

**ELECTROPHYSIOLOGICAL BRAIN MONITORING AFTER
CARDIAC ARREST WITH TEMPERATURE MANAGEMENT**

By
Ruoxian Deng

A thesis submitted to Johns Hopkins University in conformity with the requirements for
the degree of Master of Science in Engineering

Baltimore, Maryland

May, 2015

© 2015 Ruoxian Deng

All Rights Reserved

Abstract

Cardiac arrest (CA) is the leading cause of disability and death annually in the United States. Therapeutic hypothermia (TH) has been recommended as one of the standard practices for improving neurological outcome and survival to treat out-of-hospital CA patients after resuscitation. However, many clinical prognostic markers after resuscitation for predicting outcome have been less reliable under hypothermia. Therefore, there is a strong need to evaluate the prognostic value of current prognostic markers for hypoxic-ischemic brain injury after CA. The first part of this work was to review current literature and assess the prognostic value of current significant breakthroughs in neurophysiologic and electrophysiological methods for CA patients treated with TH in order to provide a comprehensive frame for future work.

Due to the restrictions of standard clinical examinations and neuroimaging techniques in detecting brain injury, electroencephalography (EEG) has emerged as one of the commonly used bed-side real-time monitoring tools for prognostication. Instead of the subjective and impractical analysis of waveform-based raw EEG signals, we applied two quantitative methods – information quantity (IQ) and sub-band IQ (SIQ) – to quantify and examine the accuracy of prognostic value of EEG markers on predicting recovery under TH in the second part of this work. Our study discovered that both IQ and SIQ accurately predict neurologic outcome at the early stage of cerebral recovery. Moreover, high-frequency oscillations (HFO) were particularly noticeable during the recovery from severe brain injury indicated by IQ, and SIQ was able to provide additional standard clinical EEG bands of interests.

The ischemic brain after CA is sensitive to trivial fluctuations of temperature. Previously, we only observed temperature management strongly affects the recovery of global EEG. However, EEG signals can be decomposed into different frequency sub-bands in clinical practices, which are related to different brain functions, and the association has not been elucidated between the recovery of each sub-band EEG and temperature management. In the third part of this work, we employed SIQ, of which indicative ability has been proven in the last part, to determine the most relevant sub-bands of EEG during brain recovery with temperature manipulation. It was found for the first time that gamma-band EEG activity, linked with high cognitive processes, was primarily affected by temperature and strongly associated with neurologic outcome, while delta-band played a role as constant component of EEG without stable relationship with temperature or outcome.

Somatosensory evoked potentials (SSEPs), especially N20 responses in human, are able to evaluate the somatosensory system functioning, which are also regarded as a reliable early prognostic marker for post-CA neurologic outcome. Transcranial direct current stimulation (tDCS) is a non-invasive technique to modulate the cerebral excitability and activity which has been confirmed by motor evoked potentials (MEPs), but it is still unclear whether it can affect the somatosensory cortex. The final part of this work preliminarily studied the alternations of excitability of somatosensory cortex by tDCS and investigated the potential of SSEPs on measuring the after-effect of tDCS.

Thesis Advisors: Dr. Xiaofeng Jia, Dr. Utpal Shashikant Bhalala and Dr. Kevin J. Yarema

Thesis Committee

Dr. Xiaofeng Jia, M. D., Ph. D. *Primary Advisor*

Associate Professor, Department of Neurosurgery, Orthopedics

University of Maryland School of Medicine;

Department of Biomedical Engineering, Anesthesiology and Critical Care Medicine

Johns Hopkins University School of Medicine

Dr. Utpal Shashikant Bhalala, M.D.

Pediatric Intensivist, Bloomberg Children's Center

Johns Hopkins Hospital;

Assistant Professor, Department of Anesthesiology and Critical Care Medicine

Johns Hopkins University

Dr. Kevin J. Yarema, Ph.D. *Committee Chair*

Associate Professor, Department of Biomedical Engineering

Johns Hopkins University

Acknowledgement

First, I would like to express my sincere appreciation to my primary advisor, Dr. Xiaofeng Jia. During my two year of master study, Dr. Jia offered me important scientific guidance, intellectual discussions, constant encouragement and support, which meant a lot to my development of scientific thinking and future career. I would also like to thank Dr. Utpal S. Bhalala and Dr. Kevin J. Yarema for their endless scientific advice and understanding. I am honored to have all of you on my thesis committee.

At our BME Department, I was given enormous opportunities of working at cutting edge with great professors and experts in various fields. My special thanks are sent to Dr. Wei Xiong from Case Western Reserve University School of Medicine for his advice on building up our new electrophysiological monitoring system and Dr. Matthew A. Koenig from University of Hawaii John A. Burns School of Medicine for his help on academic advice and discussions on neural biology.

My sincere appreciation is also due to all my previous and current lab mates, Dr. Junyun He, Dr. Rishabh Choudhary, Dr. Yuan Si, Cheng Chen, Leanne Young, Yifan Zhang and Maria Karapetkova, for their great help, encouragement and suggestions during my hard time, especially when we were relocating from JHU to University of Maryland School of Medicine.

I'm really grateful to Hang Yu, Xiaohan Hu, Jingjun Hu, Chuyang Ye, Lijuan Zeng, Qian Zuo for being great friends, who are always accompanying me, believing in me, sharing my happiness and pain in the past two years.

Finally, I would like to thank my dearest parents. Although I'm leaving my hometown for two years, their unconditional love, understanding, and support make me keep moving on.

Table of Content

List of Figures.....	xi
List of Tables.....	xv
CHAPTER 1 Brain Monitoring of Ischemic Injury and Recovery after Cardiac Arrest with Therapeutic Hypothermia	1
1.1 Introduction.....	1
1.2 Neuropathological Mechanisms of Hypoxic-Ischemic (HI) Brain Injury after Cardiac Arrest (CA)	2
1.3 The Clinical Evaluation of Neurological Outcome	3
1.4 Potential Neuroprotections for Hypoxic-Ischemic Brain Injury after Cardiac Arrest.....	4
1.4.1 Medication	4
1.4.2 Therapeutic Hypothermia (TH)	5
1.5 Neurophysiologic Brain Monitoring and Neuroimaging for Prognostication in post-CA patients.....	6
1.6 Global Electrophysiological Brain Monitoring for Prognostication in post-CA Patients.....	9
1.6.1 Prognostic Test via Electroencephalography (EEG).....	9
1.6.2 Prognostic Test via Evoked Potential (EP)	16
1.7 Cellular Electrophysiological Brain Monitoring Measurement Methods	21
1.7.1 Local Field Potentials (LFPs)	21
1.7.2 Single and Multi Unit Activity	23

1.7.3 Spiking and Burst Suppression Model.....	24
1.8 Conclusion	24
 CHAPTER 2 Quantitative EEG Markers in Severe Post-resuscitation Brain Injury with Therapeutic Hypothermia	 26
2.1 Introduction.....	26
2.2 Methods and Materials.....	27
2.2.1 Animals.....	27
2.2.2 Asphxial Cardiac Arrest and Hypothermia.....	28
2.2.3 EEG Recording and Data Analysis.....	30
2.2.4 Neurological Evaluation	31
2.2.5 Statistical Methods.....	33
2.3 Results	34
2.3.1 Temperature Recording, ABG Testing, and NDS Analysis	34
2.3.2 Quantitative EEG (qEEG) Analysis.....	35
2.3.3 Association between qEEG values and 72-hr NDS.....	35
2.3.4 Prediction of Functional Outcomes by qEEG Markers	39
2.3.5 Changes in Aggregate IQ and Aggregate SIQ with Therapeutic Hypothermia	42
2.4 Discussion.....	44
2.5 Conclusion.....	46
 CHAPTER 3 Early Quantitative Gamma-Band EEG Marker Predicts Outcomes after Cardiac Arrest and Target Temperature Management.....	 48
3.1 Introduction.....	48

3.2	Materials and Methods	50
3.2.1	Animals.....	50
3.2.2	Cardiac Arrest and Temperature Management	50
3.2.3	Sampling Method and SIQ-qEEG Analysis.....	52
3.2.4	Neurologic Evaluation	53
3.2.5	Statistical Analysis	53
3.3	Results	54
3.3.1	Temperature Management and ABG Data	54
3.3.2	Aggregate SIQ was Associated with Post-CA Functional Outcomes.....	55
3.3.3	Temporal Evolution of SIQ was Associated with Functional Outcomes in the Three Temperature Groups.....	58
3.3.4	Good Functional Outcomes were Associated with higher SIQ Values.....	64
3.3.5	Predictive Value of SIQ-qEEG Values.....	65
3.4	Discussion	73
3.5	Conclusion	76

CHAPTER 4	Effects of Transcranial Direct Current Stimulation on Somatosensory Evoked Potentials in Uninjured Rats	78
4.1	Introduction	78
4.2	Materials and Methods	81
4.2.1	Animals.....	81
4.2.2	Transcranial Direct Current Stimulation.....	81
4.2.3	SSEPs Recording and Stimulation.....	82
4.2.4	SSEPs Signal Analysis.....	83

4.2.5 Statistical Analysis	84
4.3 Results	84
4.3.1 Aggregate SSEPs Post-tDCS	86
4.3.2 Temporal Evolution of SSEPs Post-tDCS	88
4.4 Discussion.....	91
4.5 Conclusion	94
CHAPTER 5 Summary and Future Directions	95
5.1 Summary	95
5.2 Future Directions.....	96
Bibliography	98
CURRICULUM VITAE	123

List of Figures

Figure 2. 1. Representative raw EEG data, information quantity (IQ) and sub-band information quantity (SIQ) plots from the hypothermia and normothermia groups. Raw EEG signals under A, hypothermia and normothermia. B-C: The effect of hypothermia on EEG recovery was apparent with the analysis of IQ (in B) and SIQ (in C). Higher IQ was more evident in hypothermia group compared with normothermia. The high variability in IQ might be due to the HFO.

Figure 2. 2. Representative Pearson correlation (r value) plot between IQ or SIQ and 72-hr NDS. A, IQ strongly correlated with 72-hr NDS at 2 hrs after ROSC (r value: 0.718), whereas, B, SIQ have a more robust correlation with 72-hr ROSC at the same time (r value: 0.842).

Figure 2. 3 Higher aggregate IQ and SIQ values (mean±S.E.M) were found in rats with good functional outcome (72-hr NDS≥60) than in those with bad function outcome (72-hr NDS<60). *p<0.05, **p<0.01.

Figure 2. 4 In IQ, remarkable significances were observed between animals with good and bad outcomes beginning at 1 hr (good/bad: 0.51±0.03/0.34±0.03, p<0.01), 2 hrs (0.73±0.05/0.44±0.03, p<0.01), 3 hrs (0.85±0.07/0.57±0.04, p<0.01), 5 hrs (0.89±0.06/0.61±0.08, p<0.05), and 72 hrs (0.94±0.04/0.71±0.07, p<0.01), whereas notable differences in SIQ occurred at 1 hr (0.62±0.02/0.45±0.04, p<0.05). and 2 hrs (0.76±0.02/0.56±0.04, p<0.01).

Figure 2. 5 Greater recovery of IQ (mean±S.E.M) was found in rats under hypothermia

than those under normothermia. However, no significantly better recovery of SIQ (mean±S.E.M) was shown between hypothermia and normothermia groups, which is consistent with the result of 72-hr NDS. *p<0.05, **p<0.01.

Figure 2. 6 Comparison of IQ and SIQ between A, hypothermia group and B, normothermia group at different time intervals: 1-1.5 hrs, 2-2.5 hrs, 3-3.5 hrs, 4-4.5 hrs, 5-5.5 hrs, 24 hrs, 48 hrs and 72 hrs.

Figure 3. 1 The core temperature (mean±S.E.M.) was well controlled in all three temperature groups – hypothermia (33±1°C, blue), normothermia (37±0.5°C, red) and hyperthermia (39±0.5°C, green) – during the 6-hr temperature management period (highlighted).

Figure 3. 2 Examples of sub-band information quantity (SIQ) plots from the good outcome and bad outcome groups. From top to bottom, the plots represent conventional SIQ and SIQ of the sub-bands from lowest to highest frequency. Significant differences between the good and bad outcome groups were shown in the gamma band, whereas there were no differences in the delta band.

Figure 3. 3 The sub-band SIQ values in the three temperature groups at different time intervals. A, Conventional SIQ values of the hypothermia group were significantly higher than the other temperature groups from 30 mins to 2.5 hrs after ROSC. B, There were significant differences in gamma-band SIQ among the three groups at all time intervals (30 mins, 1 hr, 1.5 hrs, 2 hrs, 2.5 hrs, 3 hrs, 3.5 hrs, 48 hrs and 72 hrs). C, In the delta sub-band, a significant difference in SIQ values between the

normothermia and hyperthermia groups was seen only at 4 hrs after ROSC. * $p < 0.05$, ** $p < 0.01$.

Figure 3. 4 Representative Pearson correlation (r value) plot between SIQ value and 72-hr NDS. The gamma-band SIQ most consistently correlated with 72-hr NDS from 30 mins until 72 hrs after ROSC among all sub-bands. As shown, the gamma-band SIQ at 3 hrs after ROSC had good correlation with 72-hr NDS (r value: 0.782, $p < 0.01$).

Figure 3. 5 The comparison of SIQ-qEEG values (mean \pm S.E.M.) between the good functional outcome group (72-hr NDS \geq 60) and bad functional outcome group (NDS $<$ 60). A, Aggregate SIQ demonstrated significant differences, except in the delta-band, in conventional SIQ (good/bad: 0.80 \pm 0.02/0.65 \pm 0.02, $p < 0.01$), theta (0.86 \pm 0.02/0.75 \pm 0.02, $p < 0.01$), alpha (0.78 \pm 0.020/0.64 \pm 0.019, $p < 0.01$), beta (0.69 \pm 0.021/0.51 \pm 0.019, $p < 0.01$), and gamma (0.59 \pm 0.028/0.32 \pm 0.019, $p < 0.01$). B and C, Significant differences in conventional SIQ and gamma-band SIQ between the outcome groups were shown continuously from 30 mins to 72 hrs after ROSC. D, The delta-band SIQ showed poor discrimination between the outcome groups at most time intervals. * $p < 0.05$, ** $p < 0.01$.

Figure 3. 6 Receiver operation characteristic (ROC) curves were used to identify the optimal SIQ cut-points with area under the ROC curve > 0.8 and highest specificity for good outcome. The cut-point for gamma-band SIQ > 0.39 at 2 hrs after ROSC had a sensitivity of 0.727 and specificity of 1 with an area under ROC curve of 0.86 (shown).

Figure 4. 1 The baseline amplitude, latency and duration of SSEPs (mean±S.E.M) before cathodal and anodal tDCS. There were no significant differences found in all three parameters, demonstrating no interaction of cathodal and anodal tDCS.

Figure 4. 2 The changes in peak-to-peak amplitudes from right cortex and left cortex after anodal tDCS. A, Significantly higher amplitude was found in right cortex (1.16 ± 0.07 , $p=0.033$) compared to baseline. B, There were no significant changes found in left cortex. * $p<0.05$, ** $p<0.01$.

Figure 4. 3 After anodal stimulation, significant temporal evolutions were shown on both sides of cortex. A, From the right cortex, the amplitudes at 10 mins (0.99 ± 0.02 , $p=0.399$) and baseline were similar, but increased at 20 mins (1.13 ± 0.03 , $p=0.004$) and slightly increased to 1.20 ± 0.08 at 30 mins ($p=0.250$). B, From the left cortex, the amplitudes slightly increased with respect to baseline after anodal stimulation at 10 mins to 1.22 ± 0.16 ($p=0.208$) and then increased to 1.33 ± 0.15 ($p=0.178$) at 20 mins and notably increased to 1.55 ± 0.22 ($p=0.028$) at 30 mins.

List of Tables

Table 2. 1 Neurological Deficit Scale Score

Table 2. 2 Correlation coefficient between qEEG values and 72-hr NDS

Table 2. 3 The optimal cut-off points (sensitivity) with the highest specificity (100%) and area under ROC curve >0.8

Table 3. 1 Aggregate SIQ (mean \pm S.E.M.) in temperature groups

Table 3. 2 SIQ values (mean \pm S.E.M.) of temperature groups at different time intervals

Table 3. 3 The correlation coefficient between SIQ values and 72-hr NDS scores

Table 3. 4 SIQ values (mean \pm S.E.M.) of functional outcome condition groups at different time intervals

Table 3. 5 The correlation coefficient between good electrophysiological outcome and good functional outcome

Table 3. 6 SIQ cut-points (sensitivity) with highest specificity (100%) and area under ROC curve >0.8

Table 4. 1 The temporal changes (Mean \pm S.E.M) in latencies and durations after anodal tDCS

Table 4. 2 The temporal changes (Mean \pm S.E.M) in amplitudes and durations after anodal tDCS

CHAPTER 1 Brain Monitoring of Ischemic Injury and Recovery after Cardiac Arrest with Therapeutic Hypothermia

1.1 Introduction

Cardiac arrest (CA) affects approximately 326,200 cases annually in the United States (1). However, of these cases, approximately 10.6% of out-of-hospital, of whom 8.3% has good neurological outcome (1). Therapeutic hypothermia (TH) has been recommended by several international guidelines as a neuroprotection method for post-CA patients after the return of spontaneous circulation (ROSC) (2-5). However, the efficacy of existing prognostication parameters, as stated in the AAN reports (6), regarding functional outcome is limited because the guidelines have not been altered to consider the effects of TH. Clinical examination, brainstem reflexes, and neurophysiological monitoring retain their predictive robustness (7-9), but may lead to inconclusive results. Therefore, there is a strong need to develop reliable and noninvasive tools to improve post-CA functional outcome prognostication. Improved electrophysiological monitoring, with emphasis on electroencephalogram (EEG) and evoked potentials (EPs), can help clinicians determine the degree of neurologic injury with greater sensitivity and specificity, and can be easily implemented at the patient's bedside. The cellular electrophysiology, such as local field potential (LFP) and Multi-Unit Activity (MUA), can provide more detailed information on individual neurons or neuron populations to better understand the neuropathological

mechanism and improving the therapeutic methods for post-cardiac arrest patients.

The purpose of this narrative review is to assess the applications of neurophysiologic and electrophysiological methods and identify their advantages and limitations on monitoring post-CA brain injury and recovery to provide a comprehensive framework for future clinical prognostication.

1.2 Neuropathological Mechanisms of Hypoxic-Ischemic (HI) Brain Injury after Cardiac Arrest (CA)

Brain ischemia during CA, also known as cerebral ischemia, occurs when the blood supply to brain is blocked or reduced during CA. During brain ischemia, the cells in the brain cannot perform aerobic metabolism due to the loss of oxygen and substrate. Anaerobic metabolism within the region of brain tissue affected by ischemia generates less adenosine triphosphate (ATP). The depletion of ATP results in the dysfunction of membrane ATP-dependent Na-K pumps within several minutes after the onset on injury. A number of cytotoxic events follows, including lipolysis early changes in global ischemia consist of anoxic depolarization, which lead to changes in the intra- and extracellular, electrolyte composition (10). Due to impaired cell membrane function, extracellular sodium, chloride and calcium decrease, and potassium leak into the extracellular space (10), lactic acid and hydrogen ions (H^+) are released into the local environment. Lactic acid is an irritant which could potentially destroy cells and disrupt the normal acid-base balance in the brain, while glutamate causes excitotoxic injury (11) mediated largely through N-methyl-D-aspartate (NMDA) receptors (12). Elevated nitric

oxide causes greater and longer lasting acidosis which exacerbates cell function and edema (11). All of the above changes lead to cellular necrosis and breaking down of neuronal tissue, during ischemia (13, 14).

More oxygen, a substrate for several enzymatic oxidation processes that enhances excitotoxicity, is provided during reperfusion, which generates free radicals causing mitochondrial dysfunction (15). Free radicals then peroxidize phospholipids, particularly the cell membrane, resulting in structural damage and further loss of ionic gradients. These reactions leads to damage through lipid peroxidation, protein oxidation, and DNA fragmentation, causing cell death and cell apoptosis (16). Additionally, ischemia can induce neuroinflammation at a later stage, causing abnormal activation of microglia, or increased pro-inflammatory cytokines (17). All of the above changes harm the cells and may cause edema, leading to further depletion of the blood supply of the injury area (18, 19).

1.3 The Clinical Evaluation of Neurological Outcome

In clinical practice, the Cerebral Performance Category (CPC) is one of the commonly used methods to assess the degree of disability and neurologic outcome in post-CA patients (20, 21). There are 5 categories defined in CPC from 1 to 5: CPC 1 represents full recovery, CPC 2 represents moderate disability, CPC 3 represents severe disability, CPC 4 represents in comatose or in a persistent vegetative state and CPC 5 represents dead. The discharge CPC was also proved as a reliable positive predictor for good neurologic outcome and longer patient survival (20, 22, 23).

1.4 Potential Neuroprotections for Hypoxic-Ischemic Brain Injury after Cardiac Arrest

Therapeutic hypothermia has been recommended as the most effective treatment for out-of-hospital CA patients to improve their survival and functional outcome. Other therapies can also help recovery of cerebral activity or make a similar effect as hypothermia on cortex, but they still require additional studies before recommended for routine clinical practices.

1.4.1 Medication

Due to the glutamate excitotoxicity found in global ischemic brain after cardiac arrest, glutamate antagonists have been the primary medication administered to prevent the excitotoxicity. The glutamate antagonists, can block the binding of glutamate to its receptors, N-methyl-D-aspartate (NMDA) (24), reducing the calcium influx and avoid cell apoptosis. A large number of glutamate antagonists, such as Estrogen, Ginsenoside and Progesterone, has been discovered, but the problem occurs that how to control antagonists block the binding only when excitotoxicity happens. This problem makes these medications have unbearable side-effect or lose potency.

Other medication, i.e. antioxidants applied to control oxidative stress which is a leading cause of neuron apoptosis (25), anti protein aggregation agents (26), lithium (27) might also be able to protect post-CA ischemic brain, but more validations are required before they are recommended into clinical practices.

1.4.2 Therapeutic Hypothermia (TH)

The guideline of American Heart Association has demonstrated therapeutic hypothermia as a standard neuroprotection practice for treating out-of-hospital CA patients in clinical settings (1, 28). It has been shown that TH has the association with better neurologic recovery and prevent the secondary brain injury from cardiac arrest (29). Even trivial declines in body temperature could prevent the death of neurons (30), which initiated a rising interest of hypothermia as a mean of ischemic brain protection. The neuroprotective mechanism of hypothermia is very complicated and has not been fully elucidated. The key mechanism might be attributed to the decrease of cerebral metabolic rate and blood flow by hypothermia (31), which can prevent the accumulation and release of glutamate preventing the glutamate-mediated excitotoxicity and preserve tissue ATP levels (29). Meanwhile, hypothermia might also restrict calcium influx to further protect brain from excitotoxicity (29).

In the first 12-24 hrs after resuscitation, moderate hypothermia (32-34°C) is the recommended treatment for post-CA patient (28). However, a recent study showed that no significant difference in outcomes between the patients under mild hypothermia (36°C) and those under moderate hypothermia (33°C), which might suggest that avoiding fever may be equivalent to current hypothermic strategy to treat patients in the first 72 hrs (21). These findings will reduce the risk of hypothermia and negative rebound effect by rewarming from hypothermia.

1.5 Neurophysiologic Brain Monitoring and Neuroimaging for Prognostication in post-CA patients

Current neurophysiologic prognostication parameters include clinical examination, biochemical markers, neuroimaging and electrophysiological testing, but their reliability has been diminished due to TH intervention. The predictive performance of single biomarkers is reduced when TH is applied, suggesting that it should combine several parameters to offer greater predictive value (32).

Clinical examination, whereby pupillary and corneal responses are absent, can provide early bases for poor outcome prognostication in patients treated with both normothermia (NT) and TH patients (9, 32, 33). In contrast, motor responses 72hrs after resuscitation are no longer considered reliable predictors at Day 3 in both TH and NT groups (34).

Measurement of biochemical markers, which is a non-invasive method, provides early prognostic information about brain injury and predicts neurologic outcome after CA (35-37). Serum S-100B protein can be measured to predict outcome after CA, but it is not a commonly used method in clinical use (36). Increased neuron-specific enolase (NSE) levels > 33 ng/ml have been traditionally associated with poor outcome, but discrepancies in terms of cutoff values and subsequent neurologic recovery have discredited their reliability (34). A recent study has shown that the time evolution between Day 1 and Day 2 of the NSE levels rather than their absolute value holds better prognostication value (7). Another biochemical marker, lactate level, is also associated with neurologic outcome especially at the first 48 hrs after resuscitation from cardiac arrest. Survivors and patients with good neurologic outcome showed lower lactate levels (38). However, its prognostic

values are required the re-evaluation with the intervention of TH. The study of Bernard et al. showed that the level of lactate increased at the initiation phase of TH (33°C) and then gradually decreased (3), whereas Lazzeri et al. found that a significant reduction in serum lactate levels during TH (39) and early lactate clearance was able to predict good outcome indicated in the study of Lee et al (40).

Clinical examination and biochemical markers are largely employed for post-CA prognosis making, but are still undergoing research to account for the differences resulting from TH.

With the advances of different imaging techniques, i.e. Computed Tomography (CT), Magnetic Resonance Imaging (MRI) and Positron Emission Tomography (PET), novel imaging markers to predict long-term neurological recovery of patients after CA have been developed. CT is helpful in detecting cytotoxic edema and evaluating non-responsive post-CA patients through measuring the loss of distinction between gray and white matter. Reduced distinction was associated with mortality in comatose CA patients (41). However, the distinction is not detectable and visible within 72-hr after resuscitation, and the predictive ability of CT is limited if CT is used as an isolated prognostic tool as shown in the European Resuscitation Council Guidelines (42).

MRI, a method of detecting the alternations in cerebral protons to evaluate edema, is more sensitive than CT without using ionizing radiation or radioactive tracers. A recent study demonstrated that the abnormalities of diffusion-weighted imaging (DWI, a form of MRI), were highly sensitive to predict poor outcome (sensitivity of 98.5%) but with low specificity of 46.2% from patients following cardiac arrest (43). The additional use of

apparent diffusion coefficient (ADC), obtained by subtracting T2 signal from DWI sequences, could increase the specificity for poor outcome to 100% and the sensitivity by 38% (44). Measurement of the blood oxygenation level dependent (BOLD) signal has been found to hold important correlations with functional metabolic activity (45). Functional MRI (fMRI) was introduced to quantify BOLD signal to assess the association between the cerebral metabolism and brain functions. Since the disorders of consciousness can interrupt the BOLD signal (46), fMRI may help clinicians discover and predict the neurologic outcome in post-CA patients. But, MRI takes longer time to obtain images than CT and is limited by obtaining real-time cerebral information.

PET is a different neuroimaging technique, which can visualize the changes in cerebral metabolism not in structure. The alternations in glucose consumption, cerebral blood flow and oxygen metabolism derived from PET have the predictive value for neurologic outcome (47, 48). One of the useful measures of oxygen metabolism by PET is oxygen extraction fraction (OEF) in post-CA patients with TH. Patients with poor outcome showed notably lower OEF than those with good outcome (49).

Although neuroimaging may bring a new insight into two- or three-dimensional brain monitoring, the lack of large-sample studies, low resolution, limitation of obtaining real-time information and the absence of comparison with other established prognostic markers make neuroimaging markers solely a complementary technique with other prognostic methods for post-CA patients.

1.6 Global Electrophysiological Brain Monitoring for Prognostication in post-CA Patients

Although traditional clinical examination and biochemical markers are commonly used for an early prognostication of neurologic outcome, they fail to provide direct measurement of the degree of underlying neuronal activation (50). Also, neuroimaging markers testing is expensive and only involved in studies of limited sample size without comparison with other prognostic methods. Electrophysiological brain monitoring in the early phase of recovery can correct for these deficiency by providing both quantitative and qualitative information, with its performance largely independent of hypothermia effects.

1.6.1 Prognostic Test via Electroencephalography (EEG)

EEG monitoring of temporal and spatial characteristics, such as frequency and amplitude, is one of the most common methods and provide early information about the bedside neurophysiologic prognosis for comatose patients. EEG background reactivity and continuity have been recently identified as critical factors in predicting recovery or poor outcome (51, 52). New multimodal approaches emphasize the role of continuous EEG (cEEG) and its correlation with other neurophysiological markers, such as neuron-specific enolase (NSE) levels, as independent predictors of poor outcome (51). Other techniques aim to simplify cEEG and provide information about the recovery of EEG pattern and degree of brain injury, respectively. Automated analysis has been shown as an alternative to visual interpretation by the physician (53), but it still requires further

investigation.

Continuous Electroencephalography (cEEG)

The importance of continuous EEG (cEEG) has been increasingly recognized in monitoring brain function and predicting early outcome in ICU patients. It can improve prognostication at 72 hours, while neurologic examination performed at that time may be inconclusive (22, 54).

It has been indicated that cEEG can be applied to predict both good outcome and bad outcome based on different patterns: isoelectric (defined as no visible EEG activity), low-voltage (defined as EEG activity less than 20 μ V), burst suppression (defined as the presence of bursts, where bursts defined as amplitudes of EEG higher than 20, followed by the intervals of at least 1 sec with low-voltage suppression activity), diffuse slowing (defined as normal EEG pattern with a dominant frequency less than 8 Hz), normal or epileptiform activity (including seizures and generalized periodic discharges) (52, 55). Isoelectric, low-voltage and burst-suppression EEG patterns are associated with poor outcome (52, 56), whereas patients with good functional outcome showed normal or diffuse slowing EEG rhythm which was never found in patients with poor outcome (52, 55). Epileptiform activity is linked with poor outcome, but it is not always true (57-59).

cEEG background reactivity was defined as present if brain electrical activity of at least 10 μ V and EEG background indicated the alternation in amplitude or frequency on repetitive auditory, visual and nociceptive stimulus (60, 61). The presence of EEG reactivity was shown as a predictor of recovery of consciousness (All survivors had

background reactivity) and favorable outcome (74% of survivors), whereas the absence of reactivity had the association with mortality (Positive Predictive Value (PPV) = 1, False-positive Rate =0) (60).

The study of Cloostermans et al. also found that cEEG was the most effective predictor between the first 12-24 hours after CA and that it offered significantly better sensitivity than other electrophysiological parameters such as somatosensory evoked potentials SSEP (40% for cEEG compared to 20% for SSEP). In a prospective cohort study with 134 post-CA patients testing a multimodal approach for prognostication found that hypothermic EEG background reactivity was the best predictor for poor outcome with sensitivity of 74% with the highest area under receiving operator characteristics curve of 0.81 (51). The results showed that cEEG together with clinical examination and NSE levels had the highest prognostic accuracy of mortality and poor outcome. Another study with comatose patients has also shown correlation between unreactive EEG background and elevated NSE levels, proving that early EEG abnormalities in the first 24-48 hours are pathophysiologic signs resulting from post-anoxic neuronal injury (62). However, early presence of background reactivity does not guarantee recovery, as some patients with reactive but discontinuous background died after return to normothermia (63). Similarly, status epilepticus is now shown to depend upon the type of background reactivity of EEG as being flat, burst-suppressed, or continuous (64-66). cEEG could be useful in the first 24 hrs (65), but it is preferable to be used as part of a multimodal approach, whereby other neurophysiological factors are included, such as SSEP and neurologic examination.

Amplitude-integrated EEG (aEEG)

Amplitude-integrated EEG (aEEG) method, is increasingly used for continuous brain function monitoring of post-CA patients, as it requires less time and expertise to be interpreted (67). It is a simplified method that shows the peak-to-peak amplitude values of rectified EEG on the time-compressed semi-logarithmic scale (67, 68). aEEG method has been evaluated not only as an outcome prediction and real-time brain injury monitor in asphyctic neonates treated with hypothermia (69-71), but it is also useful as a prognostic tool for predicting outcome in post-CA adult patients with hypothermia-treatment. Rundgren. M group investigated 34 TH-treated post-CA patients: 20 patients with a continuous aEEG at normothermia after cardiac arrest returned to consciousness, but the others with abnormal aEEG pattern did not return to consciousness or died in hospital (72). In a prospective study of 55 TH treated post-CA patients, an initial continuous normal voltage (CNV) of the aEEG immediately after ROSC was a good predictor of good outcome, while a lack of CNV in the first 72 hours after ROSC was a good predictor of poor outcome (73). aEEG has been shown its ability in detecting abnormal EEG patterns commonly happening in neonates suffering in HI injury treated with hypothermia (74). Together these results demonstrate that aEEG can provide practical information on the degree of cerebral dysfunction, which can be regarded as a simpler and more reliable applied method in an ICU setting compared to the cEEG method.

Entropy-based Quantitative Electroencephalography (qEEG)

EEG monitoring methods, such as EEG background and reactivity, hold important

prognostic value about the neurological outcome of patients treated with TH (62), but prognostication is often confounded by the subjective interpretation of the neurologists who review the EEG outputs. A new automatic method based on quantitative characteristics, i.e. Burst Suppression Ratio (BSR) and approximate entropy, has been developed to measure background activity (53). The results between the visual and automated analysis correlate well, but the automatic approach was influenced by epileptiform activity and muscle artifacts among other, which required the expertise of physicians to detect the suppressed state. The same study also confirmed that BSR and approximate entropy differ significantly for good and poor outcome, with reactivity being the stronger factor compared to background discontinuity. A comparative study with 30 post-CA patients who were under hypothermia of 33°C for 24hrs revealed that elevated response entropy and state entropy during the first 24 hrs was associated with good outcome, while decreased wavelet subband entropy (WSE) and BSR in the first 24-48 hrs were strong indicators for poor outcome (75). The same study also confirmed that status epilepticus represented by decreased WSE levels was a certain predictor of mortality. Another animal study identified increased burst frequency, shorter isoelectric period, and preserved state entropy after the restoration of continuous background as associated with good outcome and survival at 96 hrs (76). On the other hand, a study in rats indicated that burst frequency was found higher in the post-CA animals treated with TH and hyperthermia compared to normothermia, which was strongly correlated with 72-hr normothermic NDS but not hypothermic or hyperthermic neurological deficit score (NDS) (77). However, burst count was time-consuming and underestimated some essential information, such as the duration of burst or suppression duration. For these

reasons, the same group developed a quantitative measures of BSR using Tsallis entropy (TsEn) and revealed that the TsEn area correlated well with functional outcome (78), while this study is still required a more involved study including temperature management before translated into clinical practice.

Another quantitative metric that has shown promising results in animals regarding differentiating good and poor outcome and the effect of temperature on recovery of cortical electrical activity is information quantity (IQ) (79, 80). Based on information theory, IQ calculates Shannon entropy based on a distribution of all wavelet coefficients and subsequent removal of the predictable component (information redundancy) using discrete wavelet transformation (DWT). However, IQ can only distinguish the changes in gross EEG. Subband IQ (SIQ) was introduced to calculate the IQ of each frequency subband, relating behavioral state to recovery possibility (81). Induced hypothermia was associated with fast recovery of gamma-band SIQ and improved functional outcomes. The further verification of this methods, nevertheless, needs to be applied on humans in clinical studies.

Bispectral Index Monitoring

Bispectral Index (BIS) monitoring is a technique that summarizes raw EEG data and is commonly used to evaluate consciousness under anesthesia. It has been suggested that BIS is a poor index of evaluation during CPR and for the prediction of ROSC (82, 83), however the technique has unconvincing data regarding its prognostic ability after CA, and thus, is not widely used. In a prospective study of 62 post-arrest patients that underwent BIS monitoring following TH, mean BIS values were higher in good outcome

patients compared to poor outcome patients at 24hrs post-resuscitation (84). The study suggests that BIS values at 24hrs post-resuscitation are correlated with neurologic outcome in patients receiving TH after CA. In another study of 83 patients with BIS monitoring following CA and TH, the BIS after the first administration of neuromuscular blockade was higher in patients with good outcomes compared to those with poor outcomes (85). Finally, a prospective cohort study of 45 comatose patients that had received TH after CA, found that a BIS of 0 was a good predictor of poor neurologic outcome, however, there was no correlation between a BIS higher than 0 and good outcome (86). This technique may be beneficial due to its simplicity and non-invasiveness, however, the conflicting results in terms of prognostic ability suggest that further research is necessary.

Cerebral Recovery Index

The Cerebral Recovery Index (CRI) was developed to assist clinicians with the prognostication of patients treated with TH after cardiac arrest and is a single numeric value that represents five qEEG parameters. In an initial single-center study of 109 patients treated with TH post-CA and cEEG monitoring, at 24 hours post-CA, $CRI < 0.29$ was associated with poor outcome (PPV =1, Negative Predictive Value (NPV) =0.71) while $CRI > 0.69$ was associated with good outcome (PPV=0.55, NPV=1) (87). This index is beneficial as it uses the clinically important information within EEG and can predict both good and bad outcome. However, given the lack of clinical data using this index, it should be used only as a complementary criterion in prognostication.

1.6.2 Prognostic Test via Evoked Potential (EP)

Although EEG monitoring is generally easy to conduct and interpret, it can be affected by external factors such as medications and sedation in the first 3 days after CPR and does not provide detailed information about the degree of injury in the higher cortical pathways in the brain. In order to avoid premature removal from ICU, evoked potentials (EPs) is used to confirm prognosis based on clinical findings, although is sensitive to muscle artifacts and relaxation(88). EP tests can provide information about the degree of functional damage of the cortical pathways upon sensory stimuli: somatosensory, motor, auditory, visual, etc., and imply the degree of likelihood of non-awakening.

Somatosensory evoked potentials (SSEPs)

Normal SSEP can be used to assess the integrity of the somatosensory pathway, the restoration of normal thalamocortical coupling, and the onset of arousal (89). Experiments have demonstrated that a significant and measurable difference existed in SSEP signals based on neurologic injury and that SSEP evolved in a predictable manner and was associated with outcome in rats after CA (90).

According to the AAN guidelines, absence of N20 component from SSEPs bilaterally up to 3 days after resuscitation has been found to be the most reliable electrophysiological biomarker for mortality or poor outcome (6). The absence of the N20 potential after stimulation of the median nerve is indicative that the patient will most probably die in a state of comatose (6, 91). The experiment results lay the groundwork for establishing the relationship between SSEPs and post-CA neurological injuries and functional outcomes. New theories promote SSEP in clinical settings to monitor patients

resuscitated from CA not only after but also during TH intervention (9). It has been identified that absence of cortical SSEP components (N20) after stimulation of the median nerve within the first 3 days after resuscitation are the reliable electrophysiological indicators of an unfavorable prognosis after therapeutic hypothermia in clinics (92). One recent study with 60 patients indicated that SSEP recorded retained high prediction value for poor neurological outcome despite TH intervention. In patients with preserved SSEP, no significant differences were found between N20 mean amplitude during therapeutic hypothermia (6-24 hours after CA) and after re-warming. In contrast, the 24 patients who showed bilaterally absent N20 did not have recovered cortical responses after re-warming. All patients with absent SSEPs during therapeutic hypothermia did not recover consciousness (93). Due to these inconsistent findings, the use of SSEP during hypothermia has yet been validated in a large hypothermic patient population to ensure that treatment benefits are not reduced and neurologists should be careful on the early only SSEP-based prognostication especially in the first 24 hrs.

Furthermore, an independent component analysis (ICA) method to separate the SSEP into early (short-latency, SL) and late (long latency, LL) responses, which were generated from the ascending pathway in both the subcortical and cortical areas, has been underway. It was shown that the recovery processes of SL- and LL-SSEPs followed different dynamics, with the SL-SSEP being restored earlier than LL-SSEPs. The SL- and LL-SSEPs represented temporal evolution of evoked response through the thalamocortical pathway and these responses were different upon injury and recovery of the thalamic and cortical regions following CA (94). Upon initiation of HI injury in a rat model with TH, LLR disappeared first, followed by the disappearance of SLR, and after a period of

isoelectric silence, SLR reappeared prior to LLR. This suggests that cortical activity, which primarily underlies the LLR, may be more vulnerable to ischemic injury than subcortical activity represented by the SLR. Compared with normothermia, hypothermia potentiated the SLR, but suppressed the LLR by delaying its recovery after CA and attenuate its amplitude, suggesting that hypothermia may selectively down-regulate cortical activity as a neuroprotective approach for the cerebral cortex (95).

While the prognostic value of SSEPs in comatose patients is well established, their clinical use is limited to studying the presence or absence of characteristic short and long latency peaks (N20 and N70 in humans). The electrophysiological examination of patients is often done 8–24 hrs after CA, due to the lack of reliable quantitative indicators for SSEP monitoring. In addition, SSEPs are only a few microvolts in amplitude and are often corrupted by biological (from nonspecific neural activity) and electrical (from instrumentation and surrounding environment) noise; waveform averaging (typically 100 to 1000 sweeps in intraoperative monitoring) is required to enhance signal quality. Also, the presence of N20 potentials cannot guarantee the good functional outcome. In order to solve the above problems, the area enclosed by the SSEP in the phase space, a space of all possible configurations of magnitudes and slopes in a signal, was investigated and introduced as a quantitative descriptor for temporal evolution of SSEP. Advanced neural monitoring systems with novel quantitative tools such as PSC (the phase space curve) and/or PSA (the phase space area) can provide real-time markers that do not require expert interpretation and offer clinicians the option to select window of interest (1–4 hrs postasphyxia) to study different components of SSEPs, simultaneously providing a better means to track injury, recovery, and the effect of neuroprotective interventions in real

time and a clinically translational means of evaluating the integrity of deep-brain regions (89). The quantitative information obtained from phase space analysis may be a valuable method in predicting both good and bad outcomes in clinical use. The second order blind identification (SOBI) technique can also be utilized to extract characteristic peak information, as new parameter from one trial of SSEP to solve noise problem. This efficient method in the identification of peak detection can offer a favorable alternative to reveal the neural transmission variation (96).

Other Diagnostic Evoked Potentials Markers

Other types of evoked potentials have not been thoroughly investigated although there has been some research on motor evoked potentials (MEPs) and auditory evoked potentials (AEPs), and their predictive value.

Presence of MEPs has long been considered to be an accurate measure of the degree of functionality of the descending cortical pathways and determine the status of the motor cortex. However, due to their high degree of sensitivity to anesthesia levels of isoflurane and ketamine and to stimulation intensity, MEPs are difficult to monitor. Previous studies have focused on using a moving average method to characterize the changes in MEP amplitudes, but this method assumes that all of signals are identical which might not be the case (97). In order to circumnavigate this issue, a statistical method has been employed to characterize MEPs by estimating the number of motor units and the potential amplitude of a single motor unit instead of using a moving average (98). The recordings showed that a decrease of anesthesia intensity resulted in increase of MEP signal amplitude.

AEPs provide information about the degree of preservation of the higher auditory cortical pathways and might help determine the likelihood of both poor outcome and chance of awakening (99). Depending on its origin, AEPs can be classified as brainstem AEPs, middle-latency AEPs (MLAEPs), and event-related AEPs (ERPs), the last being able to differentiate between different acoustic stimuli. It has been suggested that presence of mismatch negative (MMN) wave in ERPs is likely to suggest awakening of comatose patients, although it does not guarantee full functional recovery (99). A recent study, however, contended that the discriminatory performance in survivors and non-survivors is not significantly different in both TH and NT conditions, while the change in the area under the curve in the transition from TH to NT is increased in survivors compared to non-survivors (100). The study suggested that MMN presence could be observed in people with similar states of unconsciousness and could not be predictive for the final outcome, but that if the discriminatory performance changes positively in the early phase of coma, awakening will occur with 100% predictive value. Furthermore, AEPs have been associated with detecting change by a sudden change in frequency after 30ms which is particularly important for monitoring anesthesia (101). A very recent study from 2013 hypothesized that MLAEPs during anesthesia would be able to detect ROSC, survival, and neurologic outcome (102). The research group used an MLAEP monitor to determine the MLAEP index (MLAEPi) of 61 comatose patients. The MLAEPi reflected the morphology of MLAEP and the presence of the P50 component, the hippocampal CA pyramidal cells, suggests good neurologic outcome after resuscitation (102). A cut-off of 35 was established to be the threshold below which unfavorable outcome is detected with 100% sensitivity while cutoffs of 24 and 33 were

able to predict ROSC and postresuscitation survival (102).

AEPs have significant potential for predicting good outcome, which is often elusive using the standard multimodal approach (51), but studies with larger group of patients are needed to determine the veracity of this method and be implemented in the emergency room.

1.7 Cellular Electrophysiological Brain Monitoring Measurement

Methods

Although TH is used as a neuroprotective treatment for post-CA patients, it is necessary to understand the unclear fundamental mechanism for helping improving therapies. The cellular electrophysiological monitoring can be applied to investigate the alternations in activities of cerebral neurons and the neural circuit, which cannot be achieved by global electrophysiology, i.e. EEG and EPs.

1.7.1 Local Field Potentials (LFPs)

Electrophysiological brain monitoring has been expanded to include measurement of transmembrane currents and more localized events such as local field potentials (LFPs) and spikes, which can provide further information to traditional EEG recordings. LFPs originate from the firing of cortical neurons and not from action potentials, and are obtained by low-pass filtering ($<300\text{Hz}$), while spikes are the high-frequency component of the signal. The recordings are obtained using extracellular microelectrodes to measure synaptic current events over a much localized cortical region. There is some evidence that

LFPs can precede the occurrence of action potentials and could potentially be helpful for evaluation of the state of connectivity of neural pathways, while the spike temporal characteristics could signal the presence of EEG abnormalities.

In order to study the dynamics of the HI injured brain, indexes have been developed to measure anesthetic depth to quantify and understand the electroencephalogram signal and the ongoing neural processes. Local field potentials (LFPs) present advantages over the EEG diagram, as EEG is often corrupted by high frequency artifacts and electromyographic activity (103). In contrast to the EEG, in which only components below 30Hz are studied, LFPs cover a wide range of neural signals with frequencies between 1 Hz up to 300 Hz. The multitude of excitatory and inhibitory neural processes and the band-limited structure of the signals, such as gamma, alpha and beta, provide a more holistic picture of information processing in the brain during injury and recovery. For instance, high-frequency gamma-band components are preserved in LFPs and allow a better measurement of anesthetic depth compared to only the EEG. Furthermore, LFPs can be used to assess the functionality of the cortical pathways and analyze the phase-relations between the thalamus and the cortex (104, 105). A study that analyzed thalamocortical interactions discovered that at steady state there is a high degree of coherence between the thalamus and the cortex (103). Silva et al also recorded LFPs and revealed that the permutation entropy (PE) corrected for the classic burst suppression (BS) component is the most indicative component for quantifying anesthetic depth (103). Another study used LFPs to measure the vulnerability of the somatosensory responses during injury and recovery as well as during hypothermia and normothermia (106). The results suggested that the cortical function is more susceptible to HI injury than the

subcortical regions.

1.7.2 Single and Multi Unit Activity

Action potentials can be recorded with high spatial resolution from microelectrode arrays that are implanted on the cortex, and can be separated offline into single and multiunit activity (SUA, MUA) (107). The raw data are high-pass filtered followed by the application of spike detection to identify single spikes. Spike sorting is then applied to the data to discriminate SUA from MUA. The activity from single neurons will be categorized by templates such that SUA is extracted from spike sorting whereas MUA will not produce unique spike clusters after the sorting process and will instead contain spikes from multiple neurons (83, 107, 108). MUA provides more information than single-unit activity (SUA) as it accounts for smaller amplitude spike activity of the neurons around the microelectrode (109). Since MUA is generated by the spiking of several neurons it allows the study of interactions between neurons. Using a scheme of filtering and multiresolution entropy (MRE) analysis allows for spike detection and extraction of information based on entropy levels. It has been shown that employing entropy-based resolution on the MUA signal from both simulation and real time recordings, can indeed be used to describe the cortical neuron dynamics (110). LFP and MUA both underlay critical cortical processes and are interdependent, although they may differ in temporal coherence.

1.7.3 Spiking and Burst Suppression Model

According to the definition by the American Clinical Neurophysiology Society (111), spikes are short wave transients lasting $<100\text{ms}$ and can be useful in detecting abnormalities in EEG background. A novel biophysiological model of burst-suppression (BS) based on neuronal dynamics and brain metabolism has been developed to explain the periods of quiescence and spiking in the BS pattern using the ATP concentration changes (112). Cerebral metabolism, as explained by the activity of ATP-gated potassium channels (K_{ATP}) expressed in cortical and subcortical structures, was related to the observed BS pattern (112). Upon the decrease of intracellular ATP concentration, the conductance of K_{ATP} increases and K_{ATP} channels open, leading to hyperpolarization and inhibition of further spiking. The ATP concentration rises again during suppression and conductance of K_{ATP} decreases until another spike is generated. The metabolic model shows that spiking is not a simple switch on/off event and that neural activity changes in frequency depending on the oxidative stress present and the dynamics of the K_{ATP} channel. The variability of spiking that is associated with cerebral blood flow was not described by the model. There are hypotheses suggesting that slower spiking can be associated with calcium fluctuations in thalamic cells (112).

1.8 Conclusion

Therapeutic hypothermia has been considered as one of the most effective treatments for out-of-hospital CA patients for enhancing their survival and neurological function. The currently proposed multimodal approaches, combining clinical findings, biochemical

markers, and electrophysiology hold promise to facilitate the prognostication of poor outcome in post-CA patients. qEEG, SSEP and neuroimaging are able to provide accurate and objective information on the degree of HI injury and the early prediction of neurologic outcomes maximally eliminating the subjective errors by neurologists. However, the accuracy of these prognostic methods has been challenged, when used in conjunction with therapeutic hypothermia, and must be further tested by studies with larger patient groups. Absent pupillary light reflexes and SSEP are still regarded as reliable methods for the early prognostication of neurologic outcomes under hypothermia. qEEG and neuroimaging markers may bring new insights into neuromonitoring and prognostication after CA, but they still need more experiments and investigation before translated into clinical practices. Extensive cellular electrophysiology, i.e. MUA and LFP, have strong potentials for improving prognostication and therapy by assessing the thalamocortical network integrity and by offering additional cellular information to understand the underlying mechanism of therapeutic methods respectively, but have not yet become a standard practice in the emergency room.

CHAPTER 2 Quantitative EEG Markers in Severe Post-resuscitation Brain Injury with Therapeutic Hypothermia

2.1 Introduction

Approximately 326,200 cases of death and disability are caused by cardiac arrest (CA) annually in the United States (1). Only about 10.6% out-of-hospital patients survive CA, of whom 8.3% have good neurological outcome (1). Therapeutic hypothermia has been recommended as one of the most effective neuroprotection methods and a standard treatment for post-CA patients to improve survival and functional outcome after resuscitation (1, 3). However, the accuracy of some prognostic predictors for poor outcomes, such as the recovery of motor responses and biochemical markers, are challenged and less reliable under hypothermia (113). Therefore, a study to re-evaluate the current prognostic markers for different degrees of brain injuries with hypothermia is necessary.

Electroencephalography (EEG) has emerged as one of the most widely used reliable bed-side electrophysiological tools for prognostication. Due to the complicated and subjective analysis of raw EEG signals, we introduced a quantitative EEG (qEEG) method — information quantity (IQ) (79), showing objective and reliable results in predicting neurological outcome and recovery after 7-min and 9-min axphyxial CA, leading to moderate or severe brain injury, respectively (79, 80). However, IQ only

determines the recovery pattern of gross EEG signals. Thus, an alternative method, sub-band IQ (SIQ), was developed to quantify the changes during the period of injury and recovery in 5 standard clinical frequency EEG bands of interest, excluding the high-frequency oscillation (HFO) (61-122 Hz). The qEEG recovery in the bands of interest, gamma (30-60 Hz), beta (16-30 Hz), alpha (8-15 Hz), theta (4-8 Hz), and delta (below 4 Hz) (81), are potentially related to the recovery of corresponding brain functions. Both IQ and SIQ were normalized to the baseline EEG to equal 1 and dead animals had a value of 0. Higher IQ or SIQ values have been proven to be associated with good neurological outcome after moderate CA (79, 81).

Here, we describe the calculation of early IQ-qEEG and SIQ-qEEG markers as a measure of neurologic outcome, and then compared their prediction value for neurologic outcome in rats that recovered from severe brain injury after 9-min cardiac arrest with therapeutic hypothermia. We hypothesized that both IQ and SIQ qEEG markers would provide a reliable and detailed prognostic indicator after CA under therapeutic hypothermia, with the IQ marker providing additional information related to HFO activity.

2.2 Methods and Materials

2.2.1 Animals

Fourteen adult male Wistar rats (350 ± 25 g) under 9-min asphyxial CA were randomly assigned to the hypothermia ($33\pm 1^\circ\text{C}$) or normothermia ($37\pm 0.5^\circ\text{C}$) groups (n=7 per group). The experiment protocols were approved by The Johns Hopkins University

Animal Care and Use Committee.

2.2.2 Asphyxial Cardiac Arrest and Hypothermia

The asphyxial CA animal model was developed in our previous studies (79, 80). We used several life support adjustments (i.e. anesthesia, breathing circuit settings and drug requirements) for rats. 4.5% halothane mixed with 50% oxygen and 50% nitrogen at 4L/minute was carried to anesthetize the rat after the tracheal intubation with a catheter under direct laryngoscopy initially. The catheter was then connected to a mechanical ventilator (Harvard Apparatus Model 553438) with humidified 50% FiO₂ and 1.0% halothane at 50 breaths/minute, tidal volumes of 8 ml/kg and positive expiratory end pressure of 3 cm H₂O. The femoral artery and vein were cannulated (Intramedic Non-Radiopaque Polyethylene Tubing PE-50 catheters, PE 50, Becton Dickinson) to administer drugs, monitor mean artery pressure (MAP) and obtain sample of arterial blood gases (ABG). Following these preparations, baseline EEG and physiologic measurements were recorded for 5 mins with 1.0% halothane carried by a vaporizer. A 5-min washout period following the recordings of baseline with 100% oxygen for 3 mins and room air for 2 mins was implemented to prevent an anesthetic effect on the EEG signals. The rats were paralyzed with vecuronium (2 mg/kg), i.v., delivered during the 2-min washout period by room air. Global asphyxia was induced by clamping the breathing circuit and stopping mechanical ventilation for 9 mins following the 5-min washout period. CA was defined as pulse pressure <10 mmHg. Immediately after the 9-min asphyxiation, cardiopulmonary resuscitation (CPR) was performed with effective ventilation (Respiration Rate of 40/min, Tidal volumes of 8 ml/kg, positive expiratory end pressure of 0 cm H₂O), sternal chest

compressions (200 compressions/min), 100% oxygen, epinephrine (0.005 mg/kg, i.v.) and NaHCO₃ (1 mmol/kg, i.v.) until the return of spontaneous circulation (ROSC) (MAP > 60mm Hg). Then, the parameters of ventilation were adjusted to hyperventilation (Respiration Rate of 65/min, Tidal volumes of 8 ml/kg, positive expiratory end pressure of 0 cm H₂O) and maintained for 10 minutes. Subsequently, the animal was ventilated at respiration rate of 55/min at 10 mins and then 50/min at 20 mins after ROSC. The ABG was measured and monitored at 10, 20 and 40 mins after ROSC to prevent respiratory acidosis or alkalosis. No more anesthesia was given to animals during the spontaneous recovery period to reduce the effect of drugs on EEG signals. After 2 hrs, the animal was extubated and ventilation was stopped. The rat was well monitored and treated to reduce its pain and distress throughout the entire experimental period.

Hypothermia was initiated 45 mins after ROSC by external cooling using cold water and alcohol mist with an electric fan. The target core temperature of 33±1°C, measured by a temperature sensor (G2 E-mitter 870-0010-01, Mini Mitter, Sun River, OR) implanted into the peritoneal cavity 1 week before the day of cardiac arrest, was achieved within 15 mins and was maintained for 12 hrs. Rectal temperature was monitored as a reference. Since the rats were still in a comatose state within the first few hours after ROSC, a warming lamp (Thermalet TH-5, model 6333, Physiotemp, NJ, USA) was applied to avoid sharp temperature decline. At 13 hrs after ROSC, the animals were gradually re-warmed from 32-34°C to 36.5-37.5°C over 2 hrs by a heating pad and heating lamp. Normothermia was maintained after CPR at 36.5-37.5°C throughout the same time period as the hypothermia group. All animals were kept in a neonatal incubator at constant temperature of 28°C in the first 24 hrs after ROSC (79).

2.2.3 EEG Recording and Data Analysis

A two channel EEG signal from both hemispheres was recorded for 17 hrs, throughout the hypothermia, re-warming periods and 2 more recovery hours, from epidural electrodes (Plastic One, Roanoke, VA) implanted 1 week before the day cardiac arrest, by WinDaq software at a sampling rate of 250 Hz on the first day of the experiment. Serial 30-min EEG recordings were carried out at 24, 48 and 72 hrs after ROSC. The artificial noise was manually eliminated before the final data analysis. EEG electrodes were placed over parietal areas 2 mm posterior or anterior to and 2 mm lateral to bregma and a ground electrode 2 mm posterior to lambda.

In this study, we calculated the entropy-based IQ (79) and SIQ (81) in Matlab (MathWorks, Natick, MA) using our previously reported quantitative methods. In brief, Shannon entropy was calculated with a sliding temporal window technique (sliding window length $\omega=8s$, sliding step $\Delta=8s$ and the number of magnitude levels $M=20$), dividing the sampled EEG signals into equal-length windows. Second, 6 resolution decomposition coefficients, c_n^k , where $k=1,2,\dots,r+1$ representing the k^{th} subband, were obtained by discrete wavelet transform (decomposition scale $r=5$) in each temporal window. Third, since the entropy is based on probability, we determined the statistical distribution of the wavelet coefficients within each time window. To calculate the probability, $p_n^k(m)$, of each coefficient we introduced M bins I_M and calculated the occurrences of the coefficients found within each bin

$$[c_n^1, c_n^2, \dots, c_n^{r+1}] = \cup_{m=1}^M I_m \quad (1)$$

Next, the entropy formula was used to calculate the information content of the EEG

signals. The difference between IQ (Eq.2) and SIQ (Eq.3) is that IQ is obtained from the probability function for all levels of sub-band decomposition, whereas SIQ is calculated from the separately estimated probabilistic distribution in each level of decomposition. Then, the final SIQ is obtained by averaging the SIQs of all five standard clinical sub-bands of interest. Finally, we compared the changes in these values with temperature intervention and the ability to predict neurologic outcome with IQ or SIQ in severe brain injury.

$$IQ(n) = -\sum_{m=1}^M p_n(m) \log_2(p_n(m)) \quad (2)$$

$$SIQ^k(n) = -\sum_{m=1}^M p_n^k(m) \log_2(p_n^k(m)) \quad (3)$$

$$SIQ(n) = \frac{1}{r} \sum_{k=1}^r SIQ^k(n) \quad (4)$$

IQ and SIQ were normalized to the corresponding baseline values recorded before CA to allow comparison between the two temperature groups. IQ and SIQ were measured at 9 time intervals for both temperature groups: baseline (0-5 mins), CA period, 60-90 mins, 2-2.5 hrs, 3-3.5 hrs, 4-4.5 hrs, 5-5.5 hrs, 24 hrs, 48 hrs and 72 hrs.

2.2.4 Neurological Evaluation

A neurological deficit scale (NDS) score with a range of 0 (worst) to 80 (best) was used to evaluate the neurologic function of rats (Table 2.1). The NDS examination was carried out by a trained examiner blinded to temperature groups. NDS was determined at 15 hrs on the day of CA and then repeated at 24, 48 and 72 hrs after ROSC (79). Good neurologic outcome was predefined as animals with 72-hr NDS ≥ 60 and bad neurologic

outcome as animals with 72-hr NDS < 60 (80).

Table 2. 1 Neurological Deficit Scale Score

<p><u>Arousal:</u></p> <p>Alerting: Normal (0)/ Stuporous (5) / Comatose (0)</p> <p>Eye Opening: Open spontaneously (3) / Open to pain (1) / Absent (0)</p> <p>Spontaneous Respiration: Normal (6) / Abnormal (3) / Absent (0)</p> <p>Total Score : 19</p>
<p><u>Brainstem Function:</u></p> <p>Olfaction: Present (3) / Absent (0)</p> <p>Vision: Blinks to threat (3) / Absent (0)</p> <p>Pupillary Light Reflex: Present (3) / Absent (0)</p> <p>Corneal Reflex: Present (3) / Absent (0)</p> <p>Startle Reflex: Present (3) / Absent (0)</p> <p>Whisker Stimulation: Present (3) / Absent (0)</p> <p>Swallowing: Present (3) / Absent (0)</p> <p>Total Score: 21</p>
<p><u>Motor Assessment:</u></p> <p>Strength: Normal (3) / Weak movement (1) / No movement (0)</p> <p>(Each side tested and scored separately)</p> <p>Total Score: 6</p>
<p><u>Sensory Assessment:</u></p> <p>Pain: Brisk withdrawal (3) / Weak withdrawal (1) / No movement (0)</p>

(Each side tested and scored separately) Total Score: 6
<u>Motor Behavior:</u> Gait coordination: Normal (3) / Abnormal (1) / Absent (0) Balance Beam Walking: Normal (3) / Abnormal (1) / Absent (0) Total Score: 6
<u>Behavior:</u> Righting Reflex: Normal (3) / Abnormal (1) / Absent (0) Negative Geotaxis: Normal (3) / Abnormal (1) / Absent (0) Visual Placing: Normal (3) / Abnormal (1) / Absent (0) Turning Alley: Normal (3) / Abnormal (1) / Absent (0) Total Score: 12
<u>Seizures:</u> Seizures: No seizure (10) / Focal seizure (5) / Generalized seizure (0) Total Score: 10

* NDS was obtained after the recovery period on the day of CA, after 24 hrs, 48 hrs and 72 hrs.

2.2.5 Statistical Methods

The parametric variables (IQ, SIQ, temperature, ABG results) were reported as mean±S.E.M. and the non-parametric variable (NDS) were presented as median (25th-

75th interquartile). All statistics were conducted using SPSS (IBM SPSS Statistics, version 22, Armonk, NY). “Aggregate IQ or SIQ” represent the signal analyzed over the 72-hr experimental period. Parametric variables were analyzed by univariate analyses to test for the differences in IQ or SIQ between temperature groups. Non-parametric analyses were performed to test for the differences in rank order based NDS. Bivariate analyses with Pearson correlation were used to reveal the association between IQ or SIQ and 72-hr NDS. A receiver operating characteristic (ROC) curve was constructed to identify the qEEG marker optimal cut-off point with ideal sensitivity and specificity for good functional outcome. A level of $p < 0.05$ was considered significant.

2.3 Results

2.3.1 Temperature Recording, ABG Testing, and NDS Analysis

All fourteen rats' core temperature was well controlled. The target temperatures, hypothermia ($33 \pm 1^\circ\text{C}$) and normothermia ($37 \pm 0.5^\circ\text{C}$), were successfully achieved and maintained. All rats were moved to a neonatal incubator at normothermia in the first 24 hrs after ROSC. No significant differences were found in ABG values (pH, HCO_3^- , PCO_2 , PO_2) at baseline, 10 min, 20-min and 40-min after ROSC between the two temperature groups (Data not shown). Although 72-hr NDS was slightly improved in the hypothermia group (median (25th, 75th), 65 (52, 67)) compared to the normothermia group (53.5 (52.25, 66.75)), no statistically significant difference was found ($p > 0.05$), which might be due to the high mortality rate (3/7 in normothermia group and 2/7 in hypothermia group) resulting in an increased variability in the results.

2.3.2 Quantitative EEG (qEEG) Analysis

The raw EEG signals (Fig. 2.1A) were converted to IQ- (Fig. 2.1B) and SIQ- qEEG markers (Fig. 2.1C). Both IQ and SIQ decreased from baseline to the lowest points during CA, and then gradually recovered close to baseline until 72 hrs. The higher variability seen in the IQ curve might be caused by HFO (Fig. 2.1C).

2.3.3 Association between qEEG values and 72-hr NDS

Bivariate analyses indicated a significant correlation between qEEG values and 72-hr NDS (Table. 2.2). IQ-qEEG marker notably correlated with 72-hr NDS at 1 hr (r value: 0.829, $p < 0.01$), 2 hrs (0.718, $p < 0.05$) (Fig.2.2A), 24 hrs (0.723, $p < 0.05$), 72 hrs (0.844, $p < 0.01$). SIQ showed a similar significant correlation with 72-hr NDS at 1 hr (0.802, $p < 0.01$), 2 hrs (0.842, $p < 0.01$) (Fig.2.2B), 72 hrs (0.710, $p < 0.05$).

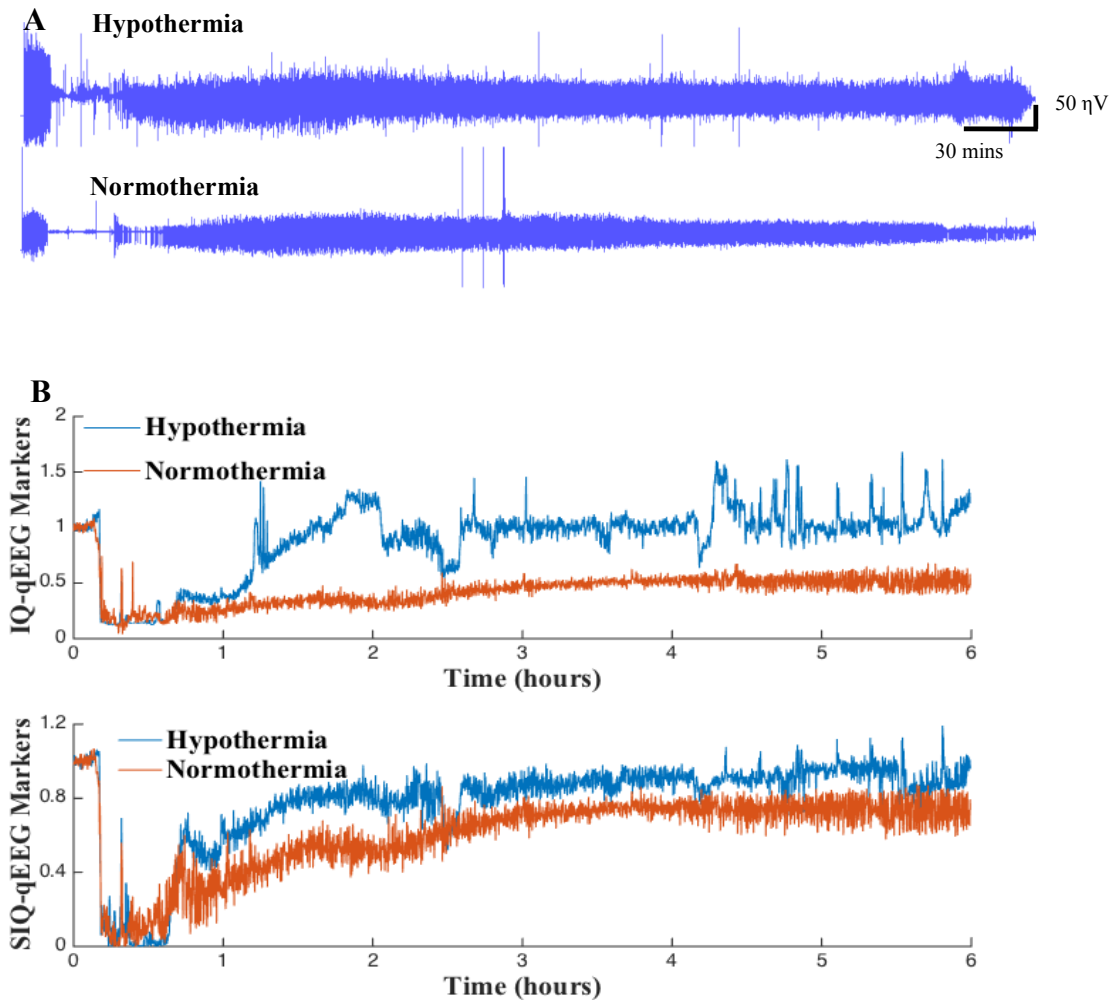


Figure 2. 1. Representative raw EEG data, information quantity (IQ) and sub-band information quantity (SIQ) plots from the hypothermia and normothermia groups. Raw EEG signals under A, hypothermia and normothermia. B-C: The effect of hypothermia on EEG recovery was apparent with the analysis of IQ (in B) and SIQ (in C). Higher IQ was more evident in hypothermia group compared with normothermia. The high variability in IQ might be due to the HFO.

Table 2. 2 Correlation coefficient between qEEG values and 72-hr NDS

qEEG Time	IQ	SIQ
1-1.5 hour	0.829**	0.802**
2-3 hour	0.718*	0.842**
3-4 hour	0.579	0.200
4-5 hour	0.523	0.111
5-6 hour	0.484	0.086
24 hour	0.723*	0.621
48 hour	0.571	0.466
72 hours	0.844**	0.710*

*p<0.05, **p<0.01

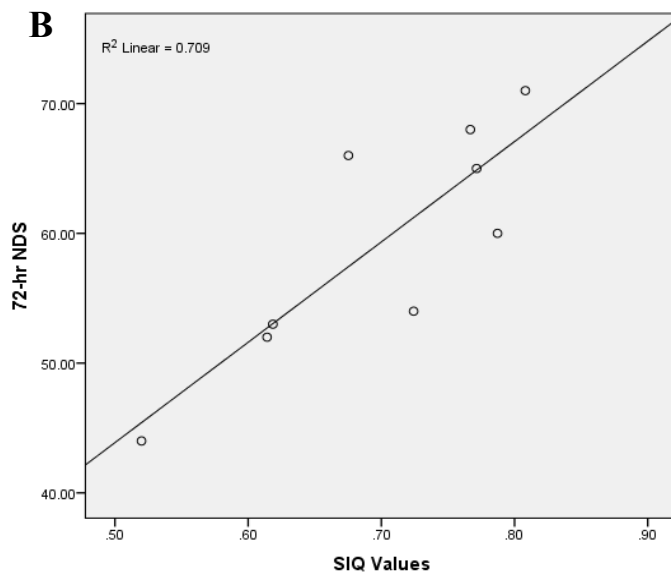
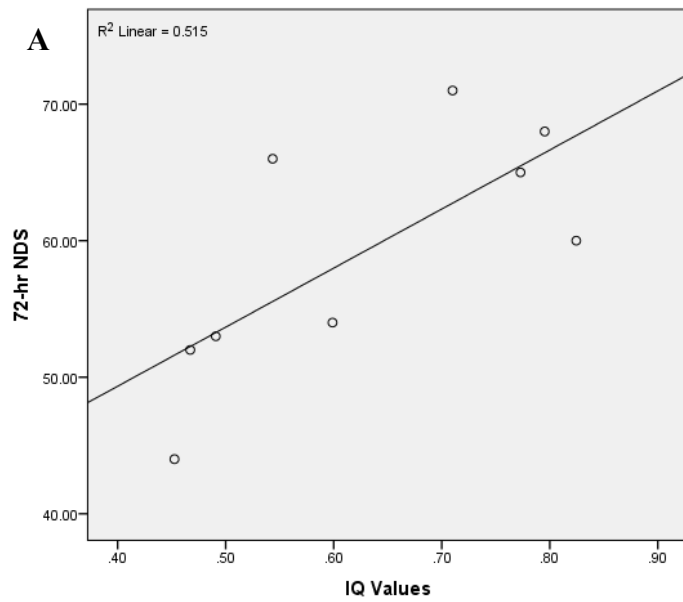


Figure 2. 2. Representative Pearson correlation (r value) plot between IQ or SIQ and 72-hr NDS. A, IQ strongly correlated with 72-hr NDS at 2 hrs after ROSC (r value: 0.718), whereas, B, SIQ have a more robust correlation with 72-hr ROSC at the same time (r value: 0.842).

2.3.4 Prediction of Functional Outcomes by qEEG Markers

By comparing the good and bad neurological functional outcome groups as defined previously, we found that the rats with good outcomes (NDS \geq 60) at 72 hrs after ROSC had higher aggregate IQ values (0.74 ± 0.04) than those with bad outcomes (NDS $<$ 60) (0.50 ± 0.03) ($p < 0.01$). The aggregate SIQ showed this similar tendency as the aggregate IQ. The rats belonging to the good outcomes group (0.73 ± 0.04) also showed higher aggregate SIQ values than those belonging to the bad outcomes group (0.59 ± 0.03) ($p < 0.01$) (Fig. 2.3).

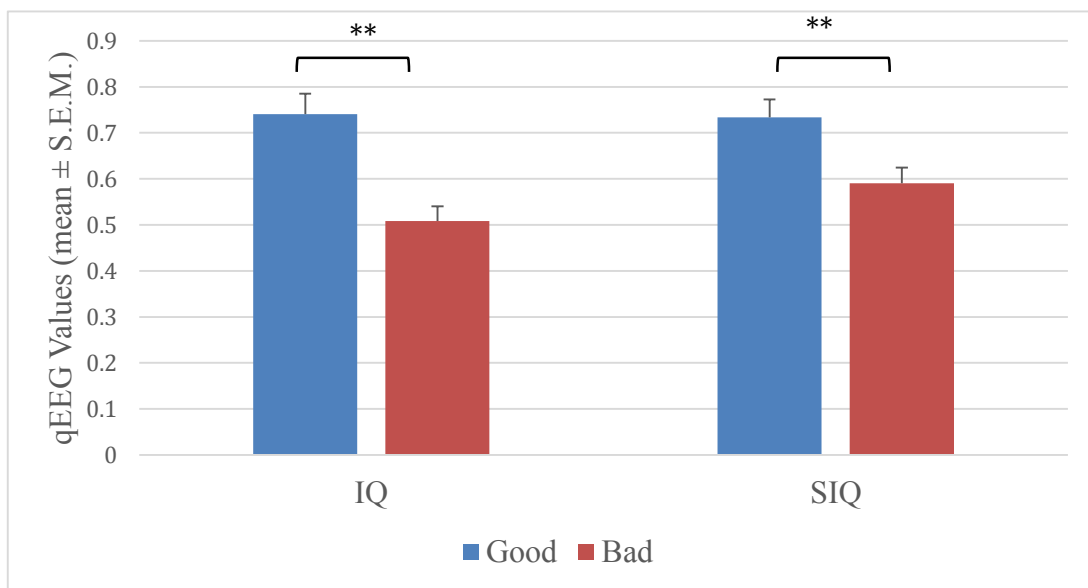


Figure 2. 3 Higher aggregate IQ and SIQ values (mean \pm S.E.M) were found in rats with good functional outcome (72-hr NDS \geq 60) than in those with bad function outcome (72-hr NDS $<$ 60). * $p < 0.05$, ** $p < 0.01$.

Significant differences between temperature groups could be found in both IQ and SIQ at different time intervals beginning at 1 hr after ROSC (Fig. 2.4).

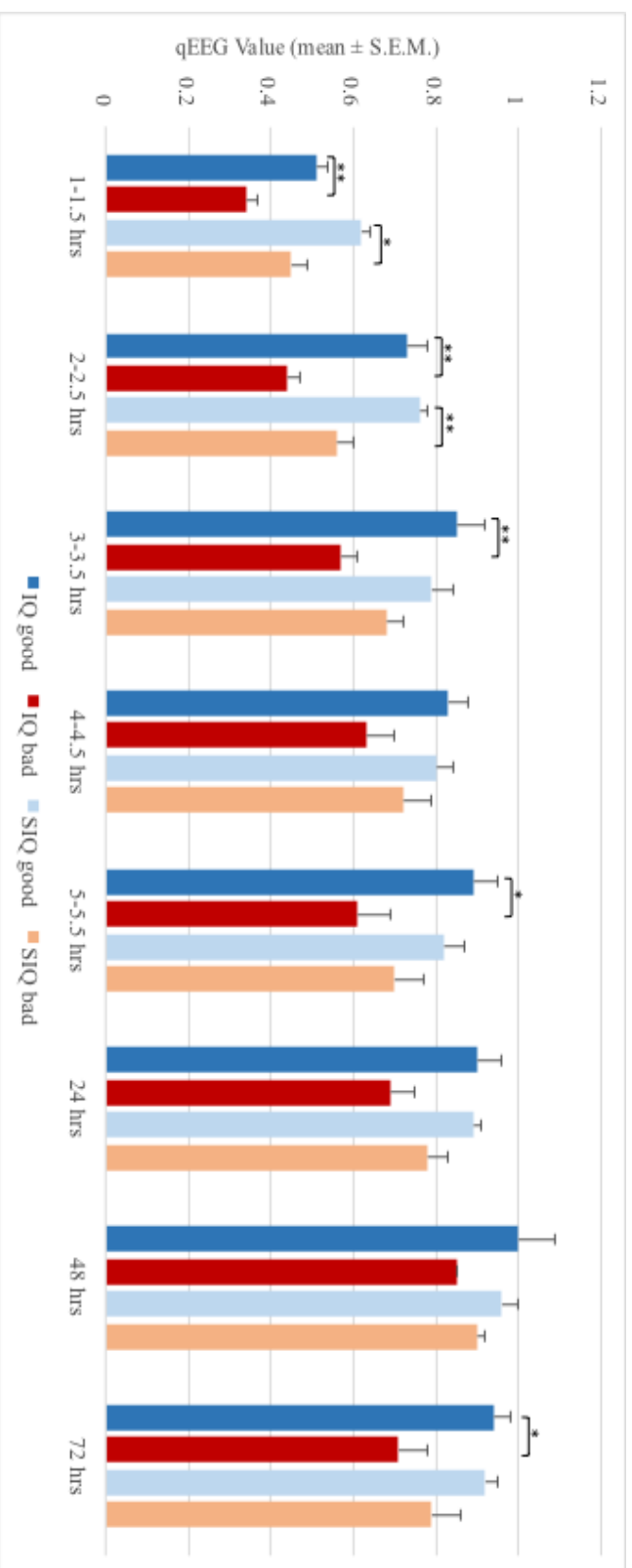


Figure 2. 4 In IQ, remarkable significances were observed between animals with good and bad outcomes beginning at 1 hr (good/bad: 0.51±0.03/0.34±0.03, p<0.01), 2 hrs (0.73±0.05/0.44±0.03, p<0.01), 3 hrs (0.85±0.07/0.57±0.04, p<0.01), 5 hrs (0.89±0.06/0.61±0.08, p<0.05), and 72 hrs (0.94±0.04/0.71±0.07, p<0.01), whereas notable differences in SIQ occurred at 1 hr (0.62±0.02/0.45±0.04, p<0.05) and 2 hrs (0.76±0.02/0.56±0.04, p<0.01).

ROC curve was used to determine the qEEG optimal cut-off points with ideal sensitivity and specificity at different time intervals for the prediction of good 72-hr functional outcome. The accurate cut-off points were defined as the highest specificity (100%) with the area under ROC curve > 0.8. They could be found in both IQ and SIQ (Table. 2.3) at 1 hr, 2 hrs and 72 hrs, with also at 3 hrs, 4 hrs, 5 hrs and 24 hrs in IQ and 24 hrs in SIQ after ROSC.

Table 2. 3 The optimal cut-off points (sensitivity) with the highest specificity (100%) and area under ROC curve >0.8

qEEG Time	IQ	SIQ
1-1.5 hour	0.47 (0.80)	0.58 (0.80)
2-3 hour	0.66 (0.80)	0.75 (0.80)
3-4 hour	0.79 (0.80)	none
4-5 hour	0.90 (0.40)	none
5-6 hour	0.87 (0.60)	none
24 hour	0.91 (0.75)	none
48 hour	none	0.93 (0.75)
72 hours	0.77 (1)	0.89 (0.80)

2.3.5 Changes in Aggregate IQ and Aggregate SIQ with Therapeutic Hypothermia

There was no significant difference in the recovery of SIQ between the hypothermia (0.66 ± 0.04) and normothermia (0.64 ± 0.04) groups ($p > 0.05$), which is consistent with the trend of 72-hr NDS. The aggregate IQ of the hypothermia group (0.65 ± 0.04) was significantly higher than the aggregate IQ of the normothermia group (0.56 ± 0.04) ($p < 0.05$). (Fig. 2.5) Nevertheless, as shown in Fig. 2.6, the IQ and SIQ values were slightly greater, although no statistical differences, in hypothermic group compared to normothermic group over the 72 hours of the study.

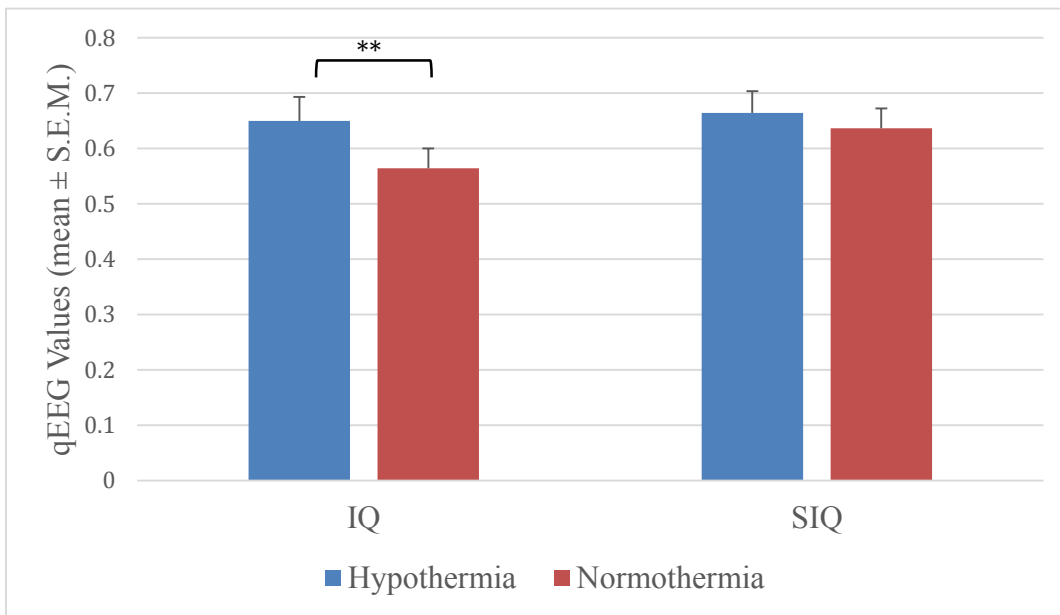


Figure 2. 5 Greater recovery of IQ (mean±S.E.M) was found in rats under hypothermia than those under normothermia. However, no significantly better recovery of SIQ (mean±S.E.M) was shown between hypothermia and normothermia groups, which is consistent with the result of 72-hr NDS. * $p < 0.05$, ** $p < 0.01$.

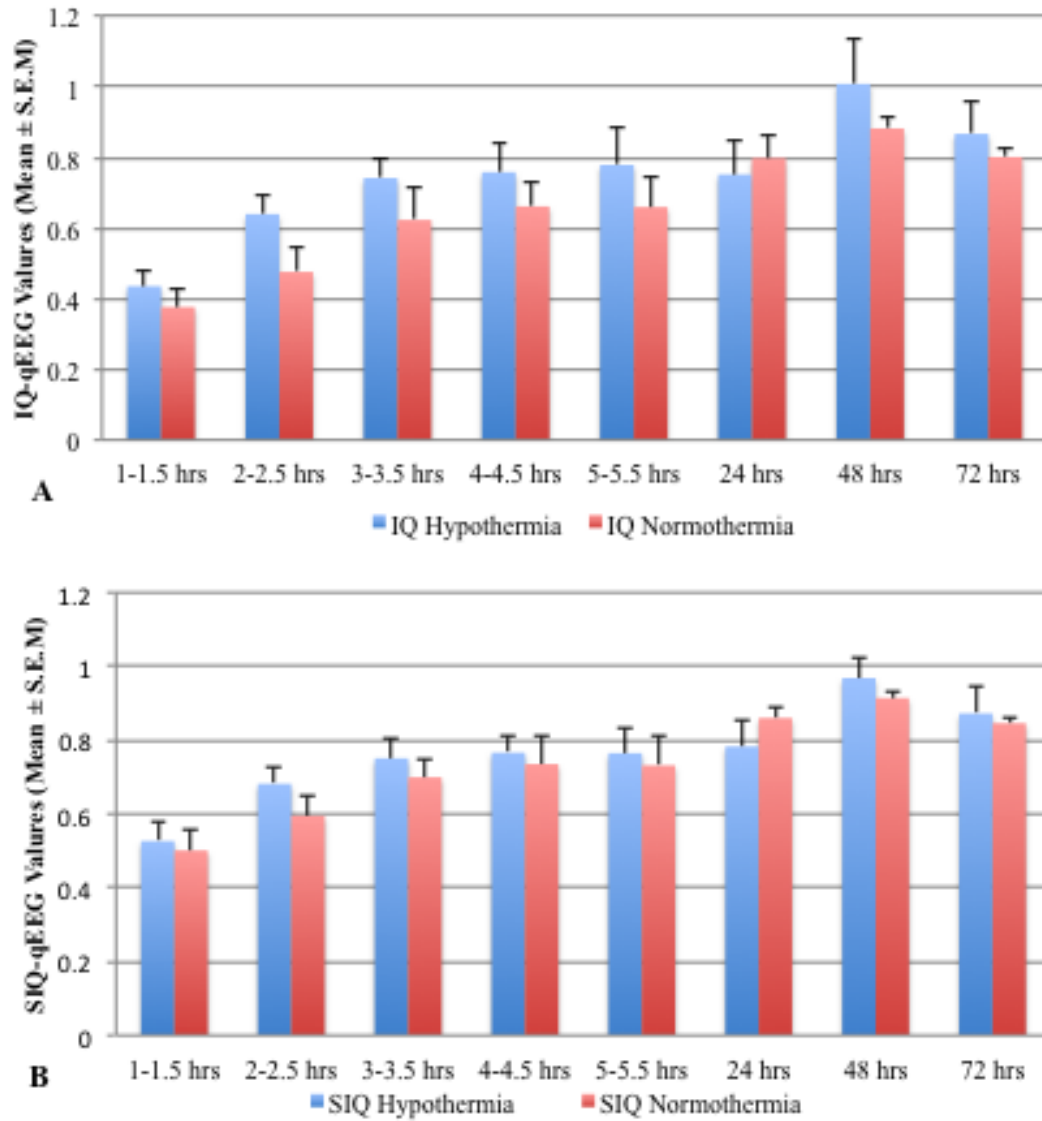


Figure 2. 6 Comparison of IQ and SIQ between A, hypothermia group and B, normothermia group at different time intervals: 1-1.5 hrs, 2-2.5 hrs, 3-3.5 hrs, 4-4.5 hrs, 5-5.5 hrs, 24 hrs, 48 hrs and 72 hrs.

2.4 Discussion

In this study, the electrophysiological recovery in severely injured post-CA brains was precisely tracked by entropy based-measures, IQ and SIQ. Both are able to accurately track the brain injury and recovery and predict the hypothermic effect on functional outcomes in the early time period after resuscitation when rats were still unresponsive.

IQ was previously introduced to quantify EEG signals and was validated by calculating the recovery of EEG entropy in both severe (79) and moderate injured brains (80) with therapeutic hypothermia. However, IQ only analyzes the gross EEG, and changes in each EEG frequency band may relate to the recovery of different brain functions. To study the cerebral changes in clinically important frequency bands, we developed a new quantitative measure, SIQ, by averaging the IQs in 5 frequency sub-bands (81). We previously found that a lower SIQ value is associated with greater injury and poor neurological outcome after CA (81). Here we applied both IQ and SIQ on the EEG of post-severe CA rats. Both IQ-qEEG and SIQ-qEEG markers were proven to be accurate predictors of 72-hr NDS and were notably higher in the good functional outcome group ($NDS \geq 60$) compared with the bad functional group ($NDS < 60$) as early as 1 hr after ROSC, while the animals still remain comatose.

Our previous study has shown that after moderate brain injury (7-min asphyxia-CA) both IQ (80) and SIQ (data not shown) accurately revealed the recovery of EEG and predicted functional outcome. Due to the high mortality rate (overall 5/14) in these post-resuscitation animals with severe brain injury, the current sample size has no power to detect the statistical difference of 72-hr NDS between the animals treated with hypothermia from the normothermia, despite the improved functional outcome from 15

hrs to 72 hrs in the hypothermia group. A similar lack of significant difference was also found in SIQ value. Interestingly, the aggregate IQ recovery after resuscitation was higher in the hypothermia group than the normothermia group in severely brain injured 9-min CA rats. When IQ was calculated, the coefficients of 6 decomposition were aggregated together to measure the distribution of the coefficients in the gross EEG, whereas the SIQ algorithm separately measured the entropy of coefficients in five different sub-bands of clinical interest and then average the results of five sub-bands to get the final SIQ value. In other words, the 6th sub-band (approximately 61-122Hz) was considered in IQ but not in SIQ. The frequency band of the 6th sub-band is identified as ripple, one of the HFOs (114, 115), which is highly associated with epileptogenesis (115, 116) and is linked to poor outcome after cardiac arrest (22, 52). The animals are more likely to generate HFOs after severe injury, resulting in the difference of prediction value between IQ and SIQ indicators. In the current study, we didn't employ continuous video recordings or other measures to show evidence of epilepsy or seizure. Further investigation is needed to investigate the sources of such HFO activity in post-CA severe brain injury.

The main focus of our study is to develop electrophysiological markers of brain injury and recovery with therapeutic hypothermia. Although the rewarming time is not our primary focus, it has been widely accepted that a slow rewarming period is beneficial. Our standard rewarming protocol was based on previous publications (117-119) such that a slow rewarming rate of 1 degree per half hour was selected, which is slow enough to preserve the benefit of hypothermia but more practical for manual temperature management. In our preliminary studies, rats with good or fair recovery spontaneously

rewarmed to normothermia in such a time frame. The designated rewarming speed was chosen to avoid additional anesthesia to cool down the animal for a slower rewarming speed. Though slower rewarming periods have been reported (120), Lu X et. al demonstrated that 1°C/hr did not alter the beneficial effect of hypothermia (121) that was shown at 0.5°C/hr. In our experiment, the actual rewarming rate of around 1.25°C/hr (34 °C at the end of hypothermia and rewarm to 36.5 °C in approximately two hours) was very close to 1°C/hr, which did not abolish the beneficial effect of therapeutic hypothermia. It has been demonstrated that our methods of manual temperature management with slow rewarming were efficient (77, 79-81, 122-124). However, the rat size is much smaller than piglets, dogs or human beings (120). In our studies, the rats usually rewarmed at the designated speed without additional manual cooling. In our rat asphyxia CA model, it's unclear whether a longer rewarming period would lead to a more beneficial effect after therapeutic hypothermia. Further studies are needed to elucidate the answer.

2.5 Conclusion

Our experiment demonstrated that HFO activities were particularly noticeable during the recovery from severe brain injury. While SIQ provides detailed sub-band EEG information related to the recovery of different brain functions, both early IQ and SIQ markers are able to accurately track recovery and predict the functional outcome from severe brain injury after CA. Development of an accurate early predictor for the recovery after ROSC from CA is the ultimate goal of neurologists and physicians. Our early qEEG markers, IQ and SIQ, are able to simplify the subjective and laborious interpretation of

EEG, which may bring new benefits to bedside cerebral monitoring if translated into clinical use.

CHAPTER 3 Early Quantitative Gamma-Band EEG Marker Predicts Outcomes after Cardiac Arrest and Target Temperature Management

3.1 Introduction

Cardiac arrest (CA) has a prevalence of approximately 424,000 cases annually in the United States (125). However, only 10.4% of out-of-hospital and 22.7% of in-hospital CA resulted in survival in 2014 (125) and surviving patients are susceptible to secondary neurological injuries. Minor fluctuations in temperature can severely affect ischemic cerebral pathological injury after CA (28). Therapeutic hypothermia and avoidance of fever have been demonstrated to improve neurological outcome and survival (2, 126-128).

Due to the limitations in detecting brain injury with standard clinical examination and structural imaging in comatose CA survivors, electroencephalography (EEG) has emerged as a widely used electrophysiological tool for prognostication (129, 130). EEG measures the sum of synchronous activity of neuronal ensembles with similar spatial orientation. Berger (131) first described alpha waves and demonstrated that EEG is characterized by different rhythms. Subsequently, a number of studies were performed to investigate the frequency content of EEG for clinical diagnostic applications. In clinical

practice, the EEG frequency bands of interests are defined as gamma (>30 Hz), beta (16-30 Hz), alpha (8-15 Hz), theta (4-8 Hz), and delta (below 4 Hz) (132). The neuronal oscillatory activities in each band represent coordinated activity (132) related to brain behavioral responses. The gamma-band, in particular, is associated with higher cortical functions such as learning, memory, perception, and consciousness (133, 134). Therefore, recovery of gamma-band activity is a pivotal target for post-CA research related to neurological recovery.

Analysis of EEG is laborious and confounded by subjective interpretation and manual pattern recognition. Quantitative EEG (qEEG) has shown promising results in studying brain injury and recovery after CA (79, 80). Based on information theory, the qEEG algorithm Information Quantity (IQ) was established in our previous studies (79) to provide an objective measure of the impact of temperature on neurological recovery after CA (80). However, IQ was only used to quantify changes in the gross EEG signal. Because changes in each EEG frequency band may relate to recovery of different brain functions, we developed the sub-band IQ (SIQ) algorithm (81). In our previous study, we quantified the information embedded in each EEG band by averaging the SIQ in 5 frequency sub-bands (referred to below as conventional SIQ) (81). We previously found that a lower conventional SIQ is associated with greater injury and poor neurological outcome after CA (81).

The recovery of SIQ in different EEG sub-bands after CA and the impact of temperature have not been elucidated. Because gamma-band activity is increased with higher cortical processes, we hypothesized that gamma-band SIQ would be strongly associated with functional outcome after CA. Second, we hypothesized that hypothermia

would be associated with better recovery of gamma-band SIQ compared to normothermia and hyperthermia.

3.2 Materials and Methods

3.2.1 Animals

We evaluated the effect of hypothermia ($33\pm 1^\circ\text{C}$), normothermia ($37\pm 0.5^\circ\text{C}$), and hyperthermia ($39\pm 0.5^\circ\text{C}$) in a rodent CA model. Twenty-four adult male Wistar rats (300–350 g, Charles River, Wilmington, MA) were randomly assigned to one of three groups: hypothermia, normothermia, or hyperthermia ($n=8$ per group). All animals underwent 7-min asphyxial CA and resuscitation followed by immediate temperature management during recovery in accordance with their assigned group. All rats had the free access to food and water, and were housed in a temperature-controlled environment with regular light/dark cycles during the whole experiment. All procedures were approved by The Johns Hopkins University Animal Care and Use Committee.

3.2.2 Cardiac Arrest and Temperature Management

The CA and resuscitation procedures were performed as previously described (77, 79, 80). Briefly, rats were intubated and ventilated with a pressure controlled ventilator. The animals were anesthetized with 1.0% halothane in 50%N₂/50%O₂ via the ventilator. The femoral artery and vein were cannulated to obtain sample arterial blood gases (ABG), continuously monitor blood pressure, and to deliver drugs. A 5-min EEG baseline

measurement with halothane was recorded, followed by a 5-min washout period without halothane to eliminate the effect of the anesthetic on the EEG recording (79). To induce paralysis, vecuronium (2mg/kg) was administered during the final 2 minutes of the washout period. Asphyxia was then induced by clamping the breathing circuit and stopping mechanical ventilation for 7 mins, thereby causing CA (pulse pressure <10mmHg). Cardiopulmonary resuscitation was performed with effective ventilation, external chest compression, epinephrine, and NaHCO₃, until return of spontaneous circulation (ROSC, pulse pressure >60mmHg).

Approximately 1 week before experiments, a telemetry temperature sensor (G2 Emitter 870-0010-01, Mini Mitter, Sun River, OR) was implanted into the peritoneal cavity to monitor the rat's core temperature. Temperature management (hypothermia or hyperthermia) was initiated immediately after ROSC and the target temperature was maintained for 6 hrs.

The hypothermia group was cooled to reach a target temperature of 33°C in 15 mins. Hypothermia was induced by a manual external cooling method using cold water and alcohol mist. The core temperature was maintained between 32-34°C for 6 hrs, after which the rewarming process began. The core temperature of the rat was gradually increased from 33°C to 37°C over 2 hours by a heating lamp and a heating pad (79, 80).

The core temperature of the normothermia group was maintained at 36.5–37.5°C for 8 hrs after ROSC. All animals were kept inside a neonatal incubator (Isolette infant incubator model C-86, Air-Shields, Hatboro, PA) for the first 24 hrs after ROSC to maintain a constant temperature after resuscitation (80).

The hyperthermia group was warmed to reach a target temperature of 39°C in 15 mins. Hyperthermia was induced by a heating pad and automatic heating lamp (Thermalet TH-5, model 6333, Physitemp Instruments, Clifton, NJ). The core temperature was maintained between 38.5-39.5°C for 6 hrs, after which the animal underwent passive cooling from 39°C to normothermia over the course of 2 hrs (80).

3.2.3 Sampling Method and SIQ-qEEG Analysis

Two-channel EEG signals were recorded via epidural screw electrodes at a sampling rate of 250 Hz (79, 80) for the first 8 hrs after ROSC for all temperature groups. At 24-, 48-, and 72-hrs after ROSC, serial 30-min EEG recordings were carried out in all animals. The noise in the signal was detected from WinDaq software (Dataq Instruments, Akron, OH) and MATLAB (MathWorks, Natick, MA) (80). Signals containing artifact were eliminated manually in the final analysis.

We computed the information content in each individual EEG frequency band using our previously established SIQ algorithm (81). Briefly, a sliding window technique was applied to the non-stationary EEG waveforms so that the waveform was divided into temporal windows representing the interval of raw EEG signals. Then, a discrete wavelet transform was used to separate the signal into sub-bands and compute the wavelet coefficients in each sub-band window. The probability functions of the wavelet coefficients were then separately estimated for each sub-band. The SIQ for each sub-band was then calculated using the probability functions and the entropy formula. Lastly, the SIQ values were averaged over all standard sub-bands of clinical interest, which was

defined as “conventional SIQ”. To compare SIQ among different groups, the SIQ values were normalized to their corresponding baseline values from the signal recorded before the initiation of CA. We calculated the SIQs from CA, every 30-min interval of raw EEG signals for the first 4 hrs, and then 24 hrs, 48 hrs and 72 hrs after ROSC.

3.2.4 Neurologic Evaluation

The neurological condition of each rat was evaluated by a Neurological Deficit Scale (NDS) score with a range of 0-80 and higher numbers representing better function. The score is based on a series of behavioral tests (79, 80). The NDS score of each animal was calculated after the recovery period on the day of CA and repeated at 24 hrs, 48 hrs and 72 hrs after ROSC. 72-hr NDS was a primary functional outcome in our study. We defined good functional outcome as rats with 72-hr NDS ≥ 60 and bad functional outcome as rats with 72-hr NDS < 60 (80).

3.2.5 Statistical Analysis

Statistical analyses were performed using a commercial statistical computer program (IBM SPSS Statistics, version 22, Armonk, NY). The parametric values of experimental groups were reported as mean \pm S.E.M. whereas nonparametric values were reported as median (interquartile range). “Aggregate SIQ” and “aggregate NDS” were defined as the SIQ values and NDS analyzed over the 72-hr study period, respectively. Univariate analyses were performed to test for differences in SIQ values and 72-hr NDS outcomes between temperature groups. Nonparametric analysis of variance was conducted to

determine the differences in NDS. The good electrophysiological outcome in each sub-band was predefined as a SIQ value greater than the mean SIQ in each temperature group at different time intervals. Bivariate analyses using the Pearson correlation were used to test for a correlation between 72-hr NDS and SIQ and the correlation between good or bad outcome using the recovery of 72-hr NDS and SIQ as defined above. A receiver operating characteristic (ROC) curve was used to identify the SIQ cutoff point with ideal sensitivity and specificity for good functional outcome (72-hr NDS \geq 60). A value of $p < 0.05$ was considered to be significant.

3.3 Results

3.3.1 Temperature Management and ABG Data

The core temperature was well controlled for all 24 rats. The three target temperatures - hypothermia ($33 \pm 1^\circ\text{C}$), normothermia ($37 \pm 0.5^\circ\text{C}$), and hyperthermia ($39 \pm 0.5^\circ\text{C}$) - were readily achieved and maintained as shown in Fig 3.1. There were no significant differences between the three groups in ABG data, including pH, PO_2 , PCO_2 bicarbonate, and O_2 saturation (data not shown).

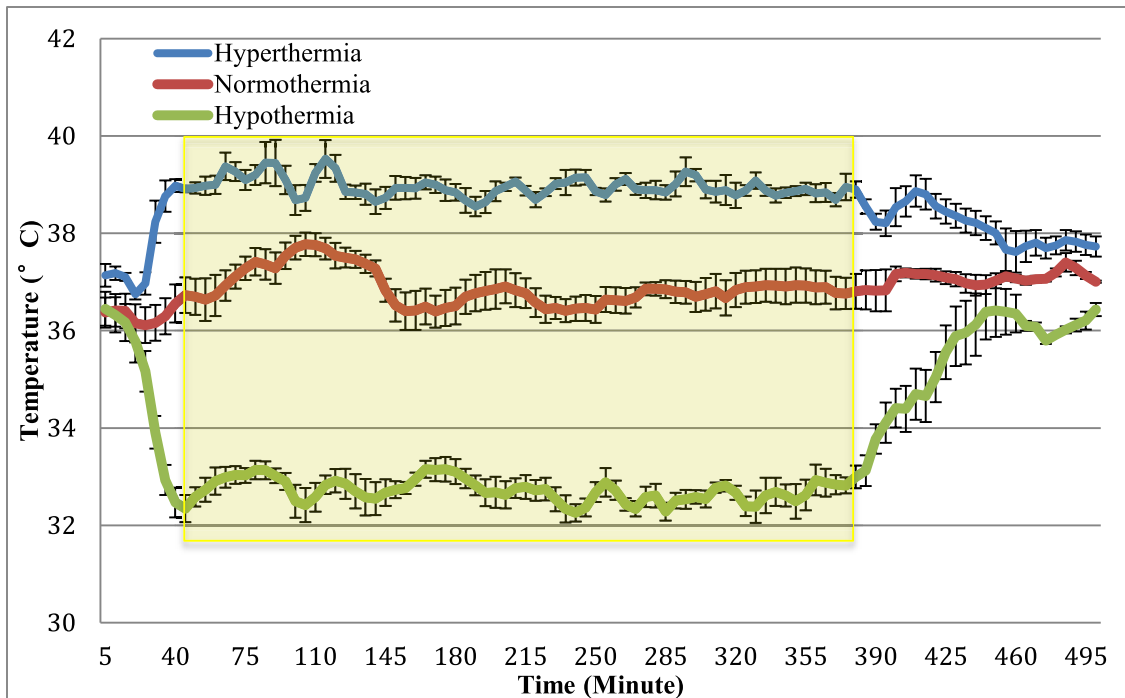


Figure 3. 1 The core temperature (mean±S.E.M.) was well controlled in all three temperature groups – hypothermia ($33\pm 1^{\circ}\text{C}$, blue), normothermia ($37\pm 0.5^{\circ}\text{C}$, red) and hyperthermia ($39\pm 0.5^{\circ}\text{C}$, green) – during the 6-hr temperature management period (highlighted).

3.3.2 Aggregate SIQ was Associated with Post-CA Functional Outcomes

We converted the raw EEG signal to SIQ values (Fig 3.2). There were significant differences in aggregate SIQ values between the three temperature groups ($p < 0.05$) (Table 3.1). Better recovery of aggregate conventional SIQ was found in the hypothermia group (0.80 ± 0.02) compared with the normothermia group (0.69 ± 0.02) ($p < 0.01$) and in the normothermia group compared with the hyperthermia group (0.66 ± 0.02) ($p < 0.05$). In

the analysis of SIQ in each sub-band, the aggregate SIQ in the gamma-band showed the same tendency as conventional SIQ. Higher aggregate SIQ values in the gamma-band were found in the hypothermia group (0.60 ± 0.03) compared with the normothermia group (0.40 ± 0.03) ($p<0.01$) and in the normothermia group compared with the hyperthermia group (0.34 ± 0.03) ($p<0.05$). The recovery of conventional SIQ and gamma-band SIQ were consistent with the aggregate NDS (median (25th, 75th)) such that the hypothermia group had a higher aggregate NDS (74 (61, 74)) than the normothermia group (49 (47, 61)) ($p<0.01$) and the normothermia group had a higher aggregate NDS compared to the hyperthermia group (43 (0, 50)) ($p<0.01$).

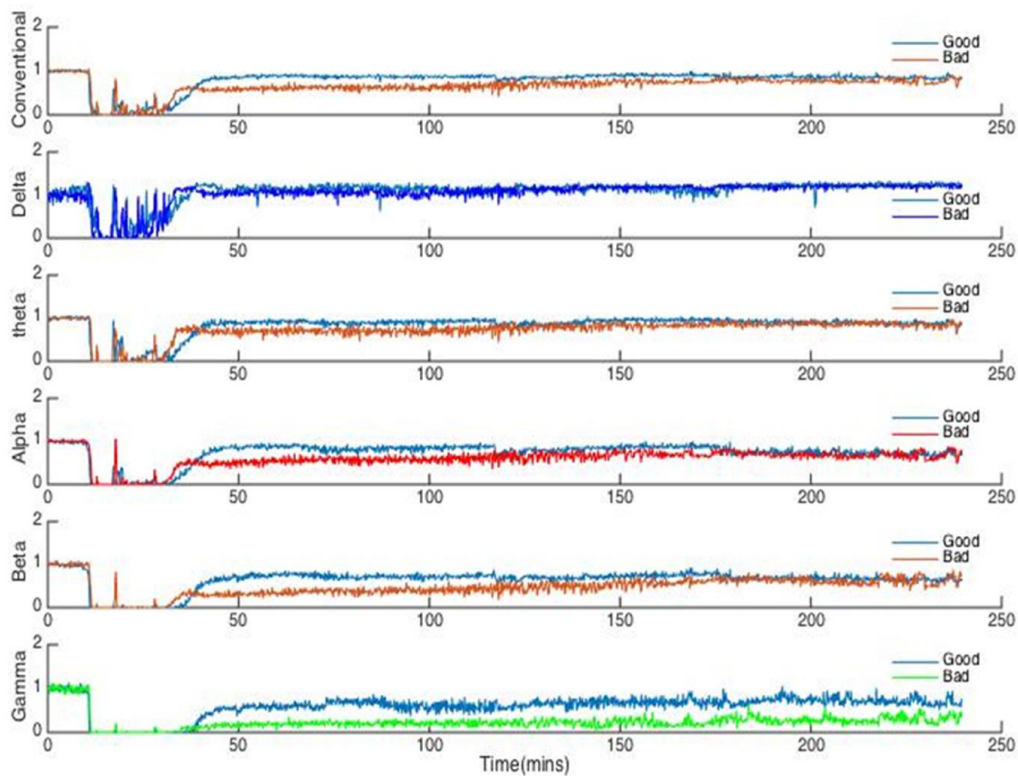


Figure 3. 2 Examples of sub-band information quantity (SIQ) plots from the good outcome and bad outcome groups. From top to bottom, the plots represent conventional

SIQ and SIQ of the sub-bands from lowest to highest frequency. Significant differences between the good and bad outcome groups were shown in the gamma band, whereas there were no differences in the delta band.

Table 3. 1 Aggregate SIQ (mean±S.E.M.) in temperature groups

Time after ROSC EEG Rhythm	Hypothermia	Normothermia	Hyperthermia
Conventional SIQ	0.80±0.02**	0.69±0.02 [†]	0.66±0.02 ^{§§}
Delta-band	1.06±0.02	1.08±0.03 [‡]	1.00±0.03 [§]
Theta-band	0.86±0.02**	0.76±0.02	0.77±0.03 ^{§§}
Alpha-band	0.79±0.02**	0.66±0.03	0.66±0.03 ^{§§}
Beta-band	0.70±0.02**	0.56±0.03	0.53±0.03 ^{§§}
Gamma-band	0.60±0.03**	0.40±0.03 [†]	0.34±0.03 ^{§§}

Hypothermia compared with normothermia, *p<0.05, **p<0.01

Normothermia compared with hyperthermia, [†]p<0.05, [‡]p<0.01

Hypothermia compared with hyperthermia, [§]p<0.05, ^{§§}p<0.01

3.3.3 Temporal Evolution of SIQ was Associated with Functional Outcomes in the Three Temperature Groups

There were significant differences in conventional SIQ (Fig 3.3A) and sub-band SIQ values except delta SIQ (Fig 3.3C) among the three temperature groups as early as 30 mins after ROSC (Table 3.2, $p < 0.05$), with the most significant differences in gamma SIQ (Fig 3.3B). Bivariate analyses showed no significant correlation between 72-hr NDS and SIQ value in the delta-band. However, significant correlations were found between the 72-hr NDS and conventional SIQ values, and SIQ values in all other sub-bands (Table 3.3) at 30 mins, 1 hr, 1.5 hrs, 2 hrs, and 2.5 hrs after ROSC. It should be noted that a significant correlation was found between 72-hr NDS and SIQ values at every time point between 30 mins and 72 hrs using the conventional SIQ, except at 4 hrs. The gamma-band SIQ showed a more robust significant correlation with 72-hr NDS at every time point after ROSC (30 mins, 0.555, $p < 0.05$; 1 hr, 0.599, $p < 0.01$; 1.5 hrs, 0.520, $p < 0.05$; then ranging 0.649-0.788 for the remaining time points, all $p < 0.01$) (Fig 3.4).

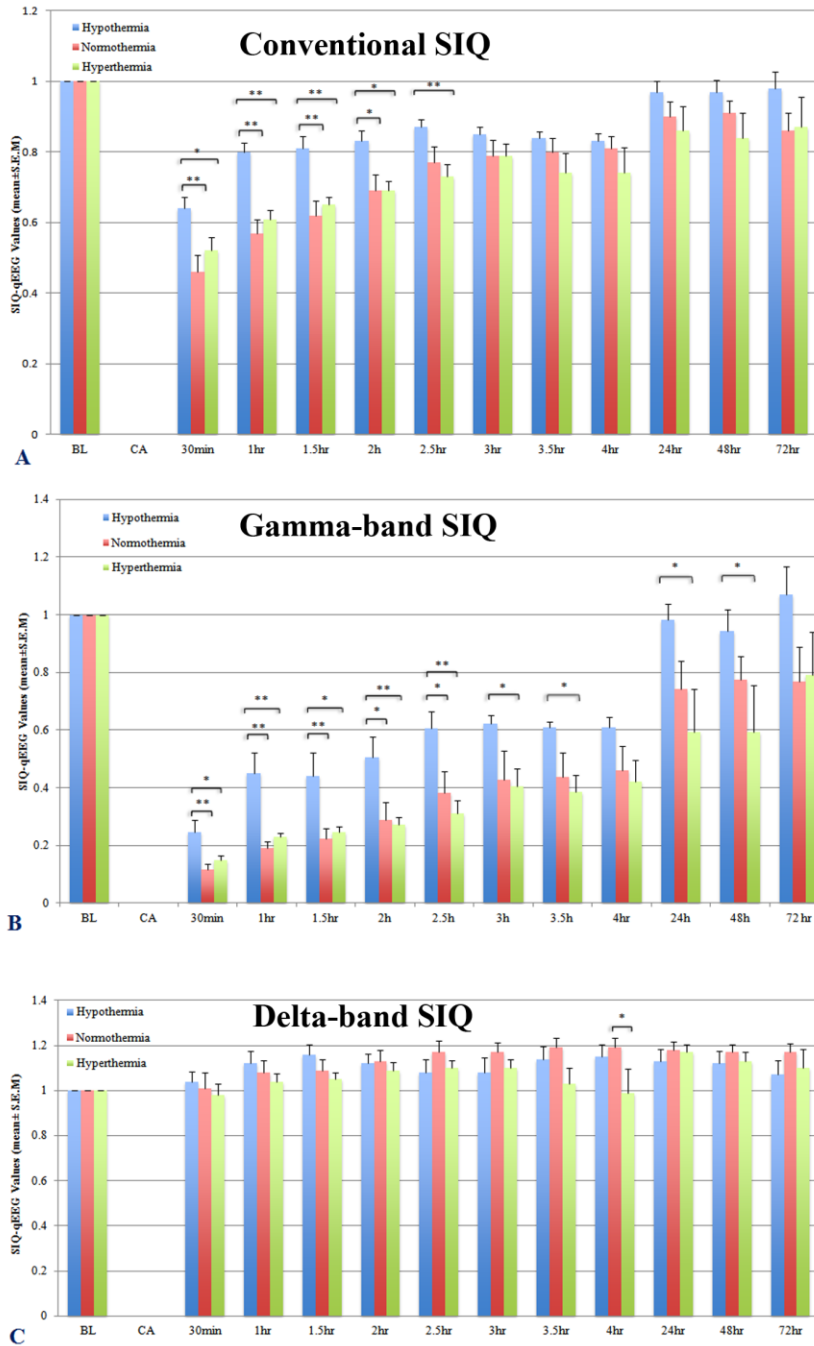


Figure 3. 3 The sub-band SIQ values in the three temperature groups at different time intervals. A, Conventional SIQ values of the hypothermia group were significantly higher than the other temperature groups from 30 mins to 2.5 hrs after ROSC. B, There were significant differences in gamma-band SIQ among the three groups at all time intervals

(30 mins, 1 hr, 1.5 hrs, 2 hrs, 2.5 hrs, 3 hrs, 3.5 hrs, 48 hrs and 72 hrs). C, In the delta sub-band, a significant difference in SIQ values between the normothermia and hyperthermia groups was seen only at 4 hrs after ROSC. * $p < 0.05$, ** $p < 0.01$.

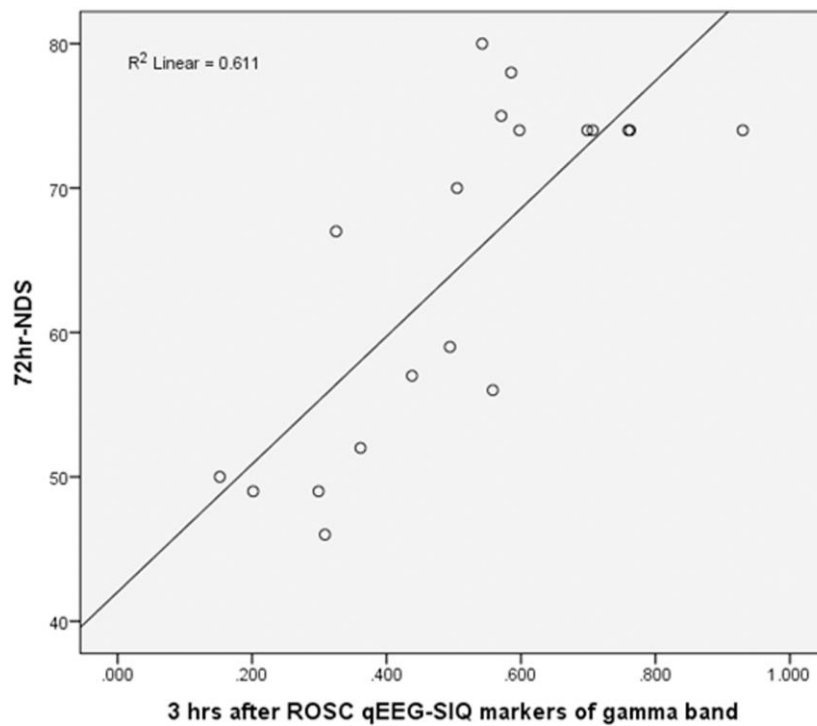


Figure 3. 4 Representative Pearson correlation (r value) plot between SIQ value and 72-hr NDS. The gamma-band SIQ most consistently correlated with 72-hr NDS from 30 mins until 72 hrs after ROSC among all sub-bands. As shown, the gamma-band SIQ at 3 hrs after ROSC had good correlation with 72-hr NDS (r value: 0.782, $p < 0.01$).

Table 3. 2 SIQ values (mean±S.E.M.) of temperature groups at different time intervals

EEG Rhythm	Time after ROSC						
	30 mins	1 hr	1.5 hrs	2 hrs	2.5 hrs	3 hrs	
Conventional	Hypothermia	0.64±0.03**	0.80±0.03**	0.81±0.03**	0.83±0.03*	0.87±0.02	0.85±0.02
	Normothermia	0.46±0.05	0.57±0.04	0.62±0.04	0.69±0.05	0.77±0.05	0.79±0.04
SIQ	Hyperthermia	0.52±0.04§	0.61±0.02§§	0.65±0.02§§	0.69±0.03§	0.73±0.04§§	0.79±0.03
	Hypothermia	1.04±0.04	1.12±0.06	1.16±0.05	1.12±0.04	1.08±0.06	1.08±0.07
Delta	Normothermia	1.01±0.07	1.08±0.05	1.09±0.05	1.13±0.05	1.17±0.05	1.17±0.04
	Hyperthermia	0.98±0.05	1.04±0.03	1.05±0.03	1.09±0.04	1.10±0.03	1.10±0.04
Theta	Hypothermia	0.78±0.03**	0.91±0.02**	0.92±0.02**	0.94±0.02*	0.96±0.02	0.93±0.03
	Normothermia	0.55±0.07	0.68±0.05	0.75±0.05	0.81±0.04	0.87±0.04	0.89±0.03
Alpha	Hyperthermia	0.65±0.05	0.75±0.03§§	0.79±0.03§	0.84±0.03§	0.87±0.03	0.93±0.03
	Hypothermia	0.65±0.04**	0.84±0.03**	0.85±0.03**	0.87±0.03**	0.92±0.03*	0.86±0.04
Beta	Normothermia	0.39±0.06	0.54±0.05	0.62±0.05	0.70±0.05	0.78±0.05	0.79±0.04
	Hyperthermia	0.49±0.05§	0.61±0.04§§	0.67±0.03§§	0.72±0.03§§	0.75±0.04§§	0.81±0.03
Gamma	Hypothermia	0.47±0.04**	0.67±0.04**	0.68±0.04**	0.73±0.05*	0.80±0.03	0.77±0.04
	Normothermia	0.24±0.05	0.36±0.04	0.44±0.05	0.54±0.07	0.65±0.07	0.67±0.06
Hyperthermia	Hypothermia	0.31±0.04§	0.42±0.03§§	0.47±0.03§§	0.54±0.04§	0.60±0.06§	0.69±0.05
	Normothermia	0.25±0.04**	0.45±0.07**	0.44±0.08**	0.51±0.07*	0.61±0.06*	0.62±0.03
Hyperthermia	Normothermia	0.12±0.02	0.19±0.02	0.22±0.04	0.29±0.06	0.38±0.07	0.43±0.10
	Hyperthermia	0.15±0.02§	0.23±0.02§§	0.25±0.02§	0.27±0.03§§	0.31±0.05§§	0.40±0.06§

Hypothermia compared with Normothermia, *p<0.05, **p<0.01

Normothermia compared with Hyperthermia, †p<0.05, ‡p<0.01

Hypothermia compared with Hyperthermia, §p<0.05, §§p<0.01

Table 3. 2 (cont.)

EEG Rhythm	Time after ROSC					
	3.5 hours	4 hours	24 hours	48 hours	72 hours	
Conventional	Hypothermia	0.84±0.02	0.83 ±0.02	0.97±0.03	0.97±0.03	0.98±0.05
	Normothermia	0.80±0.04	0.81±0.04	0.90±0.04	0.91±0.03	0.86±0.05
SIO	Hyperthermia	0.74±0.06	0.74±0.07	0.86±0.07	0.84±0.07	0.87±0.09
	Hypothermia	1.14±0.06	1.15±0.06	1.13±0.05	1.12±0.06	1.07±0.06
Delta	Normothermia	1.19±0.05	1.19±0.04 [†]	1.18±0.04	1.17±0.03	1.17±0.04
	Hyperthermia	1.03±0.07	0.99±0.11	1.17±0.03	1.13±0.04	1.10±0.09
Theta	Hypothermia	0.91±0.02	0.89±0.02	0.96±0.03	0.95±0.02	0.93±0.03
	Normothermia	0.89±0.03	0.89±0.03	0.90±0.03	0.94±0.02	0.87±0.03
Alpha	Hyperthermia	0.87±0.07	0.87±0.09	0.93±0.05	0.91±0.06	0.90±0.09
	Hypothermia	0.82±0.04	0.80±0.05	0.90±0.04	0.93±0.05	0.92±0.07
Beta	Normothermia	0.79±0.03	0.79±0.03	0.85±0.04	0.87±0.03	0.78±0.04
	Hyperthermia	0.75±0.06	0.75±0.07	0.85±0.07	0.83±0.07	0.79±0.11
Gamma	Hypothermia	0.73±0.03	0.72±0.04	0.88±0.04	0.90±0.07	0.92±0.08
	Normothermia	0.69±0.05	0.70±0.04	0.81±0.04	0.80±0.04	0.74±0.05
Hyperthermia	Hyperthermia	0.66±0.06	0.66±0.07	0.75±0.09	0.75±0.07	0.77±0.09
	Hypothermia	0.61±0.02	0.61±0.04	0.98±0.05	0.94±0.07	1.07±0.10
Hyperthermia	Normothermia	0.44±0.09	0.46±0.08	0.74±0.10	0.77±0.08	0.77±0.12
	Hyperthermia	0.39±0.06 [§]	0.42±0.08	0.59±0.15 [§]	0.59±0.16 [§]	0.79±0.15

Hypothermia compared with Normothermia, *p<0.05, **p<0.01

Normothermia compared with Hyperthermia, [†]p<0.05, [‡]p<0.01Hyperthermia compared with Hypothermia, [§]p<0.05, ^{§§}p<0.01

Table 3. 3 The correlation coefficient between SIQ values and 72-hr NDS scores

	30 min	1 hr	1.5 hrs	2 hrs	2.5 hrs	3 hrs
Conventional SIQ	0.657**	0.750**	0.686**	0.669**	0.640**	0.646**
Delta-band	0.196	0.154	0.294	0.007	-0.165	-0.187
Theta-band	0.648**	0.703**	0.664**	0.608**	0.472*	0.295
Alpha-band	0.710**	0.787**	0.739**	0.729**	0.646**	0.501*
Beta-band	0.696**	0.772**	0.699**	0.672**	0.649**	0.601**
Gamma-band	0.555*	0.599**	0.520*	0.649**	0.712**	0.782**

*p<0.05, **p<0.01

Table 3. 3 (cont.)

	3.5 hrs	4 hrs	24 hrs	48 hrs	72 hrs
Conventional SIQ	0.550*	0.437	0.643**	0.587**	0.656**
Delta-band	-0.006	0.053	-0.049	-0.137	-0.139
Theta-band	0.116	-0.041	0.471*	0.395	0.509*
Alpha-band	0.272	0.168	0.414	0.457*	0.589*
Beta-band	0.420	0.272	0.529*	0.504*	0.626**
Gamma-band	0.788**	0.667**	0.788**	0.655**	0.726**

*p<0.05, **p<0.01

3.3.4 Good Functional Outcomes were Associated with higher SIQ Values

By comparing the aggregate SIQ value (Fig. 3.5A), animals with good functional outcomes at 72 hrs had higher conventional SIQ values (0.80 ± 0.02) compared to animals with bad functional outcomes (0.65 ± 0.02) ($p<0.01$). Among the sub-bands, rats with good functional outcomes had significantly higher SIQ values compared to those with bad functional outcomes in the theta-band (0.86 ± 0.02 versus 0.75 ± 0.02 , $p<0.01$), alpha-band (0.78 ± 0.02 versus 0.64 ± 0.02 , $p<0.01$), beta-band (0.69 ± 0.02 versus 0.51 ± 0.02 , $p<0.01$), and gamma-band (0.59 ± 0.03 versus 0.32 ± 0.02 , $p<0.01$). However, there was no significant difference in the SIQ values of the delta-band.

By comparing the temporal evolution of SIQ values (Table 3.4), significant differences between animals with good and bad outcomes were seen in the high frequency bands (beta and gamma) from 30 mins to 72 hrs after ROSC except in the beta-band at 4 hrs, and in the intermediate frequency bands (theta and alpha) from 30 mins to 2.5 hrs after ROSC, with the alpha rhythm also showing significant differences at 3 hrs, 48 hrs and 72 hrs. Gamma-band SIQ (Fig 3.5C) and conventional SIQ (Fig 3.5B) most consistently discriminated between animals with good and bad functional outcomes at all time points from 30 mins to 72 hrs after ROSC. Conversely, the delta-band poorly discriminated between animals with good and bad outcomes at most time points after ROSC (except at 1.5 hrs) (Fig 3.5D).

To study the relation between good electrophysiological recovery (defined as $SIQ \geq \text{mean SIQ}$) and good functional outcome ($72\text{-hr NDS} \geq 60$), electrophysiological

recovery was strongly correlated with good functional outcome starting from 30 mins after ROSC (Table. 3.5). The conventional SIQ recovery showed significant correlation with functional outcome at 1 hr, and 2 hrs to 72 hrs, with no significant correlation at 0.5 and 1.5 hrs. The gamma-band had the strongest correlation with functional outcome as significant correlation coefficients were identified from 30 mins to 72 hrs, while the delta-band had no correlation with functional outcome.

3.3.5 Predictive Value of SIQ-qEEG Values

Receiver operation characteristic (ROC) curves were used to identify the SIQ cut-points at different intervals with optimal sensitivity and specificity for predicting good functional outcome at 72 hrs. The optimal SIQ cut-points were defined by an area under the ROC curve >0.8 and the highest specificity (100%) among all EEG sub-bands except delta. As shown in Table 3.6, the cut-points with highest sensitivity of 0.909 appeared in conventional SIQ at 1-hr and in the alpha-band at 1.5-hr post-ROSC. However, among conventional SIQ and all sub-bands, the most consistently predictive cut-points (from 30 min throughout 4 hrs and then daily until 72-hr) occurred in the gamma-band (from sensitivity of 0.273 at 30-min to 0.600 at 72-hr after ROSC). The most accurate gamma-band cut-point was at 2 hrs after ROSC, where the $SIQ > 0.39$ had sensitivity of 0.727 and specificity of 100% for prediction of good functional outcome (Fig 3.6).

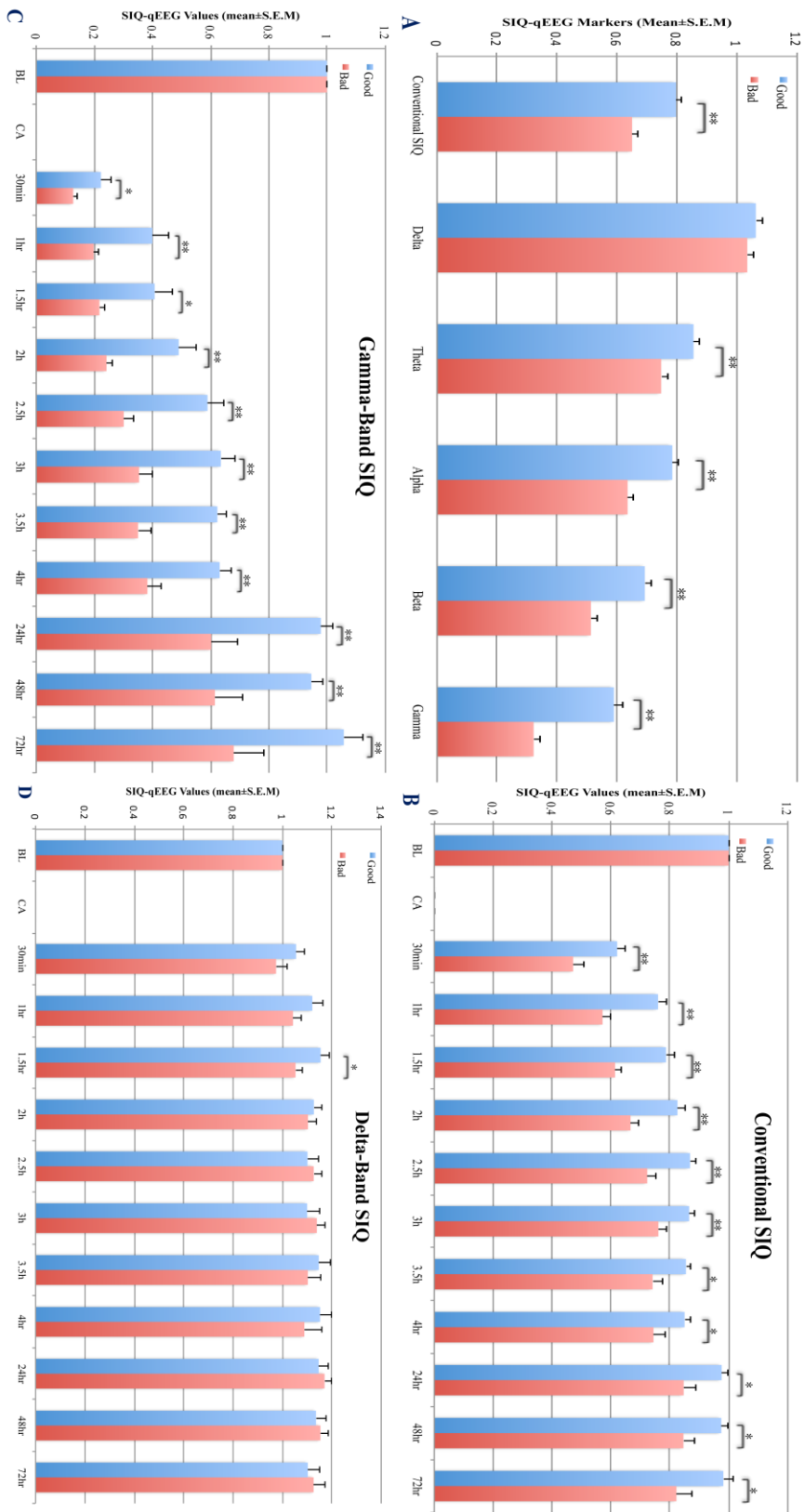


Figure 3. 5 The comparison of SIQ-qEEG values (mean ± S.E.M.) between the good functional outcome group (72-hr NDS ≥ 60) and bad functional outcome group (NDS < 60). A, Aggregate SIQ demonstrated significant differences, except in the delta-band, in conventional SIQ (good/bad: 0.80 ± 0.02 / 0.65 ± 0.02, p < 0.01), theta (0.86 ± 0.02 / 0.75 ± 0.02, p < 0.01), alpha (0.78 ± 0.02 / 0.64 ± 0.01),

p<0.01), beta (0.69±0.021/0.51±0.019, p<0.01), and gamma (0.59±0.028/0.32±0.019, p<0.01). B and C, Significant differences in conventional SIQ and gamma-band SIQ between the outcome groups were shown continuously from 30 mins to 72 hrs after ROSC. D, The delta-band SIQ showed poor discrimination between the outcome groups at most time intervals. *p<0.05, **p<0.01.

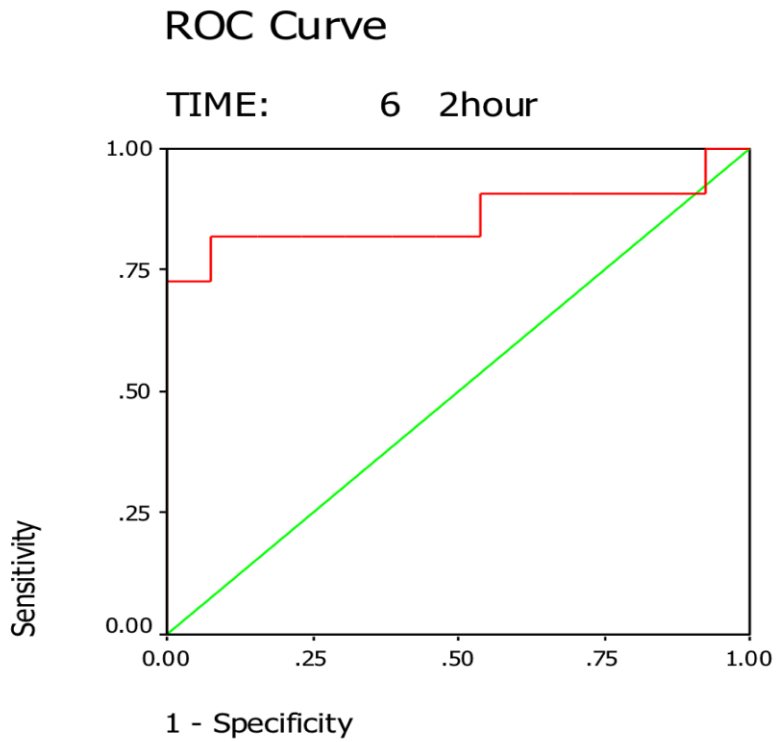


Figure 3. 6 Receiver operation characteristic (ROC) curves were used to identify the optimal SIQ cut-points with area under the ROC curve >0.8 and highest specificity for good outcome. The cut-point for gamma-band SIQ >0.39 at 2 hrs after ROSC had a sensitivity of 0.727 and specificity of 1 with an area under ROC curve of 0.86 (shown).

Table 3. 4 SIQ values (mean±S.E.M.) of functional outcome condition groups at different time intervals

EEG Rhythm	Time after ROSC					
	30 mins	1 hour	1.5 hours	2 hours	2.5 hours	3 hours
Conventional	Good 0.62±0.03**	0.76±0.03**	0.79±0.03**	0.83±0.03**	0.87±0.02**	0.87±0.02**
SIQ	Bad 0.47±0.03	0.57±0.03	0.61±0.02	0.67±0.03	0.72±0.03	0.76±0.03
	Good 1.05±0.04	1.12±0.04	1.15±0.04*	1.13±0.03	1.10±0.05	1.10±0.05
Delta	Bad 0.97±0.05	1.04±0.03	1.05±0.03	1.10±0.03	1.13±0.03	1.14±0.03
	Good 0.76±0.03**	0.88±0.02**	0.91±0.02**	0.93±0.02**	0.96±0.01**	0.94±0.02
Theta	Bad 0.58±0.05	0.70±0.03	0.75±0.03	0.81±0.03	0.86±0.03	0.89±0.03
	Good 0.63±0.04**	0.79±0.04**	0.82±0.03**	0.86±0.02**	0.90±0.02**	0.87±0.03*
Alpha	Bad 0.42±0.05	0.55±0.04	0.62±0.03	0.68±0.03	0.74±0.03	0.77±0.03
	Good 0.44±0.04**	0.61±0.04**	0.65±0.04**	0.72±0.04**	0.79±0.03**	0.79±0.03*
Beta	Bad 0.26±0.03	0.37±0.03	0.43±0.03	0.50±0.03	0.59±0.04	0.65±0.04
	Good 0.22±0.03*	0.40±0.06**	0.41±0.06*	0.49±0.06**	0.59±0.06**	0.63±0.05**
Gamma	Bad 0.13±0.02	0.20±0.02	0.22±0.02	0.24±0.02	0.30±0.03	0.35±0.05

Good Condition compared with Bad Condition, *p<0.05, **p<0.01

Table 3. 4 (cont.)

EEG Rhythm		Time after ROSC				
		3.5 hours	4 hours	24 hours	48 hours	72 hours
Conventional	Good	0.86±0.02*	0.85±0.02*	0.98±0.02*	0.98±0.02*	0.98±0.03*
SIQ	Bad	0.74±0.04	0.74±0.04	0.85±0.04	0.85±0.04	0.82±0.05
Delta	Good	1.15±0.05	1.15±0.05	1.15±0.04	1.14±0.04	1.10±0.05
	Bad	1.10±0.05	1.09±0.07	1.17±0.03	1.15±0.03	1.13±0.05
Theta	Good	0.92±0.02	0.91±0.02	0.96±0.02	0.96±0.02	0.94±0.02
	Bad	0.86±0.04	0.86±0.05	0.89±0.03	0.90±0.03	0.86±0.05
Alpha	Good	0.83±0.03	0.82±0.04	0.91±0.03	0.94±0.04*	0.91±0.05*
	Bad	0.75±0.04	0.74±0.04	0.82±0.04	0.82±0.04	0.75±0.05
Beta	Good	0.75±0.03*	0.74±0.03	0.89±0.03*	0.90±0.05*	0.90±0.05*
	Bad	0.64±0.04	0.65±0.04	0.75±0.05	0.74±0.04	0.70±0.05
Gamma	Good	0.62±0.03**	0.63±0.04**	0.98±0.04**	0.95±0.05**	1.06±0.07**
	Bad	0.35±0.04	0.38±0.05	0.60±0.09	0.61±0.09	0.68±0.10

Good Condition compared with Bad Condition, *p<0.05, **p<0.01

Table 3. 5 The correlation coefficient between good electrophysiological outcome and good functional outcome

	30 mins	1 hr	1.5 hours	2 hours	2.5 hours	3 hours
Conventional SIQ	0.367	0.832**	0.330	0.585**	0.608**	0.497*
Delta-band	0.194	0.251	0.084	-0.161	-0.161	-0.071
Theta-band	0.540**	0.678**	0.324	0.678**	0.438*	0.251
Alpha-band	0.438*	0.678**	0.151	0.678**	0.753**	0.497*
Beta-band	0.438*	0.749**	0.151	0.585**	0.608**	0.585**
Gamma-band	0.497*	0.669**	0.486*	0.664**	0.749**	0.678**

*p<0.05, **p<0.01

Table 3. 5 (cont.)

	3.5 hours	4 hours	24 hours	48 hours	72 hours
Conventional SIQ	0.510*	0.510*	0.678**	0.678**	0.489*
Delta-band	0.007	0.007	0.071	0.084	0.214
Theta-band	0.269	0.084	0.585**	0.678**	0.489*
Alpha-band	0.175	0.329	0.497*	0.497*	0.555**
Beta-band	0.438*	0.418*	0.497*	0.497*	0.555**
Gamma-band	0.678**	0.678**	0.678**	0.585**	0.592**

*p<0.05, **p<0.01

Table 3. 6 SIQ cut-points (sensitivity) with highest specificity (100%) and area under ROC curve >0.8

	30 mins	1 hr	1.5 hrs	2 hrs	2.5 hrs	3 hrs	3.5 hrs	4 hrs	24 hrs	48 hrs	72 hrs
Conventional	0.66 (0.273)	0.67 (0.909)	0.73 (0.818)	0.80 (0.727)	0.87 (0.545)	0.93 (0.182)	0.88 (0.364)	None	1.10 (0.091)	1.02 (0.364)	0.96 (0.700)
SIQ											
Delta-band	None	None	None	None	None	None	None	None	None	None	None
Theta-band	0.80 (0.273)	0.90 (0.545)	0.95 (0.273)	0.96 (0.455)	2.03 (0)	None	None	None	None	None	None
Alpha-band	0.65 (0.364)	0.71 (0.818)	0.76 (0.909)	0.81 (0.727)	0.85 (0.727)	None	None	None	None	None	None
Beta-band	0.47 (0.455)	0.52 (0.818)	0.58 (0.818)	0.70 (0.545)	0.86 (0.364)	0.94 (0.182)	None	None	None	None	0.95 (0.400)
Gamma-band	0.24 (0.273)	0.32 (0.636)	0.35 (0.636)	0.39 (0.727)	0.55 (0.545)	0.68 (0.455)	0.61 (0.545)	0.73 (0.273)	1.11 (0.182)	0.98 (0.455)	1.00 (0.600)

None: There were no cut-points with the area under ROC curve > 0.8

3.4 Discussion

In this study, recovery of SIQ-qEEG signal was associated with better functional outcomes after resuscitation from CA and targeted temperature management led to sustained improvement of SIQ values soon after ROSC. The gamma-band had the strongest and most consistent association with outcome and temperature management compared to the other EEG sub-bands. Conversely, the delta-band represented a more constant component of EEG signal and showed no consistent association with outcome or temperature management.

IQ was introduced in our prior studies to quantify EEG signal as a means of simplifying the interpretation of EEG and measuring recovery of EEG entropy (79). IQ only evaluates the information of the gross EEG without sub-band information, however. As shown in this experiment, EEG can be decomposed into different frequency sub-bands: gamma (above 30 Hz), beta (16-30 Hz), alpha (8-15 Hz), theta (4-8 Hz), and delta (below 4 Hz). The SIQ algorithm allows additional sub-band analysis to identify the most relevant sub-bands of EEG during brain recovery after CA.

The high frequency EEG signal classified into beta, and gamma frequency sub-bands are predominantly generated and synchronized by cortical mechanisms, whereas subcortical structures are responsible for the generation and synchronization of low-frequency delta-, theta- and alpha-band EEG (135). In our SIQ EEG analysis, the best recovery was in the hypothermia group in all EEG frequency sub-bands. Therapeutic hypothermia has been recommended as an effective treatment of brain injury after CA (3, 61, 125) and has been validated to improve neurological recovery and reduce ischemic neuronal injury after CA (136-138), consistent with our results.

The present study, for the first time, confirmed our hypothesis that the gamma-band makes the greatest contribution to the prognostic value of SIQ after CA. Recovery of the gamma-band SIQ was a robust, early, and consistent electrophysiological marker of better functional recovery. The association between gamma-band SIQ and outcome was stronger than conventional SIQ. This result was not surprising because gamma frequencies are considered to be an indicator of engaged intracortical networks necessary for recovery of higher order neurological processes (139). Gamma power increases with sensory stimulus (140-142), cognitive processing (143), and lexical processing (144), for example. In the cerebral cortex, gamma-band activity is increased during memory tasks, learning (145), and other advanced functional behaviors (146-148).

Significantly higher gamma-band SIQ was found in the hypothermia group than in the normothermia and hyperthermia groups. The most notable differences occurred within the first 2 hrs after ROSC when the rats remained unresponsive and neurological deficits may be obscured. Gamma-band SIQ was also strongly associated with 72-hr NDS as early as 30 mins after ROSC and was significantly higher in the good functional outcome group than the bad functional outcome group throughout the 72 hrs after ROSC. The optimal cut-points were determined by constructing ROC curves for prediction of 72-hr functional outcome. For gamma-band SIQ, a value >0.39 had exceptional sensitivity of 0.727 and specificity of 100% at 2-hr post-ROSC for prediction of good functional outcome. Similarly accurate cut-points were also found at each time point from 1 hr to 3.5 hrs.

The mechanism of alterations of gamma-band activity after CA has not been fully elucidated. Gamma frequencies are generated and synchronized by the interaction of two

neurotransmitters: gamma-aminobutyric acid (GABA), an inhibitory neurotransmitter in the mammalian nervous system, and glutamate (149, 150). Glutamate concentration is increased in the ischemic brain (151, 152), which may result in reduction of cerebral metabolism and energy consumption as a means of neuroprotection. This mechanism will prioritize energy usage for active glutamate removal to prevent excitotoxicity (153).

Hyperthermia further increases the concentration of glutamate (154), leading to excessive glutamate activity (155) and simultaneously decreases transmission of GABA (156), amplifying glutamate excitotoxicity. This mechanism may decrease high frequency EEG activity, resulting in the loss of the gamma-band in hyperthermic animals destined for poor functional recovery. Conversely, hypothermia reduces glutamate-mediated neuroexcitation and suppresses downstream secondary injuries induced by CA (3, 152, 157, 158). In this study, hypothermia mainly improved recovery of high frequency rhythms, especially in the gamma-band, which was associated with better functional outcome after CA.

We also evaluated the prognostic value of delta-band EEG and found that the delta rhythm showed poor ability to predict neurologic outcome and was not as sensitive to the temperature intervention as other sub-bands. During global ischemia, high frequency EEG rhythms are quickly suppressed and lower frequencies predominate until EEG signal is fully suppressed (159-161). After ROSC, there is early recovery of low frequency EEG signal followed by higher frequencies (162). During coma, low frequency EEG is produced by hyperpolarization of cortical neuronal membrane potentials with the absence of spontaneous synaptic potentials (163). Our studies indicate that, after ROSC, waves of low frequency bands gradually return prior to emergence from coma. Because

the delta frequency band predominates during coma, recovery of delta-band SIQ had little prognostic value. Therefore, the delta-band appears to be a constant component of EEG signal. These results confirmed our earlier findings that delta frequencies made little contribution to the prognostic value of conventional SIQ (81) or IQ (79, 80) after CA with post-resuscitation temperature management.

In the current study, we evaluated neurological outcomes with the NDS, which is heavily weighted to basic motor functions and coordination rather than more complex tasks. Because gamma-band EEG frequencies are produced during higher cognitive processes, future studies will measure the association of gamma-band recovery with more complex behaviors, such as learning and memory, after CA. These studies will help to investigate the role of gamma activity in neurological recovery in CA survivors treated with targeted temperature management.

3.5 Conclusion

This study demonstrated that temperature management had significant effects on recovery of EEG activity in different sub-bands, especially in the gamma-band. The rate of recovery of gamma-band SIQ was strongly associated with functional outcomes. This association was detectable soon after ROSC and was consistent throughout the recovery period. If translated into clinical practice, these experiments may bring new insights into real-time bedside neuromonitoring and prognostication after CA. Because EEG can be readily obtained from humans and is part of the standard clinical assessment of CA survivors, the ultimate goal of the project is to develop an accurate bedside prognostic

marker for neurological recovery based on gamma-band SIQ.

CHAPTER 4 Effects of Transcranial Direct Current Stimulation on Somatosensory Evoked Potentials in Uninjured Rats

4.1 Introduction

The transcranial direct current stimulation (tDCS), an noninvasive, safe and painless intervention with weak direct currents, is able to modulate and change cortical excitability validated from animal (164) or clinical (165-167) experiments. Compared to other transcranial stimulation techniques, such as transcranial magnetic stimulation (168) or transcranial electrical stimulation (169), the advantages of tDCS, i.e. low-tech and portable, make it one of the more commonly used methods in clinical practice (170). Although the exact mechanism of tDCS on excitability has not been elucidated, the application of tDCS was recommended as an therapeutic method for neurological and psychiatric disorders resulted from abnormalities of excitability, such as depressive illness, manic, chronic stroke and epilepsy (171-176).

tDCS has been regarded as a neuromodulatory technique to improve motor learning and motor coordination (177, 178) by changing the polarity of the resting membrane potential (179, 180) rather than directly inducing or inhibiting action potentials (181). It has been shown that the effect of tDCS on the modulation of membrane polarization in the human motor cortex depends on the current polarity. The after-effect of tDCS was monitored by the amplitude of motor evoked potentials (MEPs), which was increased by

anodal stimulation and decreased by cathodal stimulation in humans (165, 166, 178) and in animals (182, 183). Current duration is another parameter that describes the after-effects of tDCS. Longer stimulation duration resulted in increasing duration of after-effects for both humans (165-167) and animals (164) under the same stimulus intensity. Also, the potency of tDCS to induce the modulation of membrane potential was determined by the current intensity. Previous studies indicated that the stronger effects on performance by tDCS were achieved by larger current intensities (166, 184). However, the application of tDCS not only affects MEPs but also induces long-lasting variations of visual evoked potentials (VEPs) (185, 186). These studies reported conflicting findings, but it was found that the polarization of tDCS on the visual cortex facilitated or diminished the after-effects.

Some studies has found that tDCS has the ability of modifying the electrical activities in somatosensory cortex detected by somatosensory evoked potential in healthy volunteers, although their results are inconsistent (187, 188). Furthermore, Some pharmacological studies showed that Dextromethorphan, an N-methyl-D-aspartate (NMDA) receptor antagonist, was able to significantly diminish the effects of anodal and cathodal tDCS (189, 190). Interestingly, flunarizine, a calcium channel blocker, was also shown to decrease the changes in excitability of both anodal and cathodal tDCS (190). These findings suggest that the alterations of cortical excitability by tDCS depend on NMDA receptors, determined by glutamatergic synaptic plasticity, and calcium channels. Since the most important pathological mechanism of central nervous system (CNS) disorders, such as stroke or nervous system trauma, is related to glutamate excitotoxicity followed by the increase of calcium influx, tDCS can be regarded as a potential neuroprotective

method to preserve brain functions.

tDCS has been proved to induce the alteration of cortical excitability of the motor cortex (165, 166). However, it has not been elucidated whether the effect of tDCS on excitability observed in the motor cortex is also typical of other cortices. Some studies demonstrated that the modulation of sensorimotor cortical excitability is useful to relieve chronic pain or movement disorder (191). Furthermore, somatosensory pathway has been commonly used to assess the functional integrity of thalamocortical pathway and been one of the most robust and accurate neurophysiologic and prognostic parameters for brain monitoring after CNS injuries in clinical condition (90). Therefore, a study of the somatosensory cortical response, represented by SSEPs, to tDCS is necessary. Before tDCS can be used over somatosensory cortex to treat neurologic disorders, there is a strong need to study the effect of tDCS on healthy brains. Due to the effect of tDCS on the modulation of membrane polarization depending on the current polarity monitored by motor evoked potentials (165, 166, 178, 182, 183), we applied the anodal and cathodal stimulation on uninjured rats' somatosensory cortices, analyzed the peak-to-peak amplitude and duration of N10/P15, and the latency of N10, equivalent to N20 in humans, and compared these characteristics of SSEPs before and after stimulus to evaluate the tDCS' effects on the change of local cortex excitability. We hypothesized that anodal tDCS would facilitate the somatosensory cortical activities, whereas cathodal tDCS would have an opposite effect.

4.2 Materials and Methods

4.2.1 Animals

We evaluated the effect of anodal and cathodal tDCS on SSEPs in an uninjured rat model. A total of 12 adult female Wistar rats (300-350g, Charles River, Wilmington, MA) were given anodal and cathodal stimulation separately. This experimental model of tDCS was modified from the previous study of Liebetanz et.al in 2006 (183). All the experimental procedures were approved by Johns Hopkins University Animal Care and Use Committee.

4.2.2 Transcranial Direct Current Stimulation

Cathodal and anodal tDCS were applied by using a constant current stimulator (Model 2400, Keithley Instruments Inc., Cleveland, OH) to provide the continuous application of low currents in the rats. To mimic the setup in the clinical studies on humans and study the effect of tDCS on SSEPs, the current stimulations were transcranially applied on the primary somatosensory cortex (S1) of the animals. A plastic tube, which held the stimulation electrode, was positioned on the cranium over the right sensory cortex (1 mm posterior to the bregma and 3 mm right to the midline). To establish a defined contact area and a consistent position for stimulation, the tube was fixed by carboxylate dental cement (Durelon Carboxylate Cement, 3M, ESPE, St. Paul, MN) one week prior to the first day of recording SSEP after tDCS. Two adhesive electrodes were placed onto the ventral thorax of the anaesthetized rat and served as counterelectrodes. To ensure good conductivity, the tube was filled with saline solution (0.9% NaCl) for a contact area of 3.5 mm² on the skull.

A plate electrode with a contact area of 4 cm² was placed as a reference electrode onto the ventral thorax of the rat and the contact area was shaved followed by application of electrode gel (Parker Laboratories, Inc., Fairfield, NJ) before stimulation. Cathodal and anodal tDCS were applied by a constant current stimulator (Model 2400, Keithley Instruments Inc., Cleveland, OH) at a low current intensity of 100µA for 30 mins. In all experimental procedures, the animals were anesthetized by a tight-fitting facemask with 1.0% isoflurane in 50%N₂/50%O₂ via an anesthesia vaporizer (Penlon Sigma Delta, Penlon LTd., Abingdon, Oxon, UK). To prevent the interaction of cathodal and anodal stimulation, the sequence of anode or cathodal tDCS was randomized alternated on every other day.

4.2.3 SSEPs Recording and Stimulation

One week prior to stimulation under anesthesia with 2-3% isoflurane, the rats were implanted with 5 epidural screw electrodes (Plastics One, Roanoke, VA) and the plastic tube for tDCS to record the bipolar SSEPs from both cerebral hemispheres. Four recording electrodes were placed over primary somatosensory cortices near regions representing forelimbs (1 mm posterior and ± 4 mm lateral to bregma) and hindlimbs (2 mm posterior and ± 1.5 mm lateral to bregma), and a ground electrode over the right frontal lobe, as previously described (90, 192). The depth of electrode implantation was to light contact with dura matter rather than penetration into brain. Electrodes and wires, the plastic tube and the exposed skull were fixed together by carboxylate dental cement (Durelon Carboxylate Cement, 3M, ESPE, St. Paul, MN). The core temperature of the rats was maintained at normothermia (36.5–37.5°C) by using a temperature monitoring

system (Mon-a-Therm 6510, Mallinckrodt Medical Inc, St Louis, MO).

SSEP signals were recorded using Tucker Davis Technologies (TDT, Alachua, FL) data acquisition systems and software. Median nerves were stimulated through the insertion of two pairs of needle electrodes into the distal forelimbs with the application of direct current stimulation - pulse duration of 200 μ s, 6 mA, and frequency of 0.5 Hz. Signals were sampled at a frequency of 6.1 kHz. For both anodal and cathodal stimulations, baseline SSEP signals were recorded for 15 min under 1.5% isoflurane, followed by tDCS. Continuous SSEP recordings 30-minutes in duration were taken immediately after the stimulation.

4.2.4 SSEPs Signal Analysis

The forelimbs of the rats were stimulated at a frequency of 0.5 Hz alternatively, and SSEPs were recorded over the somatosensory cortex contralateral to the median-nerve stimulation. The short-latency SSEPs between 5 ms and 20 ms were used for processing. Signals were analyzed using an automated peak detection algorithm to determine the initial significant negative potential related to N10 (negative potential at the latency of 10 ms), equivalent to N20 in humans (90) and the significant positive potential related to P15 (positive potential at the latency of 15 ms). The peak-to-peak amplitudes were calculated as the difference between N10 and P15 after stimulation. Latencies were determined as the appearance of N10 with reference to stimulus time, and duration was measured as the period between N10 and P15. During the final analysis, signals containing artifact were eliminated manually and normalized to the corresponding baseline signal recorded prior to

the tDCS. Aggregate SSEPs analyzed the whole 30-min recording period (900 sweeps). To investigate the temporal evolution of SSEPs, every 300 sweeps (10-min time window) were averaged together, defining the time intervals as 10 mins, 20 mins and 30 mins, to determine the peak-to-peak amplitude, latency and duration of SSEPs.

4.2.5 Statistical Analysis

All the statistical analyses were performed using IBM SPSS Statistics 22 software (IBM, Armonk, NY). All data in this study were parametric data reported as mean \pm S.E.M. Independent-samples t-tests were used to test the changes of aggregate SSEPs and univariate analyses using ANOVA with repeated measures were applied to test the temporal evolution of SSEPs after tDCS. A value of $p < 0.05$ was regarded to be statistically significant.

4.3 Results

Twelve rats were included in the experiment and each of them were given both cathodal and anodal stimulus. The primary measures of the SSEP signal after tDCS were peak-to-peak amplitude (N10/P15), latency and duration, normalized with respect to the baseline SSEPs. There were no significant differences appearing in the baseline of these three measures between cathodal and anodal groups (Fig. 4.1).

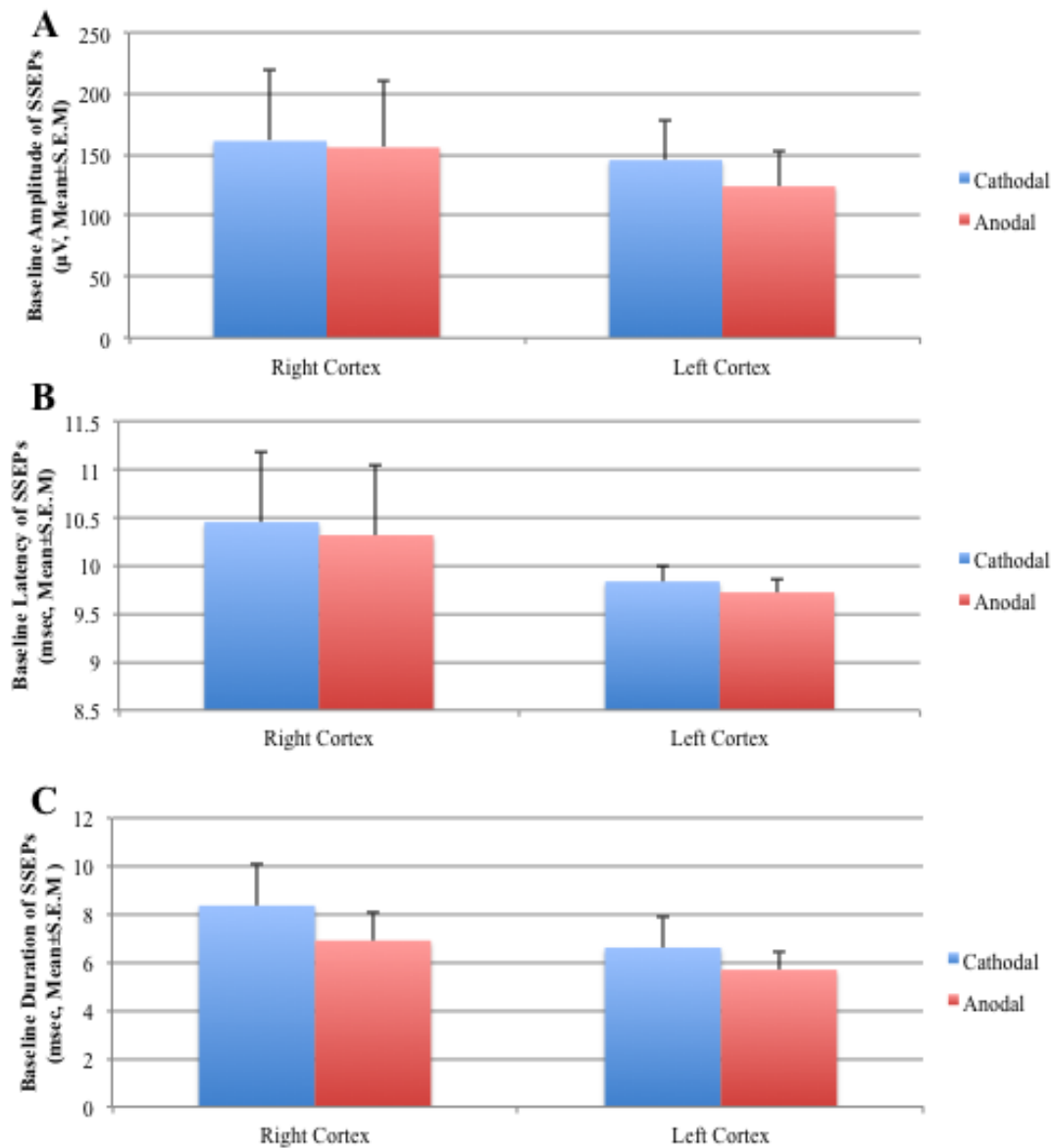


Figure 4. 1 The baseline amplitude, latency and duration of SSEPs (mean \pm S.E.M) before cathodal and anodal tDCS. There were no significant differences found in all three parameters, demonstrating no interaction of cathodal and anodal tDCS.

4.3.1 Aggregate SSEPs Post-tDCS

The differences in aggregate SSEPs were significant after anodal stimulus on the right cortex. Higher peak-to-peak amplitude of the SSEPs was found after stimulus (1.16 ± 0.07 , $p=0.033$) compared with the baseline (Fig. 4.2A). However, no significant changes were found in the latencies (1.00 ± 0.01 , $p=0.928$) and durations (0.92 ± 0.06 , $p=0.206$).

Yet, anodal stimulation on the left cortex did not cause significant changes. The amplitudes (1.23 ± 0.12 , $p=0.82$) did not show any significant difference after stimulus compared to baseline (Fig. 4.2B). Similarly, there were no significant differences in latencies (0.99 ± 0.01 , $p=0.413$) and durations (1.02 ± 0.12 , $p=0.886$) after anodal stimulation compared to baseline.

After comparing the aggregate SSEPs over 30 mins after cathodal stimulus and baseline, the peak-to-peak amplitude (Right cortex: 1.18 ± 0.150 , $p=0.263$; Left cortex: 1.17 ± 0.181 , $p=0.369$), latency (Right: 1.00 ± 0.011 , $p=0.928$; Left: 0.99 ± 0.012 , $p=0.413$) and duration (Right: 0.93 ± 0.075 , $p=0.366$; Left: 1.02 ± 0.121 ms, $p=0.885$) were similar without statistical significance on both sides of the cortex.

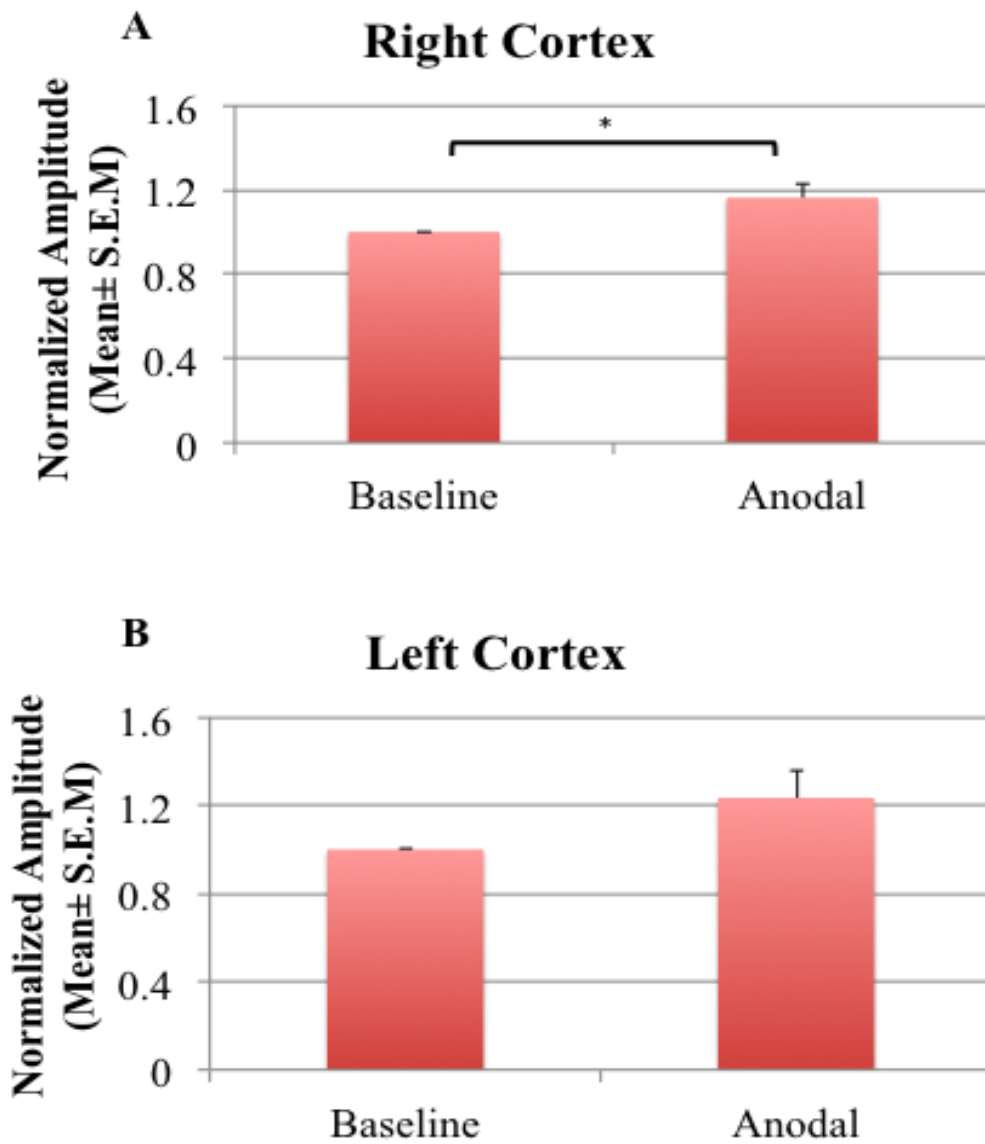


Figure 4. 2 The changes in peak-to-peak amplitudes from right cortex and left cortex after anodal tDCS. **A**, Significantly higher amplitude was found in right cortex (1.16 ± 0.07 , $p=0.033$) compared to baseline. **B**, There were no significant changes found in left cortex. * $p < 0.05$, ** $p < 0.01$.

4.3.2 Temporal Evolution of SSEPs Post-tDCS

After anodal stimulation, on the right cortex, the amplitudes at 10 mins (0.99 ± 0.02 , $p=0.399$) and baseline were similar, but increased at 20 mins (1.13 ± 0.03 , $p=0.004$) and slightly increased to 1.20 ± 0.08 at 30 mins ($p=0.250$) (Fig. 4.3A). The amplitudes at both 20 mins and 30 mins were significantly higher than the baseline ($p=0.02$, $p=0.25$, respectively). Nevertheless, there were no significant temporal changes in latencies and durations (Table 4.1).

The results of anodal tDCS to the left cortex were similar to the right cortex. The amplitudes slightly increased with respect to baseline after anodal stimulation at 10 mins to 1.22 ± 0.16 ($p=0.208$) and then increased to 1.33 ± 0.15 ($p=0.178$) at 20 mins, and finally notably increased to 1.55 ± 0.22 ($p=0.028$) at 30 mins (Fig. 4.3B). There were remarkable differences in the amplitude at 20 mins and 30 mins compared to baseline ($p=0.041$, $p=0.026$, respectively). No significant effect was seen by anodal stimulation on latencies and durations (Table 4.1).

We could not find significant temporal changes in peak-to-peak amplitudes and durations (Table 4.2) after cathodal stimulation for both sides, at any time point. However, notable changes were found in latencies at 20 mins on both sides of the cortex. For the right side, no significance of SSEP N10 latency was found in the first 10 mins, but remarkably declined to 0.97 ± 0.04 ($p=0.020$) at 20 mins and then slightly went down at 30 mins (0.96 ± 0.041 , $p=0.339$). The changes in latencies on the left side shared the same tendency as those on the right side. No significance was found on the left side initially, but latency sharply reduced to 0.99 ± 0.01 at 20 mins ($p=0.004$) and remained stable until 30 mins (0.99 ± 0.01 , $p=0.338$).

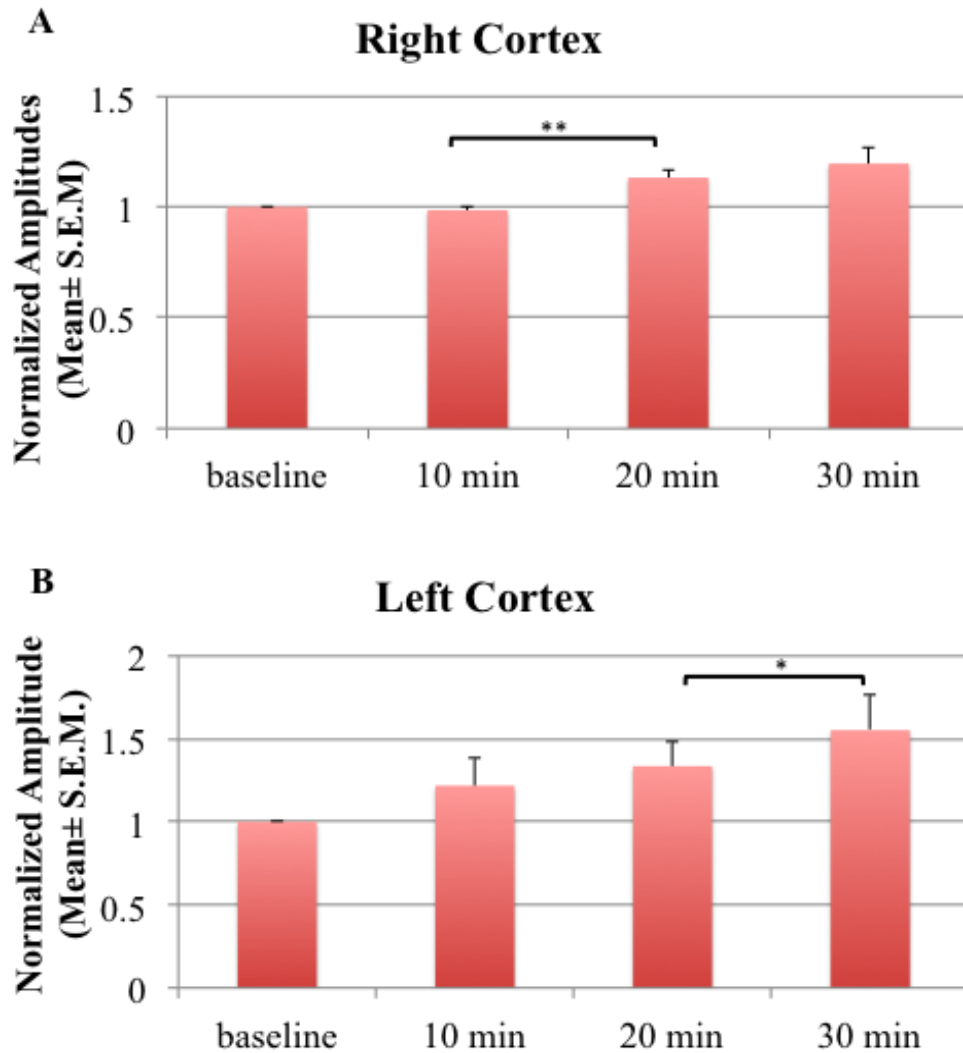


Figure 4. 3 After anodal stimulation, significant temporal evolutions were shown on both sides of cortex. A, From the right cortex, the amplitudes at 10 mins (0.99 ± 0.02 , $p=0.399$) and baseline were similar, but increased at 20 mins (1.13 ± 0.03 , $p=0.004$) and slightly increased to 1.20 ± 0.08 at 30 mins ($p=0.250$). B, From the left cortex, the amplitudes slightly increased with respect to baseline after anodal stimulation at 10 mins to 1.22 ± 0.16 ($p=0.208$) and then increased to 1.33 ± 0.15 ($p=0.178$) at 20 mins and notably increased to 1.55 ± 0.22 ($p=0.028$) at 30 mins.

Table 4. 1 The temporal changes (Mean±S.E.M) in latencies and durations after anodal tDCS

Parameters	10 min		20 min		30 min	
	Left	Right	Left	Right	Left	Right
Latency	1.00±0.002	0.97±0.035	0.99±0.004	0.97±0.036	1.00±0.009	0.97±0.035
Duration	0.98±0.018	1.01±0.037	1.00±0.027	0.98±0.055	0.93±0.084	0.88±0.063

Table 4. 2 The temporal changes (Mean±S.E.M) in amplitudes and durations after anodal tDCS

Parameters	10 min		20 min		30 min	
	Left	Right	Left	Right	Left	Right
Amplitude	0.99±0.026	0.93±0.054	1.08±0.082	1.03±0.075	1.22±0.147	1.11±0.116
Duration	1.02±0.016	1.00±0.010	0.98±0.038	0.97±0.038	1.03±0.120	0.93±0.066

4.4 Discussion

In order to clarify the effect of tDCS to the somatosensory cortex, we quantified and evaluated three parameters of SSEPs: N10/P15 peak-to-peak amplitude and duration, and latency of N10, to indicate the polarity-dependent effects of tDCS on excitability of the afferent somatosensory pathway in uninjured rats. Our results showed that 30-min 100 μ A anodal tDCS to the somatosensory cortex resulted in a long-lasting significant increase in amplitude evoked by contralateral median-nerve stimulus, whereas no effects were found after cathodal tDCS. No comparable effects of tDCS on latency or duration on both sides of the cortex were seen, except for the significant reduction in latency at 20 mins after cathodal stimulus.

Previously, the effect of tDCS on the shifts of somatosensory cortical excitability has been studied. However, these previous experiments reported contradictory conclusions (187, 188). Matsunaga et al indicated that anodal tDCS applied on the motor cortex amplified the amplitude of N30 SSEP components whereas cathodal tDCS had no effect. Conversely, a notable decrease was shown in the N20 amplitude after cathodal tDCS on the somatosensory cortex, while no significant change was shown in N20 and N30 activity after anodal stimulation in the study by Dieckhofer A et al.

Our animal experiment suggests that anodal stimulation could elevate somatosensory cortical excitability, similar to the enhancing effect of anodal tDCS to the human motor cortex (165, 166), demonstrating the possibility of measuring and quantifying the SSEP signals instead of MEPs to investigate the excitability modulation by tDCS. MEPs could be severely affected by external factors such as anesthetics (193), which may lead to more artificial noise in signals and impact the accuracy of the results of the analysis in

behavior or locomotion studies. Rather, SSEPs were stable and consistent throughout our present study, as was shown by the lack of significant differences in amplitudes, latencies and durations between the baseline and cathodal and anodal stimulation.

Although the exact mechanism of tDCS on the change of excitability has not been fully understood, many studies indicated that anodal stimulation depolarizes the resting potential of many perpendicular-oriented neurons directly under the point of stimulus, inducing a long-lasting elevation of the cortical activity and excitability after the end of stimulation (164, 180, 194). In our analysis of SSEPs, the growth in N10/P15 peak-to-peak amplitudes lasted for 30 mins after the 30-min anodal stimulation. These long-lasting effects depend on protein synthesis (195) with the change in levels of cAMP (196) and calcium (197), and result in the alternations in synaptic transmission (188). These findings confirmed by subsequent pharmacological studies that the polarity-dependent alteration of resting membrane potential, resulted from long-time tDCS, leads to the changes in synaptic strength via modulating NMDA receptor activity (189). One interesting phenomena that occurred after anodal stimulation was a lack of significant increases in the first 10-min amplitude on both sides of the cortex, followed by a notable increase at 20 mins and 30 mins. This may be due to the 10-min reaction period being too short in time for neurotransmitters to be released, bind to and activate the receptors, the efficacy of which being elevated by anodal tDCS.

It was unexpected that the anodal stimulation would elevate excitability but the cathodal stimulation could not induce the diminution on SSEPs. Previous studies demonstrated that cathodal stimulation had opposite effects to anodal stimulation, inducing the moderation of motor cortical activity (166, 182, 183). Nevertheless, other

experiments showed that the change of excitability was only sensitive to one-polarity tDCS in the motor system (198), visual system (199) and even somatosensory system (170, 187, 188), corresponding to our experimental results. Another interesting result was the small and insignificant increase of latencies after cathodal stimulation. This phenomena may be explained by the cathodal stimulation being unable to counteract the excitation induced by median-nerve stimulus. The activation caused by anodal stimulation, however, might be amplified after median-nerve stimulus to the somatosensory cortex. This might lead to the significant “positive” after-effects after anodal stimulation but the absence of “negative” effects by cathodal stimulation. The final reason for the different results from previous studies might be due to the current density we applied on the rat’s cortex. The animal’s cortex was stimulated with the current density of 2.86, approximately half of the density used by other groups (182, 183), but much higher than the clinical standard range of 0.028-0.057 mA/cm² (165, 200). The differences in current density might cause a different current propagation over the cortex.

The high current density of tDCS, outside of the clinical range, applied in our experiment is the potential limitation of this study, though it is in the safety range for rats (183, 201). No muscular twitching or epileptic-like activity was found during or after tDCS, also suggesting the safety level of the stimulation on the somatosensory cortex. However, further animal studies are required to mimic clinical practices to maintain the post-tDCS effect without any functional damage to the brain.

4.5 Conclusion

In conclusion, this study demonstrated that the anodal transcranial direct current stimulation could significantly enhance the N10/P15 peak-to-peak amplitude of SSEPs safely. This elevation was detectable throughout the whole 30-min post stimulation, whereas no effects could be found after cathodal tDCS. Our results further proved that transcranial direct current stimulation is a reliable noninvasive technique to modulate the excitability of somatosensory cortex as shown for the motor cortex. With the large number of neurologic disorders caused by abnormal excitability in cerebral activity, these effects of tDCS on somatosensory cortex might bring a new insight into clinical use. Also, the feasibility of tDCS in rats on SSEPs suggests that this technique can be used to explore more potential therapeutic methods in many pre-clinical studies on animal models of neurological and neuropsychiatric diseases associated with cortical polarization.

CHAPTER 5 Summary and Future

Directions

5.1 Summary

This thesis work mainly investigated and evaluated the accuracy of two quantitative EEG markers (qEEG), information quantitative (IQ) and sub-band information quantitative (SIQ) in predicting neurologic recovery from severe hypoxic-ischemic injury with therapeutic hypothermia, studied the alternations of each EEG sub-band in moderate brain injury and their associations with neurologic outcome in moderately injured brains with temperature management, and quantified and assessed the ability of somatosensory evoked potentials (SSEPs) on detecting the after-effects of transcranial direct current stimulation (tDCS) on somatosensory cortex.

In summary, this work:

- Reviewed current clinical standards, therapeutic methods for post-CA brain injury, neurophysiologic and physiological methods for predicting neurologic outcome.
- Applied IQ and SIQ to evaluate the benefits of therapeutic hypothermia on severe brain injury and assess their accuracy of predicting neurologic outcome. We found that both quantitative markers were able to provide early accurate predictions, but SIQ was able to offer additional sub-band EEG information related to the recovery of different brain functions. High-frequency oscillations were particularly remarkable during the recovery from severe brain injury.

- Employed SIQ to investigate the changes in different standard clinical EEG sub-band after moderate brain injury and recovery with temperature management.
- Characterized the association between gamma-band SIQ and temperature manipulation after cardiac arrest. For the first time we showed that recovery of gamma-band SIQ-qEEG marker was strongly associated with functional outcomes after CA. Induced hypothermia was associated with faster recovery of gamma-band SIQ and improved functional outcomes.
- Explored the post-CA changes in delta-band with targeted temperature manipulation. The delta-band represented a more constant component of EEG signals and showed no consistent correlation with outcome or temperature management.
- Investigated the ability of somatosensory evoked potentials (SSEPs) to evaluate the effect of transcranial direct current stimulation (tDCS) on the somatosensory system. We found that anodal tDCS was able to enhance N10/P15 peak-to-peak amplitude of SSEPs, consistent with the findings obtained from motor evoked potentials (MEPs). Thus, we concluded that tDCS could modulate the excitability not only on motor cortex but on somatosensory cortex, which could be detected by SSEPs.

5.2 Future Directions

Current findings and methods in this work laid a foundation for the future studies including:

- Study of the effect of mild hypothermia (34-36 °C) on EEG by using IQ or SIQ.
- Exploration and validation of the cut-off points obtained from IQ or SIQ on post-CA patients to help in translating these two methods into clinical practices.
- Application of the cut-off points to guide the duration and intensity of induced hypothermia.
- Development of an optimal multimodal algorithm including IQ-qEEG, SIQ-qEEG markers and neuroimaging.
- Investigation the effect of tDCS on post-CA somatosensory cortex.

Bibliography

1. Mozaffarian D, Benjamin EJ, Go AS, et al. Heart disease and stroke statistics--2015 update: a report from the American Heart Association. *Circulation* 2015;131(4):e29-322.
2. Hypothermia after Cardiac Arrest Study G. Mild therapeutic hypothermia to improve the neurologic outcome after cardiac arrest. *N Engl J Med* 2002;346(8):549-556.
3. Bernard SA, Gray TW, Buist MD, et al. Treatment of comatose survivors of out-of-hospital cardiac arrest with induced hypothermia. *The New England journal of medicine* 2002;346(8):557-563.
4. Holzer M. Targeted temperature management for comatose survivors of cardiac arrest. *N Engl J Med* 2010;363(13):1256-1264.
5. Neumar RW, Nolan JP, Adrie C, et al. ILCOR Consensus Statement Post – Cardiac Arrest Syndrome Epidemiology , Pathophysiology , Treatment , and Prognostication Resuscitation (American Heart Association , Australian and New Zealand Resuscitation Council of Asia , and the Resuscitation Council. 2013.
6. Wijdicks EFM, Hijdra a, Young GB, et al. Practice parameter: prediction of outcome in comatose survivors after cardiopulmonary resuscitation (an evidence-based review): report of the Quality Standards Subcommittee of the American Academy of Neurology. *Neurology* 2006;67:203-210.
7. Huntgeburth M, Adler C, Rosenkranz S, et al. Changes in Neuron-Specific Enolase are More Suitable Than Its Absolute Serum Levels for the Prediction of Neurologic Outcome in Hypothermia-Treated Patients with Out-of-Hospital Cardiac

Arrest. Neurocritical care 2013.

8. Cronberg T, Rundgren M, Westhall E, et al. Neuron-specific enolase correlates with other prognostic markers after cardiac arrest. *Neurology* 2011;77:623-630.
9. Bouwes A, Binnekade JM, Kuiper Ma, et al. Prognosis of coma after therapeutic hypothermia: a prospective cohort study. *Annals of neurology* 2012;71:206-212.
10. Geocadin RG, Koenig MA, Jia X, et al. Management of brain injury after resuscitation from cardiac arrest. *Neurologic clinics* 2008;26(2):487-506, ix.
11. Vaagenes P, Ginsberg M, Ebmeyer U, et al. Cerebral resuscitation from cardiac arrest: pathophysiologic mechanisms. *Crit Care Med* 1996;24(2 Suppl):S57-68.
12. Lipton SA, Rosenberg PA. Excitatory Amino-Acids as a Final Common Pathway for Neurologic Disorders. *New Engl J Med* 1994;330(9):613-622.
13. Traystman RJ, Kirsch JR, Koehler RC. Oxygen radical mechanisms of brain injury following ischemia and reperfusion. *Journal of applied physiology* 1991;71(4):1185-1195.
14. Majno G, Joris I. Apoptosis, oncosis, and necrosis. An overview of cell death. *Am J Pathol* 1995;146(1):3-15.
15. Chan PH. Role of oxidants in ischemic brain damage. *Stroke; a journal of cerebral circulation* 1996;27(6):1124-1129.
16. Chan PH. Reactive oxygen radicals in signaling and damage in the ischemic brain. *Journal of cerebral blood flow and metabolism : official journal of the International Society of Cerebral Blood Flow and Metabolism* 2001;21(1):2-14.
17. Bhalala US, Koehler RC, Kannan S. Neuroinflammation and neuroimmune dysregulation after acute hypoxic-ischemic injury of developing brain. *Frontiers in*

pediatrics 2014;2:144.

18. Zheng Z, Yenari MA. Post-ischemic inflammation: molecular mechanisms and therapeutic implications. *Neurological research* 2004;26(8):884-892.

19. Liu F, McCullough LD. Inflammatory responses in hypoxic ischemic encephalopathy. *Acta pharmacologica Sinica* 2013;34(9):1121-1130.

20. Phelps R, Dumas F, Maynard C, et al. Cerebral Performance Category and long-term prognosis following out-of-hospital cardiac arrest. *Crit Care Med* 2013;41(5):1252-1257.

21. Nielsen N, Wetterslev J, Cronberg T, et al. Targeted temperature management at 33 degrees C versus 36 degrees C after cardiac arrest. *The New England journal of medicine* 2013;369(23):2197-2206.

22. Rossetti AO, Oddo M, Logroscino G, et al. Prognostication after cardiac arrest and hypothermia: a prospective study. *Annals of neurology* 2010;67(3):301-307.

23. Hsu CH, Li J, Cinousis MJ, et al. Cerebral performance category at hospital discharge predicts long-term survival of cardiac arrest survivors receiving targeted temperature management*. *Critical care medicine* 2014;42(12):2575-2581.

24. Rothman S. Synaptic release of excitatory amino acid neurotransmitter mediates anoxic neuronal death. *The Journal of neuroscience : the official journal of the Society for Neuroscience* 1984;4(7):1884-1891.

25. Andersen JK. Oxidative stress in neurodegeneration: cause or consequence? *Nature medicine* 2004;10 Suppl:S18-25.

26. Ge P, Luo Y, Wang H, et al. Anti-protein aggregation is a potential target for preventing delayed neuronal death after transient ischemia. *Medical hypotheses*

2009;73(6):994-995.

27. Leeds PR, Yu F, Wang Z, et al. A new avenue for lithium: intervention in traumatic brain injury. *ACS chemical neuroscience* 2014;5(6):422-433.

28. Neumar RW, Nolan JP, Adrie C, et al. Post-cardiac arrest syndrome: epidemiology, pathophysiology, treatment, and prognostication. A consensus statement from the International Liaison Committee on Resuscitation (American Heart Association, Australian and New Zealand Council on Resuscitation, European Resuscitation Council, Heart and Stroke Foundation of Canada, InterAmerican Heart Foundation, Resuscitation Council of Asia, and the Resuscitation Council of Southern Africa); the American Heart Association Emergency Cardiovascular Care Committee; the Council on Cardiovascular Surgery and Anesthesia; the Council on Cardiopulmonary, Perioperative, and Critical Care; the Council on Clinical Cardiology; and the Stroke Council. *Circulation* 2008;118(23):2452-2483.

29. Yenari MA, Han HS. Neuroprotective mechanisms of hypothermia in brain ischaemia. *Nature reviews Neuroscience* 2012;13(4):267-278.

30. Busto R, Dietrich WD, Globus MY, et al. Small differences in intraschemic brain temperature critically determine the extent of ischemic neuronal injury. *Journal of cerebral blood flow and metabolism : official journal of the International Society of Cerebral Blood Flow and Metabolism* 1987;7(6):729-738.

31. Erecinska M, Thoresen M, Silver IA. Effects of hypothermia on energy metabolism in Mammalian central nervous system. *Journal of cerebral blood flow and metabolism : official journal of the International Society of Cerebral Blood Flow and Metabolism* 2003;23(5):513-530.

32. Fugate JE, Wijdicks EFM, Mandrekar J, et al. Predictors of neurologic outcome in hypothermia after cardiac arrest. *Annals of neurology* 2010;68:907-914.
33. Greer DM, Yang J, Scripko PD, et al. Clinical examination for prognostication in comatose cardiac arrest patients. *Resuscitation* 2013;84:1546-1551.
34. Samaniego EA, Mlynash M, Caulfield AF, et al. Sedation Confounds Outcome Prediction in Cardiac Arrest Survivors Treated with Hypothermia. 2011;15:113-119.
35. Wojtczak-Soska K, Lelonek M. S-100B protein: An early prognostic marker after cardiac arrest. *Cardiology journal* 2010;17(5):532-536.
36. Shinozaki K, Oda S, Sadahiro T, et al. Serum S-100B is superior to neuron-specific enolase as an early prognostic biomarker for neurological outcome following cardiopulmonary resuscitation. *Resuscitation* 2009;80(8):870-875.
37. Almaraz AC, Bobrow BJ, Wingerchuk DM, et al. Serum neuron specific enolase to predict neurological outcome after cardiopulmonary resuscitation: a critically appraised topic. *The neurologist* 2009;15(1):44-48.
38. Kliegel A, Losert H, Sterz F, et al. Serial lactate determinations for prediction of outcome after cardiac arrest. *Medicine* 2004;83(5):274-279.
39. Lazzeri C, Gensini GF, Sori A, et al. Dynamic behaviour of lactate values during mild hypothermia in patients with cardiac arrest. *European heart journal Acute cardiovascular care* 2014;3(2):176-182.
40. Lee TR, Kang MJ, Cha WC, et al. Better lactate clearance associated with good neurologic outcome in survivors who treated with therapeutic hypothermia after out-of-hospital cardiac arrest. *Critical care* 2013;17(5):R260.
41. Torbey MT, Selim M, Knorr J, et al. Quantitative analysis of the loss of

distinction between gray and white matter in comatose patients after cardiac arrest. *Stroke; a journal of cerebral circulation* 2000;31(9):2163-2167.

42. Deakin CD, Nolan JP, Soar J, et al. European Resuscitation Council Guidelines for Resuscitation 2010 Section 4. Adult advanced life support. *Resuscitation* 2010;81(10):1305-1352.

43. Greer D, Scripko P, Bartscher J, et al. Clinical MRI interpretation for outcome prediction in cardiac arrest. *Neurocritical care* 2012;17(2):240-244.

44. Wijman CA, Mlynash M, Caulfield AF, et al. Prognostic value of brain diffusion-weighted imaging after cardiac arrest. *Annals of neurology* 2009;65(4):394-402.

45. Schmitz B, Bock C, Hoehn-Berlage M, et al. Recovery of the rodent brain after cardiac arrest: a functional MRI study. *Magnetic resonance in medicine : official journal of the Society of Magnetic Resonance in Medicine / Society of Magnetic Resonance in Medicine* 1998;39:783-788.

46. Gofton TE, Chouinard PA, Young GB, et al. Functional MRI study of the primary somatosensory cortex in comatose survivors of cardiac arrest. *Experimental neurology* 2009;217(2):320-327.

47. Rudolf J, Sobesky J, Ghaemi M, et al. The correlation between cerebral glucose metabolism and benzodiazepine receptor density in the acute vegetative state. *European journal of neurology : the official journal of the European Federation of Neurological Societies* 2002;9(6):671-677.

48. Edgren E, Enblad P, Grenvik A, et al. Cerebral blood flow and metabolism after cardiopulmonary resuscitation. A pathophysiologic and prognostic positron emission tomography pilot study. *Resuscitation* 2003;57(2):161-170.

49. Nakamura T, Kuroda Y, Torigoe N, et al. Cerebral metabolism monitoring during hypothermia following resuscitation from cardiopulmonary arrest. *Acta neurochirurgica Supplement* 2008;102:203-206.
50. Madhok J, Wu D, Xiong W, et al. Hypothermia amplifies somatosensory-evoked potentials in uninjured rats. *J Neurosurg Anesthesiol* 2012;24(3):197-202.
51. Oddo M, Rossetti AO. Early Multimodal Outcome Prediction After Cardiac Arrest in Patients Treated With Hypothermia. *Critical care medicine* 2014:18-21.
52. Cloostermans MC, van Meulen FB, Eertman CJ, et al. Continuous electroencephalography monitoring for early prediction of neurological outcome in postanoxic patients after cardiac arrest: a prospective cohort study. *Critical care medicine* 2012;40(10):2867-2875.
53. Noirhomme Q, Lehembre R, Lugo ZDR, et al. Automated analysis of background EEG and reactivity during therapeutic hypothermia in comatose patients after cardiac arrest. *Clinical EEG and neuroscience* 2014;45:6-13.
54. Al Thenayan E, Savard M, Sharpe M, et al. Predictors of poor neurologic outcome after induced mild hypothermia following cardiac arrest. *Neurology* 2008;71(19):1535-1537.
55. Maher D, Tran H, Nuno M, et al. Continuous electroencephalogram patterns are suggestive of eventual neurologic outcomes in post-cardiac arrest patients treated with therapeutic hypothermia. *Journal of critical care* 2015;30(1):121-125.
56. Lee YC, Phan TG, Jolley DJ, et al. Accuracy of clinical signs, SEP, and EEG in predicting outcome of hypoxic coma: a meta-analysis. *Neurology* 2010;74(7):572-580.
57. Rossetti AO, Logroscino G, Liaudet L, et al. Status epilepticus: an independent

outcome predictor after cerebral anoxia. *Neurology* 2007;69(3):255-260.

58. Rossetti AO, Oddo M, Liaudet L, et al. Predictors of awakening from postanoxic status epilepticus after therapeutic hypothermia. *Neurology* 2009;72(8):744-749.

59. San-Juan OD, Chiappa KH, Costello DJ, et al. Periodic epileptiform discharges in hypoxic encephalopathy: BiPLEDs and GPEDs as a poor prognosis for survival. *Seizure* 2009;18(5):365-368.

60. Rossetti AO, Urbano LA, Delodder F, et al. Prognostic value of continuous EEG monitoring during therapeutic hypothermia after cardiac arrest. *Critical care* 2010;14(5):R173.

61. Fugate JE, Wijdicks EF, Mandrekar J, et al. Predictors of neurologic outcome in hypothermia after cardiac arrest. *Ann Neurol* 2010;68(6):907-914.

62. Rossetti AO, Carrera E, Oddo M. Early EEG correlates of neuronal injury after brain anoxia. *Neurology* 2012;78:796-802.

63. Tsetsou S, Oddo M, Rossetti AO. Clinical outcome after a reactive hypothermic EEG following cardiac arrest. *Neurocritical care* 2013;19:283-286.

64. Rossetti AO, Oddo M, Liaudet L, et al. Predictors of awakening from postanoxic status epilepticus after therapeutic hypothermia. *Neurology* 2009;72:744-749.

65. Sadaka F, Doerr D, Hindia J, et al. Continuous Electroencephalogram in Comatose Postcardiac Arrest Syndrome Patients Treated With Therapeutic Hypothermia: Outcome Prediction Study. *Journal of intensive care medicine* 2014.

66. Rundgren M, Westhall E, Cronberg T, et al. Continuous amplitude-integrated electroencephalogram predicts outcome in hypothermia-treated cardiac arrest patients. *Critical care medicine* 2010;38:1838-1844.

67. Hellstrom-Westas L, Rosen I. Continuous brain-function monitoring: state of the art in clinical practice. *Seminars in fetal & neonatal medicine* 2006;11(6):503-511.
68. Mastrangelo M, Fiocchi I, Fontana P, et al. Acute neonatal encephalopathy and seizures recurrence: a combined aEEG/EEG study. *Seizure : the journal of the British Epilepsy Association* 2013;22(9):703-707.
69. Thorngren-Jerneck K, Hellstrom-Westas L, Ryding E, et al. Cerebral glucose metabolism and early EEG/aEEG in term newborn infants with hypoxic-ischemic encephalopathy. *Pediatr Res* 2003;54(6):854-860.
70. Toet MC, Hellstrom-Westas L, Groenendaal F, et al. Amplitude integrated EEG 3 and 6 hours after birth in full term neonates with hypoxic-ischaemic encephalopathy. *Arch Dis Child Fetal Neonatal Ed* 1999;81(1):F19-23.
71. van Rooij LGM, Toet MC, Osredkar D, et al. Recovery of amplitude integrated electroencephalographic background patterns within 24 hours of perinatal asphyxia. *Arch Dis Child-Fetal* 2005;90(3):245-251.
72. Rundgren M, Rosen I, Friberg H. Amplitude-integrated EEG (aEEG) predicts outcome after cardiac arrest and induced hypothermia. *Intensive Care Med* 2006;32(6):836-842.
73. Oh SH, Park KN, Kim YM, et al. The prognostic value of continuous amplitude-integrated electroencephalogram applied immediately after return of spontaneous circulation in therapeutic hypothermia-treated cardiac arrest patients. *Resuscitation* 2013;84(2):200-205.
74. Shah DK, Wusthoff CJ, Clarke P, et al. Electrographic seizures are associated with brain injury in newborns undergoing therapeutic hypothermia. *Archives of disease in*

childhood Fetal and neonatal edition 2014;99(3):F219-224.

75. Wennervirta JE, Ermes MJ, Tiainen SM, et al. Hypothermia-treated cardiac arrest patients with good neurological outcome differ early in quantitative variables of EEG suppression and epileptiform activity. *Critical care medicine* 2009;37:2427-2435.

76. Chen B, Song F-Q, Sun L-L, et al. Improved early postresuscitation EEG activity for animals treated with hypothermia predicted 96 hr neurological outcome and survival in a rat model of cardiac arrest. *BioMed research international* 2013;2013:312137.

77. Jia X, Koenig MA, Venkatraman A, et al. Post-cardiac arrest temperature manipulation alters early EEG bursting in rats. *Resuscitation* 2008;78(3):367-373.

78. Dandan Z, Jia X, Ding H, et al. Application of Tsallis entropy to EEG: quantifying the presence of burst suppression after asphyxial cardiac arrest in rats. *IEEE transactions on bio-medical engineering* 2010;57(4):867-874.

79. Shin HC, Tong S, Yamashita S, et al. Quantitative EEG and effect of hypothermia on brain recovery after cardiac arrest. *IEEE transactions on bio-medical engineering* 2006;53(6):1016-1023.

80. Jia X, Koenig MA, Nickl R, et al. Early electrophysiologic markers predict functional outcome associated with temperature manipulation after cardiac arrest in rats. *Critical care medicine* 2008;36(6):1909-1916.

81. Shin HC, Jia X, Nickl R, et al. A subband-based information measure of EEG during brain injury and recovery after cardiac arrest. *IEEE transactions on bio-medical engineering* 2008;55(8):1985-1990.

82. Chollet-Xemard C, Combes X, Soupizet F, et al. Bispectral index monitoring is useless during cardiac arrest patients' resuscitation. *Resuscitation* 2009;80(2):213-216.

83. Fatovich DM, Jacobs IG, Celenza A, et al. An observational study of bispectral index monitoring for out of hospital cardiac arrest. *Resuscitation* 2006;69(2):207-212.
84. Leary M, Fried DA, Gaieski DF, et al. Neurologic prognostication and bispectral index monitoring after resuscitation from cardiac arrest. *Resuscitation* 2010;81(9):1133-1137.
85. Seder DB, Fraser GL, Robbins T, et al. The bispectral index and suppression ratio are very early predictors of neurological outcome during therapeutic hypothermia after cardiac arrest. *Intensive care medicine* 2010;36(2):281-288.
86. Stammet P, Werer C, Mertens L, et al. Bispectral index (BIS) helps predicting bad neurological outcome in comatose survivors after cardiac arrest and induced therapeutic hypothermia. *Resuscitation* 2009;80(4):437-442.
87. Tjepkema-Cloostermans MC, van Meulen FB, Meinsma G, et al. A Cerebral Recovery Index (CRI) for early prognosis in patients after cardiac arrest. *Critical care* 2013;17(5):R252.
88. Friberg H, Rundgren M, Westhall E, et al. Continuous evaluation of neurological prognosis after cardiac arrest. *Acta anaesthesiologica Scandinavica* 2013;57:6-15.
89. Madhok J, Maybhate A, Xiong W, et al. Quantitative assessment of somatosensory-evoked potentials after cardiac arrest in rats: Prognostication of functional outcomes. *Critical care medicine* 2010;38(8):1709-1717.
90. Xiong W, Koenig MA, Madhok J, et al. Evolution of Somatosensory Evoked Potentials after Cardiac Arrest induced hypoxic-ischemic injury. *Resuscitation* 2010;81(7):893-897.
91. Marion DW. Coma due to cardiac arrest: prognosis and contemporary treatment.

F1000 medicine reports 2009;1:1-5.

92. Thomke F. Assessing Prognosis Following Cardiopulmonary Resuscitation and Therapeutic Hypothermia-a Critical Discussion of Recent Studies. *Dtsch Arztebl Int* 2013;110(9):137-U112.

93. Grippo A, Carrai R, Fossi S, et al. Absent SEP during therapeutic hypothermia did not reappear after re-warming in comatose patients following cardiac arrest. *Minerva anesthesiologica* 2013;79(4):360-369.

94. Wu D, Anastassios B, Xiong W, et al. Study of the origin of short- and long-latency SSEP during recovery from brain ischemia in a rat model. *Neuroscience letters* 2010;485(3):157-161.

95. Wu D, Xiong W, Jia XF, et al. Short- and long-latency somatosensory neuronal responses reveal selective brain injury and effect of hypothermia in global hypoxic ischemia. *Journal of neurophysiology* 2012;107(4):1164-1171.

96. Ma Y, Hu Y, Valentin N, et al. Time jitter of somatosensory evoked potentials in recovery from hypoxic-ischemic brain injury. *J Neurosci Meth* 2011;201(2):355-360.

97. Agrawal G, Iyer S, All AH. A comparative study of recording procedures for motor evoked potential signals. Conference proceedings : Annual International Conference of the IEEE Engineering in Medicine and Biology Society IEEE Engineering in Medicine and Biology Society Conference 2009;2009:2086-2089.

98. Ma Y, Thakor NV, Jia X. Statistical model applied to motor evoked potentials analysis. *Conf Proc IEEE Eng Med Biol Soc* 2011;2011:2001-2004.

99. Rodriguez Ra, Bussière M, Froeschl M, et al. Auditory-evoked potentials during coma: do they improve our prediction of awakening in comatose patients? *Journal of*

critical care 2014;29:93-100.

100. Tzovara A, Rossetti AO, Spierer L, et al. Progression of auditory discrimination based on neural decoding predicts awakening from coma. *Brain : a journal of neurology* 2013;136:81-89.

101. Slabu L, Escera C, Grimm S, et al. Early change detection in humans as revealed by auditory brainstem and middle-latency evoked potentials. *The European journal of neuroscience* 2010;32:859-865.

102. Tsurukiri J, Mishima S, Ohta S. Initial middle latency auditory evoked potentials index helps to predict resuscitated outcomes in patients with cardiac arrest. *The American journal of emergency medicine* 2013;31:895-899.

103. Silva A, Cardoso-Cruz H, Silva F, et al. Comparison of anesthetic depth indexes based on thalamocortical local field potentials in rats. *Anesthesiology* 2010;112:355-363.

104. Chen C, Maybhate A, Israel D, et al. Assessing thalamocortical functional connectivity with Granger causality. *IEEE Trans Neural Syst Rehabil Eng* 2013;21(5):725-733.

105. Maybhate A, Chen C, Akbari Y, et al. Band specific changes in thalamocortical synchrony in field potentials after cardiac arrest induced global hypoxia. *Conference proceedings : Annual International Conference of the IEEE Engineering in Medicine and Biology Society IEEE Engineering in Medicine and Biology Society Annual Conference* 2013;2013:7112-7115.

106. Wu D, Xiong W, Jia X, et al. Short- and long-latency somatosensory neuronal responses reveal selective brain injury and effect of hypothermia in global hypoxic ischemia. *Journal of neurophysiology* 2012;107:1164-1171.

107. Waldert S, Pistohl T, Braun C, et al. A review on directional information in neural signals for brain-machine interfaces. *Journal of physiology*, Paris 2009;103(3-5):244-254.
108. Brown TM, Banks JR, Piggins HD. A novel suction electrode recording technique for monitoring circadian rhythms in single and multiunit discharge from brain slices. *Journal of neuroscience methods* 2006;156(1-2):173-181.
109. Choi YS, Koenig MA, Jia XF, et al. Quantifying Time-Varying Multiunit Neural Activity Using Entropy-Based Measures. *Ieee T Bio-Med Eng* 2010;57(11):2771-2777.
110. Choi YS, Koenig MA, Jia X, et al. Multiresolution entropy measure for neuronal multiunit activity. *Conf Proc IEEE Eng Med Biol Soc* 2009;2009:4715-4718.
111. Tsuchida TN, Wusthoff CJ, Shellhaas Ra, et al. American clinical neurophysiology society standardized EEG terminology and categorization for the description of continuous EEG monitoring in neonates: report of the American Clinical Neurophysiology Society critical care monitoring committee. *Journal of clinical neurophysiology : official publication of the American Electroencephalographic Society* 2013;30:161-173.
112. Ching S, Purdon PL, Vijayan S, et al. A neurophysiological-metabolic model for burst suppression. *Proceedings of the National Academy of Sciences of the United States of America* 2012;109:3095-3100.
113. Bouwes A, Binnekade JM, Kuiper MA, et al. Prognosis of coma after therapeutic hypothermia: a prospective cohort study. *Annals of neurology* 2012;71(2):206-212.
114. Bragin A, Engel J, Jr., Wilson CL, et al. High-frequency oscillations in human brain. *Hippocampus* 1999;9(2):137-142.
115. Bragin A, Wilson CL, Staba RJ, et al. Interictal high-frequency oscillations (80-

500 Hz) in the human epileptic brain: entorhinal cortex. *Annals of neurology* 2002;52(4):407-415.

116. Jacobs J, Levan P, Chatillon CE, et al. High frequency oscillations in intracranial EEGs mark epileptogenicity rather than lesion type. *Brain : a journal of neurology* 2009;132(Pt 4):1022-1037.

117. Coimbra C, Wieloch T. Moderate hypothermia mitigates neuronal damage in the rat brain when initiated several hours following transient cerebral ischemia. *Acta neuropathologica* 1994;87(4):325-331.

118. Berger C, Xia F, Kohrmann M, et al. Hypothermia in acute stroke--slow versus fast rewarming an experimental study in rats. *Experimental neurology* 2007;204(1):131-137.

119. Eshel G, Reisler G, Berkovitch M, et al. Comparison of fast versus slow rewarming following acute moderate hypothermia in rats. *Paediatric anaesthesia* 2002;12(3):235-242.

120. Wang B, Armstrong JS, Lee JH, et al. Rewarming from therapeutic hypothermia induces cortical neuron apoptosis in a swine model of neonatal hypoxic-ischemic encephalopathy. *Journal of cerebral blood flow and metabolism : official journal of the International Society of Cerebral Blood Flow and Metabolism* 2015.

121. Lu X, Ma L, Sun S, et al. The effects of the rate of postresuscitation rewarming following hypothermia on outcomes of cardiopulmonary resuscitation in a rat model. *Critical care medicine* 2014;42(2):e106-113.

122. Jia X, Koenig MA, Shin HC, et al. Quantitative EEG and neurological recovery with therapeutic hypothermia after asphyxial cardiac arrest in rats. *Brain research*

2006;1111(1):166-175.

123. Jia X, Koenig MA, Shin HC, et al. Improving neurological outcomes post-cardiac arrest in a rat model: immediate hypothermia and quantitative EEG monitoring. *Resuscitation* 2008;76(3):431-442.

124. Wu D, Xiong W, Jia X, et al. Short- and long-latency somatosensory neuronal responses reveal selective brain injury and effect of hypothermia in global hypoxic ischemia. *Journal of neurophysiology* 2012;107(4):1164-1171.

125. Go AS, Mozaffarian D, Roger VL, et al. Heart disease and stroke statistics--2014 update: a report from the American Heart Association. *Circulation* 2014;129(3):e28-e292.

126. Leary M, Grossestreuer AV, Iannacone S, et al. Pyrexia and neurologic outcomes after therapeutic hypothermia for cardiac arrest. *Resuscitation* 2013;84(8):1056-1061.

127. Bro-Jeppesen J, Hassager C, Wanscher M, et al. Post-hypothermia fever is associated with increased mortality after out-of-hospital cardiac arrest. *Resuscitation* 2013;84(12):1734-1740.

128. Bernard SA, Gray TW, Buist MD, et al. Treatment of comatose survivors of out-of-hospital cardiac arrest with induced hypothermia. *New Engl J Med* 2002;346(8):557-563.

129. Thomassen A, Sorensen K, Wernberg M. The prognostic value of EEG in coma survivors after cardiac arrest. *Acta Anaesthesiol Scand* 1978;22(5):483-490.

130. Binnie CD, Prior PF, Lloyd DS, et al. Electroencephalographic prediction of fatal anoxic brain damage after resuscitation from cardiac arrest. *Br Med J* 1970;4(5730):265-268.

131. Berger H. Über das elektrenkephalogramm des menschen. *European Archives of*

Psychiatry and Clinical Neuroscience 1929;87(1):527-570.

132. Buzsaki G, Draguhn A. Neuronal oscillations in cortical networks. *Science* 2004;304(5679):1926-1929.

133. Uhlhaas PJ, Pipa G, Lima B, et al. Neural synchrony in cortical networks: history, concept and current status. *Frontiers in integrative neuroscience* 2009;3:17.

134. Uhlhaas PJ, Singer W. Abnormal neural oscillations and synchrony in schizophrenia. *Nature reviews Neuroscience* 2010;11(2):100-113.

135. Uhlhaas PJ, Singer W. Neural synchrony in brain disorders: relevance for cognitive dysfunctions and pathophysiology. *Neuron* 2006;52(1):155-168.

136. Horn M, Schlote W, Henrich HA. Global cerebral ischemia and subsequent selective hypothermia. A neuropathological and morphometrical study on ischemic neuronal damage in cat. *Acta neuropathologica* 1991;81(4):443-449.

137. D'Cruz BJ, Fertig KC, Filiano AJ, et al. Hypothermic reperfusion after cardiac arrest augments brain-derived neurotrophic factor activation. *Journal of cerebral blood flow and metabolism : official journal of the International Society of Cerebral Blood Flow and Metabolism* 2002;22(7):843-851.

138. Hicks SD, DeFranco DB, Callaway CW. Hypothermia during reperfusion after asphyxial cardiac arrest improves functional recovery and selectively alters stress-induced protein expression. *J Cereb Blood Flow Metab* 2000;20(3):520-530.

139. Jia X, Kohn A. Gamma rhythms in the brain. *PLoS biology* 2011;9(4):e1001045.

140. Singer W, Gray CM. Visual feature integration and the temporal correlation hypothesis. *Annual review of neuroscience* 1995;18:555-586.

141. Basar E, Basar-Eroglu C, Rahn E, et al. Sensory and cognitive components of

brain resonance responses. An analysis of responsiveness in human and cat brain upon visual and auditory stimulation. *Acta oto-laryngologica Supplementum* 1991;491:25-34; discussion 35.

142. Adrian ED. Olfactory reactions in the brain of the hedgehog. *The Journal of physiology* 1942;100(4):459-473.

143. Kaiser J, Lutzenberger W. Human gamma-band activity: a window to cognitive processing. *Neuroreport* 2005;16(3):207-211.

144. Pulvermuller F, Lutzenberger W, Preissl H, et al. Spectral responses in the gamma-band: physiological signs of higher cognitive processes? *Neuroreport* 1995;6(15):2059-2064.

145. Miltner WH, Braun C, Arnold M, et al. Coherence of gamma-band EEG activity as a basis for associative learning. *Nature* 1999;397(6718):434-436.

146. Llinas R, Ribary U. Coherent 40-Hz oscillation characterizes dream state in humans. *Proceedings of the National Academy of Sciences of the United States of America* 1993;90(5):2078-2081.

147. Elbert T, Rockstroh B, Lutzenberger W, et al. *Self-regulation of the brain and behavior*: Springer; 1984.

148. Steriade M, Amzica F, Contreras D. Synchronization of fast (30-40 Hz) spontaneous cortical rhythms during brain activation. *The Journal of neuroscience : the official journal of the Society for Neuroscience* 1996;16(1):392-417.

149. Traub RD, Bibbig A, LeBeau FE, et al. Cellular mechanisms of neuronal population oscillations in the hippocampus in vitro. *Annual review of neuroscience* 2004;27:247-278.

150. Wang XJ, Buzsaki G. Gamma oscillation by synaptic inhibition in a hippocampal interneuronal network model. *The Journal of neuroscience : the official journal of the Society for Neuroscience* 1996;16(20):6402-6413.
151. White BC, Sullivan JM, DeGracia DJ, et al. Brain ischemia and reperfusion: molecular mechanisms of neuronal injury. *Journal of the neurological sciences* 2000;179(S 1-2):1-33.
152. Oku K, Kuboyama K, Safar P, et al. Cerebral and systemic arteriovenous oxygen monitoring after cardiac arrest. Inadequate cerebral oxygen delivery. *Resuscitation* 1994;27(2):141-152.
153. Dirnagl U, Iadecola C, Moskowitz MA. Pathobiology of ischaemic stroke: an integrated view. *Trends in neurosciences* 1999;22(9):391-397.
154. Morimoto T, Nagao H, Yoshimatsu M, et al. Pathogenic role of glutamate in hyperthermia-induced seizures. *Epilepsia* 1993;34(3):447-452.
155. Suehiro E, Fujisawa H, Ito H, et al. Brain temperature modifies glutamate neurotoxicity in vivo. *Journal of neurotrauma* 1999;16(4):285-297.
156. Qu L, Liu X, Wu C, et al. Hyperthermia decreases GABAergic synaptic transmission in hippocampal neurons of immature rats. *Neurobiology of disease* 2007;27(3):320-327.
157. Busto R, Globus MY, Dietrich WD, et al. Effect of mild hypothermia on ischemia-induced release of neurotransmitters and free fatty acids in rat brain. *Stroke; a journal of cerebral circulation* 1989;20(7):904-910.
158. Nolan JP, Morley PT, Vanden Hoek TL, et al. Therapeutic hypothermia after cardiac arrest: an advisory statement by the advanced life support task force of the

International Liaison Committee on Resuscitation. *Circulation* 2003;108(1):118-121.

159. Sharbrough FW, Messick JM, Jr., Sundt TM, Jr. Correlation of continuous electroencephalograms with cerebral blood flow measurements during carotid endarterectomy. *Stroke; a journal of cerebral circulation* 1973;4(4):674-683.

160. Hossmann KA. Viability thresholds and the penumbra of focal ischemia. *Annals of neurology* 1994;36(4):557-565.

161. Jordan KG. Emergency EEG and continuous EEG monitoring in acute ischemic stroke. *Journal of clinical neurophysiology : official publication of the American Electroencephalographic Society* 2004;21(5):341-352.

162. Kawakami S, Hossmann KA. Electrophysiological recovery after compression ischemia of the rat brain. *Journal of neurology* 1977;217(1):31-42.

163. Amzica F, Kroeger D. Cellular mechanisms underlying EEG waveforms during coma. *Epilepsia* 2011;52 Suppl 8:25-27.

164. Bindman LJ, Lippold OC, Redfearn JW. The Action of Brief Polarizing Currents on the Cerebral Cortex of the Rat (1) during Current Flow and (2) in the Production of Long-Lasting after-Effects. *The Journal of physiology* 1964;172:369-382.

165. Nitsche MA, Paulus W. Sustained excitability elevations induced by transcranial DC motor cortex stimulation in humans. *Neurology* 2001;57(10):1899-1901.

166. Nitsche MA, Paulus W. Excitability changes induced in the human motor cortex by weak transcranial direct current stimulation. *The Journal of physiology* 2000;527 Pt 3:633-639.

167. Nitsche MA, Nitsche MS, Klein CC, et al. Level of action of cathodal DC polarisation induced inhibition of the human motor cortex. *Clinical neurophysiology :*

official journal of the International Federation of Clinical Neurophysiology
2003;114(4):600-604.

168. Barker AT, Jalinous R, Freeston IL. Non-invasive magnetic stimulation of human motor cortex. *Lancet* 1985;1(8437):1106-1107.

169. Merton PA, Morton HB. Stimulation of the cerebral cortex in the intact human subject. *Nature* 1980;285(5762):227.

170. Rogalewski A, Breitenstein C, Nitsche MA, et al. Transcranial direct current stimulation disrupts tactile perception. *The European journal of neuroscience* 2004;20(1):313-316.

171. Costain R, Redfearn JW, Lippold OC. A Controlled Trial of the Therapeutic Effect of Polarization of the Brain in Depressive Illness. *The British journal of psychiatry : the journal of mental science* 1964;110:786-799.

172. Carney MW. Negative polarisation of the brain in the treatment of manic states. *Irish journal of medical science* 1969;8(3):133-135.

173. Fregni F, Boggio PS, Lima MC, et al. A sham-controlled, phase II trial of transcranial direct current stimulation for the treatment of central pain in traumatic spinal cord injury. *Pain* 2006;122(1-2):197-209.

174. Fregni F, Boggio PS, Nitsche MA, et al. Treatment of major depression with transcranial direct current stimulation. *Bipolar Disord* 2006;8(2):203-204.

175. Hummel F, Celnik P, Giraux P, et al. Effects of non-invasive cortical stimulation on skilled motor function in chronic stroke. *Brain* 2005;128(Pt 3):490-499.

176. Auvichayapat N, Rotenberg A, Gersner R, et al. Transcranial direct current stimulation for treatment of refractory childhood focal epilepsy. *Brain stimulation*

2013;6(4):696-700.

177. Antal A, Nitsche MA, Kruse W, et al. Direct current stimulation over V5 enhances visuomotor coordination by improving motion perception in humans. *Journal of cognitive neuroscience* 2004;16(4):521-527.

178. Nitsche MA, Schauenburg A, Lang N, et al. Facilitation of implicit motor learning by weak transcranial direct current stimulation of the primary motor cortex in the human. *J Cogn Neurosci* 2003;15(4):619-626.

179. Creutzfeldt OD, Fromm GH, Kapp H. Influence of transcortical d-c currents on cortical neuronal activity. *Experimental neurology* 1962;5:436-452.

180. Purpura DP, McMurtry JG. Intracellular Activities and Evoked Potential Changes during Polarization of Motor Cortex. *Journal of neurophysiology* 1965;28:166-185.

181. Nitsche MA, Cohen LG, Wassermann EM, et al. Transcranial direct current stimulation: State of the art 2008. *Brain stimulation* 2008;1(3):206-223.

182. Cambiaghi M, Velikova S, Gonzalez-Rosa JJ, et al. Brain transcranial direct current stimulation modulates motor excitability in mice. *Eur J Neurosci* 2010;31(4):704-709.

183. Liebetanz D, Klinker F, Hering D, et al. Anticonvulsant effects of transcranial direct-current stimulation (tDCS) in the rat cortical ramp model of focal epilepsy. *Epilepsia* 2006;47(7):1216-1224.

184. Iyer MB, Mattu U, Grafman J, et al. Safety and cognitive effect of frontal DC brain polarization in healthy individuals. *Neurology* 2005;64(5):872-875.

185. Accornero N, Li Voti P, La Riccia M, et al. Visual evoked potentials modulation during direct current cortical polarization. *Experimental brain research* 2007;178(2):261-

266.

186. Antal A, Kincses TZ, Nitsche MA, et al. Excitability changes induced in the human primary visual cortex by transcranial direct current stimulation: direct electrophysiological evidence. *Investigative ophthalmology & visual science* 2004;45(2):702-707.

187. Dieckhofer A, Waberski TD, Nitsche M, et al. Transcranial direct current stimulation applied over the somatosensory cortex - differential effect on low and high frequency SEPs. *Clinical neurophysiology : official journal of the International Federation of Clinical Neurophysiology* 2006;117(10):2221-2227.

188. Matsunaga K, Nitsche MA, Tsuji S, et al. Effect of transcranial DC sensorimotor cortex stimulation on somatosensory evoked potentials in humans. *Clinical neurophysiology : official journal of the International Federation of Clinical Neurophysiology* 2004;115(2):456-460.

189. Liebetanz D, Nitsche MA, Tergau F, et al. Pharmacological approach to the mechanisms of transcranial DC-stimulation-induced after-effects of human motor cortex excitability. *Brain* 2002;125(Pt 10):2238-2247.

190. Nitsche MA, Fricke K, Henschke U, et al. Pharmacological modulation of cortical excitability shifts induced by transcranial direct current stimulation in humans. *The Journal of physiology* 2003;553(Pt 1):293-301.

191. Lefaucheur JP, Drouot X, Keravel Y, et al. Pain relief induced by repetitive transcranial magnetic stimulation of precentral cortex. *Neuroreport* 2001;12(13):2963-2965.

192. Madhok J, Maybhate A, Xiong W, et al. Quantitative assessment of

somatosensory-evoked potentials after cardiac arrest in rats: prognostication of functional outcomes. *Critical care medicine* 2010;38(8):1709-1717.

193. Cheng G, Kendig JJ. Enflurane directly depresses glutamate AMPA and NMDA currents in mouse spinal cord motor neurons independent of actions on GABAA or glycine receptors. *Anesthesiology* 2000;93(4):1075-1084.

194. Bindman LJ, Lippold OC, Redfearn JW. Long-lasting changes in the level of the electrical activity of the cerebral cortex produced by polarizing currents. *Nature* 1962;196:584-585.

195. Gartside IB. Mechanisms of sustained increases of firing rate of neurones in the rat cerebral cortex after polarization: role of protein synthesis. *Nature* 1968;220(5165):383-384.

196. Hattori Y, Moriwaki A, Hori Y. Biphasic effects of polarizing current on adenosine-sensitive generation of cyclic AMP in rat cerebral cortex. *Neuroscience letters* 1990;116(3):320-324.

197. Islam N, Aftabuddin M, Moriwaki A, et al. Increase in the calcium level following anodal polarization in the rat brain. *Brain research* 1995;684(2):206-208.

198. Priori A. Brain polarization in humans: a reappraisal of an old tool for prolonged non-invasive modulation of brain excitability. *Clin Neurophysiol* 2003;114(4):589-595.

199. Antal A, Nitsche MA, Paulus W. External modulation of visual perception in humans. *Neuroreport* 2001;12(16):3553-3555.

200. Nitsche MA, Doemkes S, Karakose T, et al. Shaping the effects of transcranial direct current stimulation of the human motor cortex. *J Neurophysiol* 2007;97(4):3109-3117.

201. Liebetanz D, Koch R, Mayenfels S, et al. Safety limits of cathodal transcranial direct current stimulation in rats. *Clin Neurophysiol* 2009;120(6):1161-1167.

CURRICULUM VITAE

RUOXIAN DENG

116 W UNIVERSITY PKWY, APT.835, BALTIMORE, MD, USA 21210

PHONE: 410-245-8481

EMAIL:RDENG.JHU@GMAIL.COM

Education

M.S. (May. 2015 Expected)

**Department of Biomedical Engineering, Whiting School of Engineering, Johns
Hopkins University, Baltimore, MD**

- GPA: 3.74/4;
- Fully Funded by Department Assistantship, NIH R01HL118084 and AHA
09SDG2110140 Grants

B.S. (Jun.2012)

**School of Medical Instrument and Food Engineering, University of Shanghai for
Science and Technology (USST), Shanghai, China**

- Major: Biomedical Engineering.

- Overall GPA: 89.5/100; Major GPA (specialized courses): 92.3/100
- Winner of Academic Excellence Scholarship (every semester) and National Scholarship(senior).

Research and Professional Experience

Research Assistant (Sep. 2013-Present)

Prof. Xiaofeng Jia

Department of Biomedical Engineering, Johns Hopkins University, Baltimore, USA & Department of Neurosurgery, University of Maryland School of Medicine, Baltimore, USA

- Receiving practical trainings in building asphyxial cardiac arrest and cardiopulmonary animal model, electrode implantation over cortices, rat's body temperature manipulation, immunofluorescence staining, etc.
- Engaging in applying the subband-based information (SIQ) measure of EEG to assess neurological recovery with therapeutic hypothermia in severe and moderate asphyxial cardiac arrest (CA) rodent model.
- Studying in using quantitative measure of somatosensory-evoked potentials (SSEP) to predict neurological outcome after resuscitation from moderate CA with temperature management.
- Assisted in the study on the effect of temperature modulation on spike activities of cortical and thalamic neurons in an uninjured rodent model.

- Participated in the investigation on the application of bone marrow stromal cells on functional recovery of denervated skeletal muscles.

Volunteer Research Assistant (Nov.2012-Jan. 2013)

Prof. Xiaofeng Jia

Department of Biomedical Engineering, Johns Hopkins University, Baltimore, USA

- Participated in the study on the effect of transcranial stimulation on evoked potential.

Research Assistant to Project Director (Jul. 2012 – Aug.2013)

Shanghai InnoStar Bio-Tech Co., Ltd., Shanghai, China

- Engaged in general pharmacology studies and new drug development researches.
- Assisted in performing animal surgeries and conducting experimental data-analysis.

Research Assistant Trainee (Oct. 2011- Jun. 2012)

Shanghai InnoStar Bio-Tech Co., Ltd., Shanghai, China

- Assisted in completing performance qualification and validation of JET & implantable telemetry systems in Beagle dogs' and cynomolgus monkeys' cardiovascular & respiratory systems.
- Engaged in meta-analysis for studies on the association between cytochrome P450 2E1 RsaI/PstI polymorphism with risk of anti-tuberculosis drug-induced liver injury.

Assistant to Application Specialist (Trainee) (Jun. 2011 - Oct. 2011)

Data Sciences International (DSI), Shanghai Office, China

- Learned about the principle of operation about physiological signal telemetry systems, Ponemah Software, etc.
- Installed and debugged experiment instruments for customers.

Research Assistant Trainee (Jun. 2010 - Sep. 2010 & Jan. 2011- Mar. 2011)

**Shanghai Institute of Traumatology & Orthopedics, Ruijin Hospital, Shanghai
Jiao Tong University School of Medicine, Shanghai, China**

- Received practical trainings in immunohistochemistry, cell culture, PCR, RT-PCR, etc.
- Participated in the investigation of hypoxia inducible factor (HIF) pathway in bone formation and the applications of desferrioxamine (DFO) in bone repair.
- Studied the regulatory effects of hemin on mesenchymal stem cell proliferation and differentiation.

Publications

- **Deng R**, Young L, Jia X. The Subband-based EEG Marker and Neurological Outcome with Temperature Manipulation after Cardiac Arrest. The XXVIIth International Symposium on Cerebral Blood Flow, Metabolism and Function & XIIth International Conference, June 27-30, 2015, Vancouver, Canada.

- Si Y, Li J, **Deng R**, Jia X. The Effect of Bone Marrow Stromal Cells on Functional Recovery of Denervated Skeletal Muscles. The 7th Annual Maryland Stem Cell Research Symposium, December 2, 2014, Silver Spring, Maryland.
- Tang N, **Deng R** (co-first author), Wang Y, Lin M, Li H, Qiu Y, Hong M, Zhou G. GSTM1 and GSTT1 Null Polymorphisms and Susceptibility to Anti-tuberculosis Drug-induced Liver Injury: a Meta-Analysis. *Int J Tuberc Lung Dis*, 2013, 17(1):17-25
- **Deng R**, Yang T, Wang Y, Tang N. CYP2E1 RsaI/PstI Polymorphism and Risk of Anti-tuberculosis Drug-induced Liver Injury: A Meta-Analysis. *Int J Tuberc Lung Dis*, 2012, 16(12):1574-81.
- **Deng R**, Feng S, Wan C, Zhang L, Ran R, Deng L. Hemin Boosts Mice Mesenchymal Stem Cell Proliferation by Down-Regulation of Cell Cycle Regulator p21. The 9th Stem Cell Research & Therapeutics Conference, October 24- 26, 2012, Philadelphia, Pennsylvania.
- Zhang W, Li G, **Deng R**, Deng L, Qiu S. New Bone Formation in a True Bone Ceramic Scaffold Loaded with Desferrioxamine in the Treatment of Segmental Bone Defect: a Preliminary Study. *J Orthop Sci*, 2012, 17: 289-98.
- Zhao J, Zhao Q, Zhang L, **Deng R**, Qi J, Zhou Q, Wang J, Lin L, Deng L. Preliminary Study of Mechanism of Delayed Early Fracture Healing in Ovariectomized Mice. *Journal of Shanghai Jiaotong University (Medical Science)*, 2011, 31: 890-4 (Chinese).
- Zeng W, Zhang W, Wang J, **Deng R**, Zhou Q, Wei L, Qi J, Deng L. Effects of Hypoxia Pathway on Multipotential Differentiation of Bone Marrow Stromal

Stem Cells. Journal of Shanghai Jiaotong University (Medical Science), 2011, 31:
913-7 (Chinese).

Computer Skills

- Professional in C language, Ponemah Software, MATLAB, Qt Creator, Stata, SAS, SPSS, Protel 99 SE, UG.
- Quite familiar with LINUX operation system.

Teaching Experience

Teaching Assistant (Sep.2014-Present)

- Lab for System Bioengineering I
- Lab for System Bioengineering II

Grader (Sep.2013-May.2014)

- Molecules and Cells
- Systems and Controls